INDEX
(FOUR REPORTS FOLLOW THIS INDEX PAGE)

Synthesis and Characterization Alkali Metal Salts Containing Trapped Hydrino

Performed at Rowan University
Glassboro, New Jersey

College of Liberal Arts and Sciences
Departments of Chemistry and Biochemistry
Prof. Amos Mugweru
Prof. K.V. Ramanujachary
Ms Heather Peterson
Mr. John Kong
Mr. Anthony Cirri

May 2009

Synthesis and Characterization Alkali Metal Salts Containing Trapped Hydrino

Prof. Amos Mugweru, Prof. K.V. Ramanujachary, Ms Heather Peterson, Mr. John Kong and Mr. Anthony Cirri

Rowan University

Chemistry and Biochemistry

Glassboro NJ, 08028

Summary

In this work, potassium chloride and potassium iodide salts containing a new form of hydrogen (hydrino) were synthesized. Characterization using solid state MAS ^{1}H NMR of potassium chloride salt containing the hydrino hydrogen (KH*Cl) gave spectral features at -4.50 ppm and 1.20 ppm relative to tetramethylsilane (TMS) while liquid ^{1}H NMR gave less intense peaks at 1.20 ppm versus TMS. MAS ^{1}H NMR of potassium iodide salt containing the hydrino hydrogen (KH*I) gave an intense broad peak at approximately -2.45 ppm relative to TMS while liquid ^{1}H NMR showed a very intense peak at approximately 1.258 ppm. These unusual upfield shifted peaks relative to the respective ordinary molecular hydrogen (4.5 ppm in liquid NMR) and hydride (0.8 and 1.1 ppm in MAS ^{1}H NMR) ^{1}H NMR peak locations are similar to those reported by BLP. Samples synthesized using chemicals provided by BLP also yielded similar MAS ^{1}H NMR spectral features. BLP has attributed these peaks *to* lower energy hydrogen (hydrino) as hydride ions (-4.5 and -2.45 ppm in MAS ^{1}H NMR) and molecular hydrino gas (1.2 ppm in liquid ^{1}H NMR). Neutron diffraction studies indicate the possibility of trapped interstitial atoms although the exact nature of these could not be established unambiguously. Elemental analysis on these salts containing hydrino hydrogen showed negligible amounts of Be, Cr, Mn, Ni, Co, Zn, As, Ag, Cd, Sb, Ba and Pb. These results are supportive of the possibility of having lower electronic states of hydrogen.

Introduction

BLP has made claims of the existence of a hydrogen where the single electron resides in a lower energy state called *hydrinos* [1-8]. The transition to such a state is induced by the presence of a catalyst and atomic hydrogen [1-8]. It has been claimed that the alkali metal halide is capable of trapping this lower energy hydrogen as a high binding energy hydride ion also called the hydrino hydride ion. If these claims are verified then it is reasonable to envision a potentially novel and revolutionary energy source.

In this work, we have used chemicals supplied by BLP and synthesized several alkali halido hydrides, (KH*X, X= Cl and I) containing hydrino hydride ions trapped in the lattice of the alkali halides. The procedure is outlined below. We also purchased our own chemicals and synthesized in-house samples of these compounds. Synthesis of KH*X included the reaction of KCl or KI with hydrogen in the presence of catalysts [2-5, 7, 8]. These reactions were carried at temperatures in the range of 500^{o}C to 600^{o}C in a kiln for 68 hours. BLP has claimed that the high binding energy hydrides have a smaller radius relative to the normal hydride which in turn enhance the shielding. The observed upfield shifts in the NMR spectra has been attributed to the increased shielding.

The objective of the work at the Chemistry and Biochemistry Department at Rowan was to synthesize and characterize hydrino-hydride ions trapped in the lattice of alkali halides and compare the results with those obtained from BLP materials

Synthesis of Alkali Salts with Trapped Hydrino

Chemicals and Procedures

KCl and KI (both with a purity better than 99.5%) were procured from VWR, potassium sticks from Strem Chemicals, and nickel screen (Ni, 20x20 mesh plain, 0.014 inch in diameter) was purchased from the Unique Wire Weaving Company. K_2CO_3 and H_2O_2 were also purchased from VWR.

In preparation for the reaction, the salts were first dried in a flask under a vacuum of approximately 50 mTorr at 200^{o}C for 14 hours and then transferred to the glove box. The potassium sticks were washed three times with anhydrous hexane inside the glove box. Nickel screen was washed with a water solution containing 20 wt % K_2CO_3 and 5 % H_2O_2 and then with deionizer water and dried at 100 ^{o}C overnight.

For the synthesis of KH*Cl, a clean stainless steel reactor was transferred to the glove box after drying in the oven overnight at 120^{o}C and lined with about 43 grams of nickel screen. A stainless steel crucible was then placed in the reactor. The oxide layer on the surface of potassium was peeled off with a penknife. About 1.6 g of the shinny potassium was weighed and placed on the bottom of stainless steel crucible. 20 grams of KCl was then weighed and placed in the stainless steel crucible to cover the potassium. The reactor was tightly closed and was checked for any leaks before placing the reaction was started. The reactor was pumped down to a final vacuum of < 30 mTorr.

For synthesis of KH*I, 15.0 grams of dry Raney Ni 2800 was weighed inside the glove box and placed in the stainless steel crucibles. Approximately 1.0 g of potassium metal was also weighed inside the glove box and placed in a smaller stainless steel crucible. 20 grams of KI was then weighed and spread over the potassium metal inside the smaller crucible. The crucible was subsequently transferred to the larger crucible and placed on the bottom of the reactor before sealing and evacuation. The reaction temperature for this synthesis was 500^{o}C. The rest of the procedure was similar synthesis of KH*Cl.

After evacuation of the reactors, hydrogen gas (5 PSIG pressure) was slowly introduced and the temperature was gradually increased to 600^{o}C. The reactor pressure was maintained at 5 PSIG for the next 68 hours. In some experiments, the pressure was checked and more hydrogen added every 30 minutes if needed to maintain 5 PSIG. After the completion of the experiment, the kiln was shut down and allowed to cool naturally. At about 300^{o}C, the kiln's lid was opened to hasten the cooling. The reactor was pressurized with helium after the reactor temperature had dropped to 50^{o}C.

The reactor assembly was transferred to the Ar-filled glove box after closing all the valves. The hydrogen containing salts were retrieved and placed in a vial. Nearly 1.0 gram of the sample was sent out for solid state MAS ^{1}H NMR studies. This procedure was repeated several times to ensure the reproducibility during the months of January to May. Liquid NMR studies of these samples were taken at Rowan University. Solid state MAS ^{1}H NMR results, liquid ^{1}H NMR, as well as elemental analysis, and neutron diffraction studies were carried out.

For solution ^{1}H NMR measurements, KH*X samples were first washed in DMF-d_7 solvent in a glove box. The clear liquid, just above the solid material, was transferred to an NMR tube (attached to a vacuum line for sealing) and then flame-sealed for NMR analysis. Proton NMR was recorded using a 400 MHz Varian Oxford AS400 NMR system. Solution ^{1}H NMR spectra of these salts were obtained in the DMF-d_7 solvent. All NMR specra were relative to TMS.

Elemental analysis of the salt was done using inductively coupled plasma mass spectrometry (Agilent 7500, ICP-MS) and using standard analytical procedures.

Results and Discussions

Characterization of Hydrino Containing KCl Salts

Figure 1 shows the solid state MAS ^{1}H NMR spectrum of KH*Cl sample prepared using chemicals provided by BLP using the procedure described above. Two peaks were observed, one intense peak at around -4.469 ppm and another less intense centered at 1.197 ppm. Other samples synthesized using BLP chemicals yielded similar spectra.

Figure 2 shows the MAS ^{1}H NMR spectrum of the KCl salt purchased by Rowan from VWR. Two peaks with low intensity centered at around 1.13 ppm and at 4.298 ppm were observed, and no peaks upfield of TMS were detected. BLP reported that the MAS ^{1}H NMR of mixtures of KCl and KH show an H_2 peak at 4.3 ppm and KH in two chemical environments at 1.1 and 0.8 ppm [3,5]. KH is air sensitive and not present in KCl. The peak at 1.1 ppm has been found only in salts that contain a hydrino catalyst [2] and H_2. The peak at 1.1 ppm has been observed by other researchers who could not assign it [9]. It is observed along with the known H_2 peak at about 4.3 ppm. BLP attributes the peak to interstitial $H_2(1/4)$ [2]. MAS ^{1}H NMR spectra of some additional KH*Cl salts synthesized using Rowan procured reagents are shown in Figures 3 and 4. Two intense peaks were obtained, one at -4.5 ppm and another at 1.201 ppm. All syntheses showed considerable reproducibility as each sample yielded the similar spectra.

Solid State ^{1}H NMR clearly shows an upfield shifted peak at -4.50 ppm and a peak at 1.20 ppm which BLP has attributed to hydrino hydride ion and molecular hydrino, $H_2(1/4)$, respectively. The unusual upfield shifted peaks were consistently observed at these positions in the samples as

repeated runs yielded similar spectra. We cannot assign negative upfield shifted peaks to any known compound from the literature as ordinary alkali hydrides alone or when mixed with alkali halides only show down-field shifted peaks.

Solution ^{1}H NMR spectrum of KH*Cl in DMF-d_7 as the solvent is shown in figure 5. Four peaks were observed, a singlet at 8.030ppm and two solvent peak quintets centered at 2.907 ppm, and 2.715 ppm. Another singlet is also visible at 3.379 ppm due to presence of residual water in DMF. There was no clear upfield shifted peak at -3.80 ppm that was observed by BLP [2]; although, a less intense peak at 1.25 ppm assigned to $H_2(1/4)$ by BLP [2] was apparent (Figure 5 insert).

Neutron diffraction studies of KH*Cl and KCl used in the synthesis indicated that interstitial atoms could be trapped in the KCl lattice. Figure 6 shows the neutron diffraction pattern KCl while figure 7 shows the neutron diffraction pattern of KH*Cl. This initial result leads us to believe that indeed hydrogen could be the atom in the salt but exactly in what form is still not clear to us. We have planned more neutron diffraction studies.

Elemental analysis of KH*Cl using ICP-MS yielded the following results: Be (less than 1 ppb) , Cr (3.0 ppb) , Mn (less than 1.0 ppb), Ni (less than 1.0 ppb) , Co (< 1.0 ppb) , Zn (about 1.0 ppb) , As (about 1.6 ppb), Ag (7.4 ppb), Cd (< 1.0ppb), Sb (1.8 ppb), Ba (<1.0 ppb) and Pb (0.3 ppb). These concentrations were too low to influence the reaction or the NMR results.

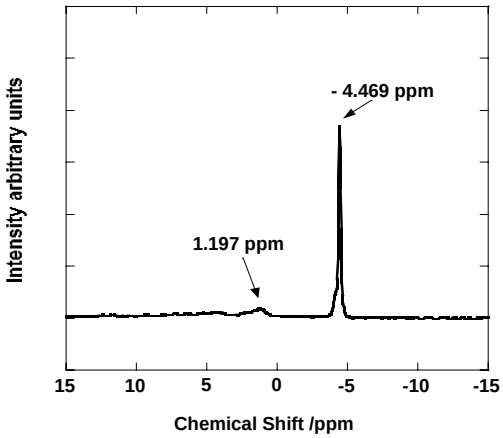

Fig. 1. Solid state MAS ^{1}H NMR spectrum of sample prepared using BLP chemicals.

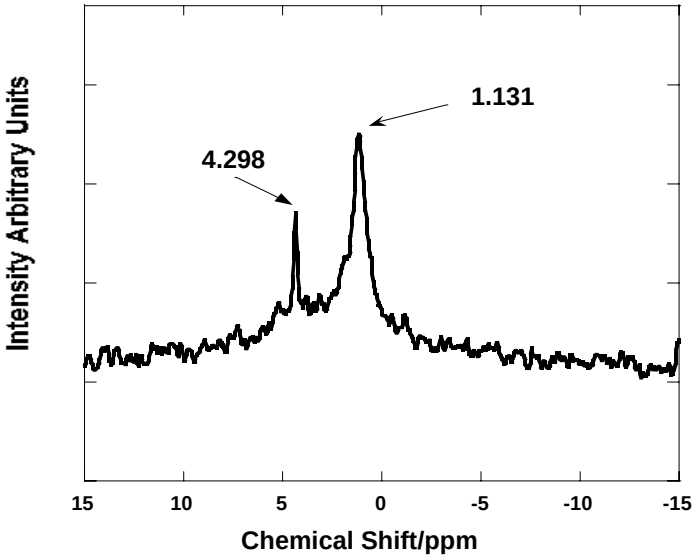

Fig. 2. MAS ^{1}H NMR spectrum of KCl bought from VWR.

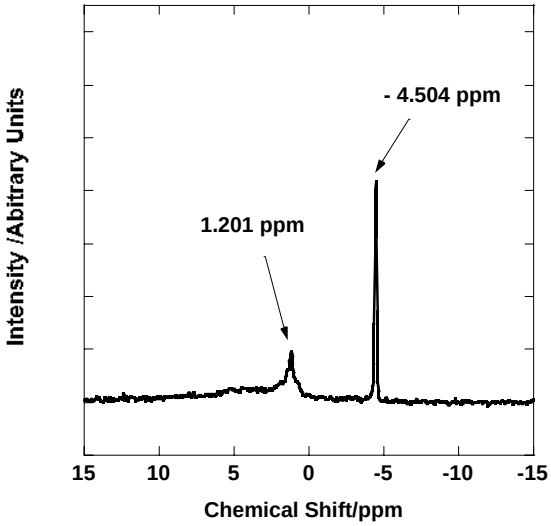

Fig. 3. MAS ^{1}H NMR spectrum of KH*Cl synthesized using chemicals purchased by Rowan.

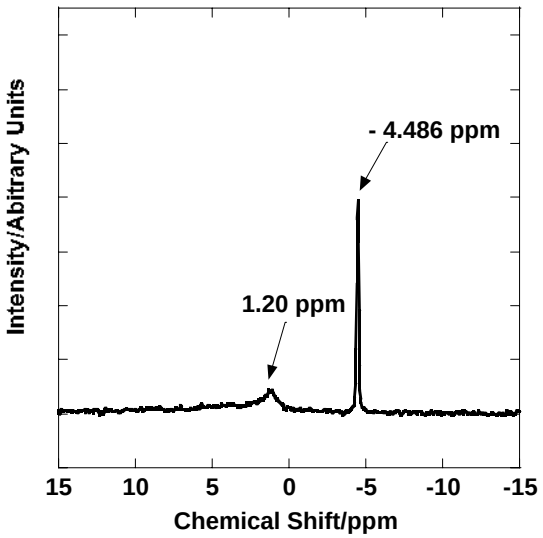

Fig. 4. MAS ^{1}H NMR spectrum of KH*Cl synthesized on Feb 24, 2009 using chemicals procured by Rowan.

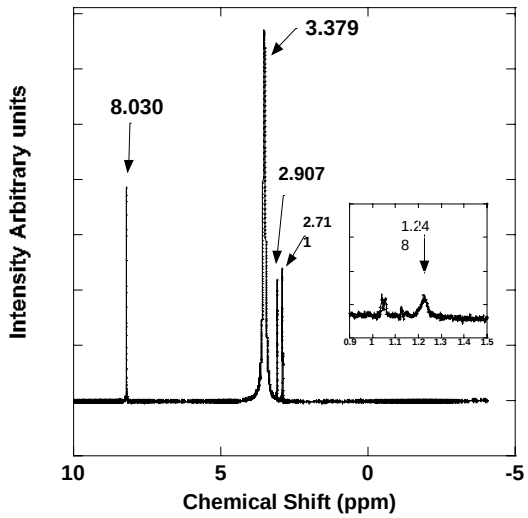

Fig. 5. Liquid ^{1}H NMR spectra of KH*Cl synthesized on April 14, 2009 using chemicals procured by Rowan.

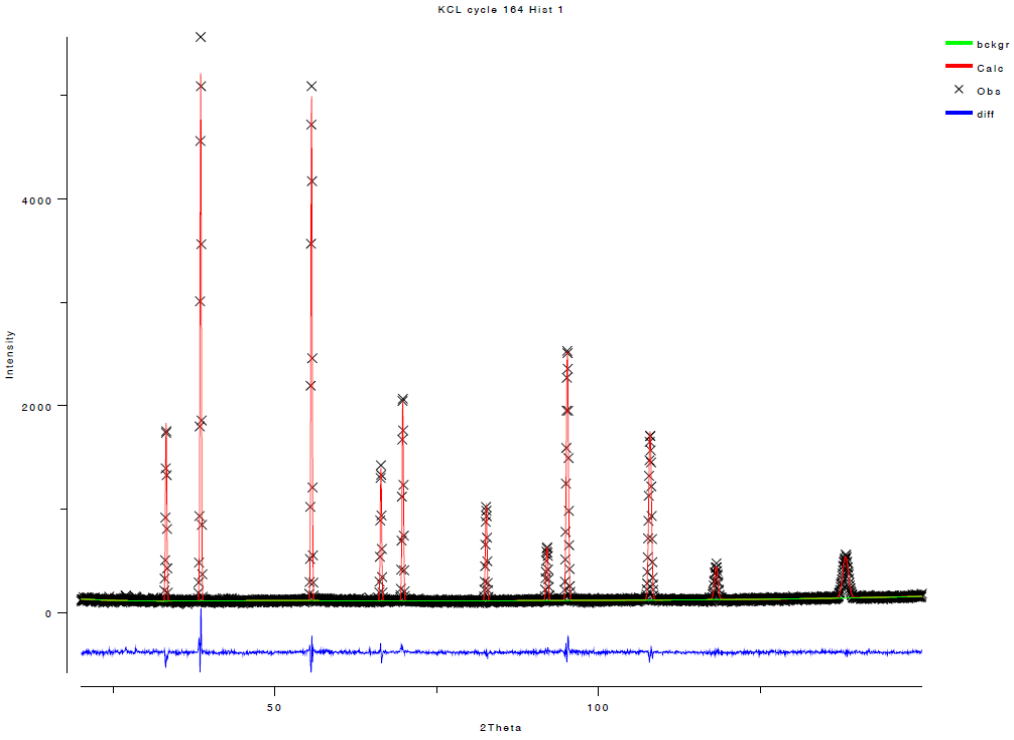

Fig. 6. Neutron diffraction spectra of KCl.

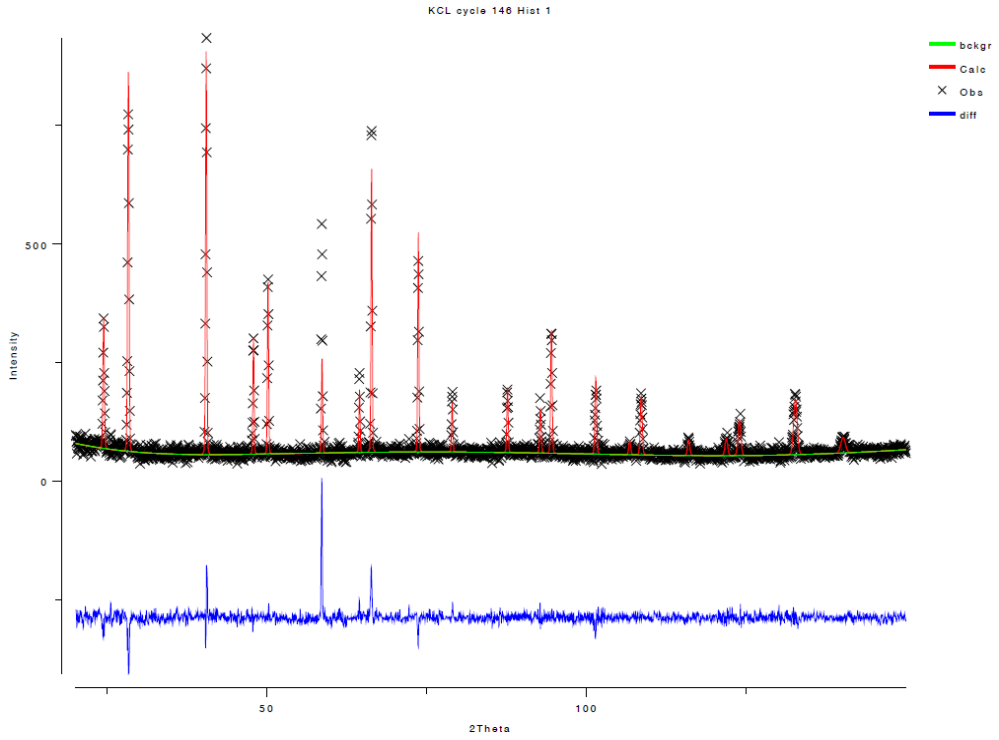

Fig.7. Neutron diffraction pattern of KH*Cl.

Characterization of Hydrino Containing KI Salts

Figure 8 shows the solid state MAS ^{1}H NMR spectrum of a KH*I sample prepared using chemicals provided by BLP using the procedures discusses previously. One broad intense peak at around -2.4 ppm, a less intense 1.051 ppm and broad peaks centered at -19.1 ppm and 13.9 ppm, which are the side bands of -2.4 ppm peak, were observed. Other samples synthesized using BLP chemicals yielded similar spectra.

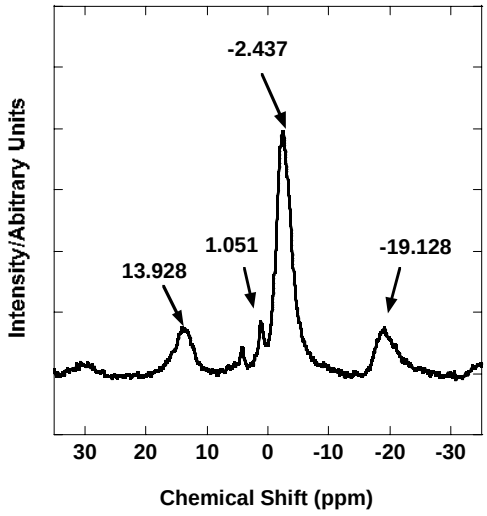

Fig. 8. MAS ^{1}H NMR spectra of KH*I sample prepared using chemicals provided by BLP.

Using our own chemicals and protocols discussed previously, we synthesized KH*I. MAS ^{1}H NMR spectra of some of the KH*I salts synthesized are shown in Figures 9 and 10. One broad intense peak was obtained, at between -2.3 ppm and -2.7 ppm. A less intense broad peak was observed at approximately 1 ppm. The sidebands of the about -2.4 ppm peak were observed at about -19 ppm and 13ppm. The synthesis was reproducible as repetition of sample synthesis yielded the same spectra.

Previously BLP published results show MAS ^{1}H NMR spectra with broad peaks at around -2.31 ppm and 1.13 ppm versus TMS. According to BLP, the upfield shifted peak at around -2.31 ppm is due to a hydrino hydride ion, $H^-(1/4)$ shifted compared to the –4.4 ppm peak in KH*Cl by a matrix effect that also broadens the peak, whereas the peak at around 1.05 ppm is due to trapped molecular hydrino gas $H_2(1/4)$. Other than the halide, the main hydrogen dissociator used in this synthesis was Raney Ni as opposed to Ni screen in the synthesis of KH*Cl. KH*Cl gives very sharp peaks (Figures 1, 3, and 4). The narrow peak width obtained with KH*Cl points to a free ion rotating. In the literature no compounds have been found with the kind of protons contained in these

compounds. We are planning to carry out neutron diffraction studies of this salt to indentify any interstitial atoms present.

The solution ^{1}H NMR spectrum of KH*I synthesized in our lab using DMF-d_7 as the solvent is shown in Figure 11. Four solvent peaks were observed, a singlet at 8.030ppm and two quintets centered at 2.898 ppm, and 2.686 ppm. Another singlet is also visible at 3.498 ppm due to presence of residual water in DMF. There was also a huge peak at 1.258 ppm which was not due to the DMF solvent. Samples synthesized using BLP chemicals and our own chemicals have shown consistent unusual liquid ^{1}H NMR peaks at approximately 1.258 ppm. BLP's published results also include another less intense peak at -3.79 ppm in addition to the peak at 1.21 ppm [2]. BLP has attributed the upfield shifted peaks at -3.79 ppm to $H^-(1/4)$ while the one at approximately 1.21 is assigned to H_2 (1/4). Our liquid ^{1}H NMR spectra did not show the less intense peaks at -3.79 ppm but an unusually large peak at 1.258 ppm was obtained which matched the $H_2(1/4)$. This huge peak may also be formed through conversion of H^- (1/4) to hydrino gas $H_2(1/4)$.

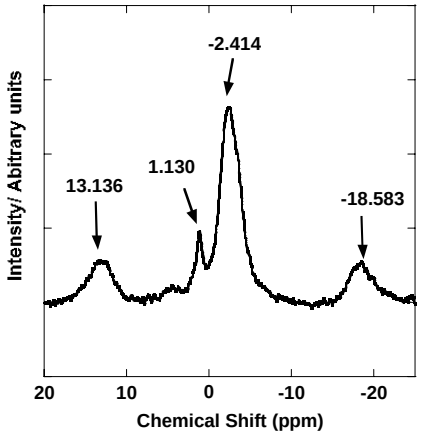

Fig. 9. MAS ^{1}H NMR spectrum of KH*I synthesized on April 15, 2009 using chemicals procured by Rowan.

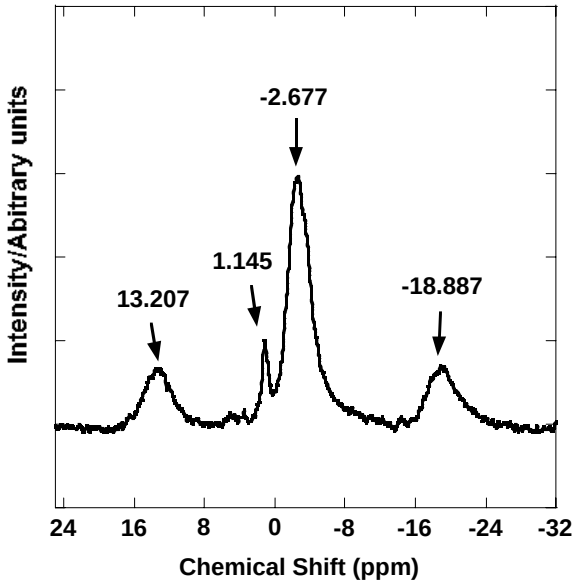

Fig. 10. MAS ^{1}H NMR spectrum of KH*I synthesized on April 28, 2009 using chemicals procured by Rowan.

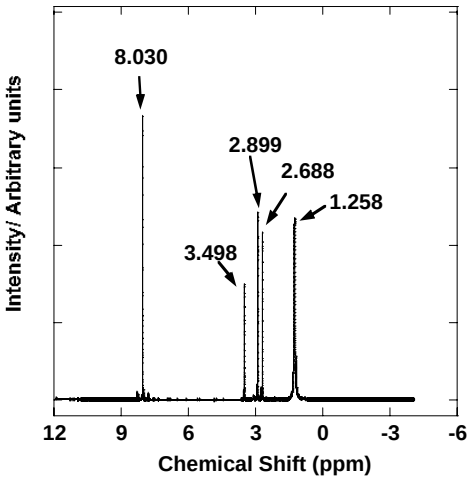

Fig. 11. Liquid ^{1}H NMR spectrum of KH*I synthesized on April 28, 2009 using chemicals procured by Rowan.

Conclusions and Further Work

The solid state MAS ^{1}H NMR spectra of KH*Cl and KH*I synthesized using chemicals purchased by Rowan and those provided by BLP have shown similar and consistent unusual upfield shifted peaks relative to those of ordinary H species. From KH*Cl we observed peaks at around 1.20 and -4.50 ppm while KH*I shows broad, high intensity peaks at around -2.3 to -2.7 ppm. BLP has attributed these upfield shifted peak at -4.50 ppm and -2.3 ppm to $H^-(1/4)$ while the ones at approximately 1.21 ppm and 1.1 ppm to $H_2(1/4)$ [2]. Liquid ^{1}H NMR studies show less intense peaks at 1.248 ppm for KH*Cl while strong peaks were observed for KH*I at 1.258 ppm.

Neutron diffraction studies on these samples point to presence of trapped atoms in the crystal lattice of these salts. According to our elemental analysis results using ICP-MS, we do not see significant amount of other elements that could play a role in the synthesis. Accordingly, we have ruled out the role of other elements in these reactions. Although we have not concluded our work in the area of characterization, we are not aware of any hydride compounds in the literature based on elemental analysis that gives these upfield-shifted peaks. This gives credence to presence of hydrinos trapped in these salts.

To precisely confirm the presence of hydrino hydride ions and molecular hydrino in these salts we plan to perform further neutron diffraction. After obtaining the diffraction pattern, we plan to drive off the trapped interstitial atoms through heating and obtain the pattern again. The pattern should resemble either KCl or KI, after driving off the hydrino gas.

References

1. Mills, R.L., L. Y, and K. Akhtar, Spectroscopic Observation of Helium-Ion and Hydrogen-Catalyzed Hydrino Transitions. **Submitted**.

2. Mills, R.L., G. Zhao, K. Akhtar, Z. Chang, J. He, Y. Lu, W. Good, G. Chu, and B. Dhandapani, Commercializable power source from forming new states of hydrogen. *International Journal of Hydrogen Energy*, **2009**. 34(2): p. 573-614.

3. R.L Mills, B.D., Mark Nansteel, Jiliang He, Tina Shannon, Alex Echezuria, Synthesis and characterization of novel hydride compounds. *International Journal of Hydrogen Energy*, **2001**. 26: p. 339-367.

4. Mills, R.L. and P. Ray, Spectroscopic identification of a novel catalytic reaction of potassium and atomic hydrogen and the hydride ion product. *International Journal of Hydrogen Energy*, **2002**. 27(2): p. 183-192.

5. Mills, R.L., Synthesis and Characterization of potassium iodo hydride. *International Journal of Hydrogen Energy*, **2000**. 25: p. 1185-1203.

6. Mills, R., The Grand Unified Theory of Classical Quantum Mechanics. June 2008 Edition, http://www.blacklightpower.com/theory/bookdownload.shml.

7. Mills, R.L., J. Dong, W. Good, and A. Voigt, Minimum heat of formation of potassium iodo hydride. *International Journal of Hydrogen Energy*, **2001**. 26(11): p. 1199-1208.

8. Mills, R.L., P. Ray, B. Dhandapani, W. Good, P. Jansson, and M. Nansteel, Spectroscopic and NMR identification of novel hydride ions in fractional quantum energy states formed by an exothermic reaction of atomic hydrogen with certain catalysts. *Eur Phys J Appl Phys*, **2004**. 28: p. 83-10.

9. Lu C, Hu J, Kwak JH, Yang Z, Ren R, Markmaitree T, et. al., Study the Effects of Mechanical Activation on Li-N-H systems with ^{1}H and ^{6}Li solid-dtate NMR. *Journal of Power Sources* 2007; 170:419-24.

Report on Synthesis and Studies of "Generation 2" Lower Energy Hydrogen Chemicals

Performed at Rowan University
Glassboro, New Jersey

College of Liberal Arts & Sciences

Departments of Chemistry & BioChemistry

Prof. Amos Mugweru

Prof. K.V. Ramanujachary

Heather Peterson

John Kong

August 10, 2009

Report on synthesis and studies of "Generation 2" lower energy hydrogen chemicals

Prof. Amos Mugweru, Prof. K.V. Ramanujachary, Ms Heather Peterson, and Mr. John Kong

Rowan University

Chemistry and Biochemistry

Glassboro NJ, 08028

The primary aim of this work was to reproduce the synthesis and conduct studies of BLP generation-2 chemistry. This phase of the work is a continuation of prior work that involved studies on the lower energy state of hydrogen. During the current reporting period, sodium or potassium hydride, magnesium or calcium metal powder, titanium carbide or activated carbon support material and several halide salts were loaded in a cell and were heated to initiate the reaction. The products of the reaction, including the gases generated, were collected and analyzed. Gaseous products were analyzed using gas chromatography and mass spectrometry. The solid product was analyzed using X-ray diffraction (XRD). The reaction pathway was determined based on the starting materials and the post reaction products determined by chemical analysis. In most of the reactions the presence of magnesium hydride, the metal of metal halide reactant and an alkali halide salt were observed. A small amount of magnesium halide was also observed. However, the starting metal halide salt was absent in all the products. Liquid ^{1}H NMR spectra after extraction with DMF-d_7 showed a very intense peak at approximately 1.258 ppm and at -3.84 ppm which BLP previously attributed to a lower energy hydrogen (hydrino) as molecular hydrino gas and hydrino hydride ions, respectively. The heat generated for each reaction was determined by carrying out the calorimetric studies in the Department of Engineering. For the different reaction mixtures approximately 1.6–6.5 times more energy than the maximum expected for conventional chemistry was observed. Temperature programmed desorption studies was used to rule out presence of water and/or CO/CO_2 in the starting materials. In what follows, we present some of experimental studies that were carried out at Rowan.

Background

In our prior report, we reproducibly synthesized "hydrino" trapped compounds using procedures provided by BLP. In the same study, we were able to confirm the unusal state of hydrogen, "hydrino," using both liquid ^{1}H NMR and MAS ^{1}H NMR studies. For the generation of the unusual state of hydrogen, we employed a method in which alkaline halides were heated in the presence of hydrogen and a catalyst to form hydrinos. According to BLP, the alkali metal halide is capable of trapping the lower energy hydrogen as a high binding energy hydride ion [also called the hydrino hydride ion as well as molecular hydrino]. In this report, we report the results from studying BLP generation 2 chemistry. BLP has been conducting studies on generation 2 chemistry that they claim will potentially lead to a new energy source. In the generation 2 chemistry, (we witnessed at BLP and performed at Rowan University), sodium or potassium hydride, magnesium or calcium powder, a support material, and a metal halide were mixed and heated to initiate the reaction. Calorimetric studies as well as chemical characterization of the reaction products were performed using XRD, GC, MS, and TPD techniques. Liquid ^{1}H NMR was also carried out on some of the samples. We report here the results of these reactions carried out at Rowan using chemicals procured by us, and using both 0.05 mole (5X) and 0.5 mole (50X) scale reactors. We initially assessed possible chemical reactions occurring and their energies. The enthalpies of the most energetic reactions possible were compared with the actual heat measured calorimetrically in the smaller 5X reactors and larger 50X reactors.

Chemicals and Procedures

Titanium carbide, TiC, tin iodide, SnI_2 (99%), iron bromide, $FeBr_2$ (98+%), magnesium metal powder, Mg (99.8%), potassium hydride, KH (30-35% wt% in mineral oil), indium chloride, InCl (99.995%), cobalt iodide, CoI_2 (99.5%), europium bromide, $EuBr_2$ (99.99%), manganese iodide, MnI_2 (98%), calcium, Ca (98.8%), and silver chloride, AgCl (99.9%) were all supplied by Alfa Aesar. The anhydrous hexane ($\geq$99%) was supplied by Sigma Aldrich and sulfur hexafluoride, SF_6 (99.9%) was from GTS-Welco. In preparation for the first reaction, titanium carbide was first dried in a flask under a vacuum of approximately 50 mTorr at 200 °C for 14 hours and then transferred to the glove box. The potassium hydride was washed inside the glove box with anhydrous hexane four times after decanting the mineral oil. The KH was further dried in the anti-chamber of the glove box for 4 hours to remove residual hexane and other organic residues, and later transferred into a

sealed container within the glove box. As will be described later, temperature programmed desorption (TPD) studies were done on the starting materials, manganese iodide, titanium carbide and other salts to quantify any condensable gas(es) such as water and/or CO_2/CO present.

For a 50X reaction, 83.0 grams of KH, 50.0 grams of Mg, 200.0 grams of TiC and 154.0 grams of MnI_2 were weighed and thoroughly mixed in a large beaker inside the glove box. A 2 liter cell was transferred to a glove box and the reaction mixture was quantitatively transferred into the cell and then the cell closed. The loaded cell was taken to the Technology Park in Rowan University where calorimetric studies were carried out. For a 5X reactor, 8.30 grams of KH, 5.0 grams of Mg, 20.0 grams of TiC and 15.40 grams of MnI_2 were used. The reaction was repeated with MnI_2 replaced by $FeBr_2$, SnI_2, InCl, CoI_2, $EuBr_2$ AgCl and SF_6.

For the solution ^1H NMR measurements, a post reaction sample from NaH +MgH_2 + activated carbon and 0.03 moles of SF_6 gas was extracted using DMF-d_7 solvent in a glove box. The clear liquid, just above the solid material, was transferred to an NMR tube and tightly capped. ^1H NMR was recorded using a 400 MHz Varian Oxford AS400 NMR system. All chemical shifts in ^1H NMR spectra were relative to TMS.

Temperature programmed desorption (TPD) studies

The desorption behavior of materials was stuided using a Chembet 3000 chemisorption unit of Quantchrome Corporation with a thermal conductivity detector (TCD). The initial task of this phase of analysis was to quantify water present, if any, in starting materials. Argon was used as a carrier gas, and dry ice was used for the separation of water (by condensation) during the course of desorption experiments. Appromately 0.1 grams of the sample was loaded into the TPD cell under argon environment. The cell was then placed in a thermal heater and connected to a gas line (including stainless steel tubing and reservoir). Any condensed water would be carried into the TCD analyzer when the dry ice dewar was removed and the trap was thawed to room temperature. Appendix A shows the TPD traces of the starting materials (TiC and MnI_2) suggesting a negligible amount of water and CO_2 present in the materials.

An independent TPD analysis was also performed using the ideal gas law. Approximately 0.1 grams of the starting chemical sample was loaded into a TPD cell under argon, the cell was then placed in a thermal heater and connected to a gas line (including stainless steel tubing and reservoir). Before heating, the sample and gas line were evacuated to $\sim 10^{-5}$ Torr of pressure. The cell was then heated

slowly to ~500 °C in order to desorb all of the water present in the sample. The evolved gas was expanded into a reservoir of known volume. The gas line was then submerged into a liquid nitrogen dewar in order to condense any water vapor or other gas(es) present from the thermal desorption. After evacuating the noncondensable gases, the cold trap was removed to allow the reservoir to reach room temperature and evaporate any condensed gas with temperature increases. In the experiment, cell temperature, room temperature, and gas pressure were monitored and recorded by a Labview program.

The quantity of gas obtained could be calculated using the ideal gas law (Equation 1) using the measured pressure, temperature and volume.

$$PV = nRT \quad (1)$$

The results of the TPD of the TiC and MnI_2 starting materials are given in Appendix A. Since liquid nitrogen was used as the cold trap, any gas with a boiling point above –196 °C would have been condensed. As shown, the total condensable gas was negligible; thus, the material contained minute quantities of H_2O (and/or CO_2 and CO) from both TiC and MnI_2. Their contribution to the heat energy of the reaction was considered to be small enough to be neglected in the heat balance calculations.

Analysis of reaction products

Before collecting the gas for MS and GC analysis, the pressure and volume of the gas in reactor was measured by connecting the reactor to a pre-evacuated reservoir (known volume) with a pressure gauge. Using the known combined volume, measured pressure and temperature, the moles of gas were determined using the ideal gas law. The gas from the reaction was then transferred to an empty cell for mass spectroscopic identification and quantitative gas chromatography. Gas chromatography (GC) showed that most of the gas generated during the reaction was methane. Figure 1 shows the gas chromatogram of the gases generated during the reaction. Argon is already present as all the chemical manipulations are carried out in this atmosphere. The gas was loaded into a six-port rotary valve from gas container with a gas line before the injection Prior to the gas sample loading, the sample loop (~3 ml) in the six-port rotary valve was sufficiently evacuated (~10^{-5} torr) to remove any residual gas/contaminant. The oven temperature was set at 80 °C, the injector was set to 100 °C, and the detector was set to 120 °C. Helium was the carrier gas and a flow rate of 43.4 ml/min was employed. Calibrations using pure gases H_2, CH_4, CO, and CO_2 were

performed prior to testing. Figure 2 shows the mass spectrum of the gases generated during the reaction. To quantify the amount of methane found in the gaseous phase, a calibration curve of methane gas was obtained (Appendix A). In the case of the reaction mixture 83g KH +50g Mg + 200g TiC + 154g MnI_2 a quantitative analysis of the gaseous phase indicated that 16.0% volume of the gas produced was methane. Since the total gas pressure was about 1 atm, and the volume of methane was 384 ml (2400 ml × 16%), the moles of methane in the product was 0.01575 mole (room temperature 24 °C).

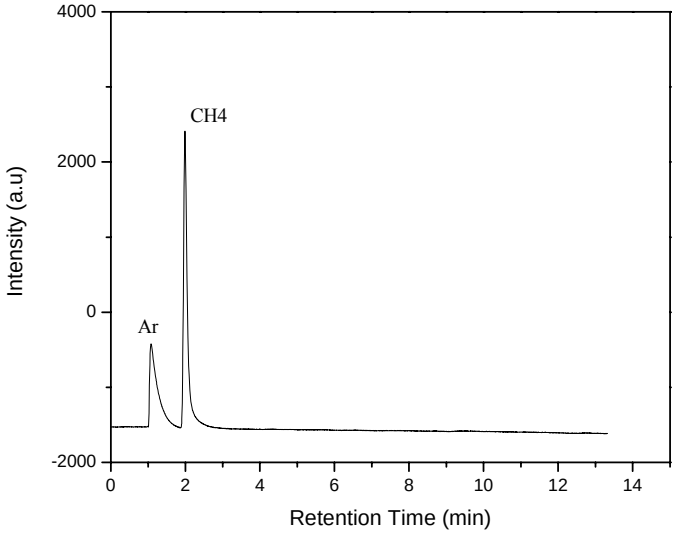

Figure 1. Gas chromatograph of contents of gas phase following the reaction.

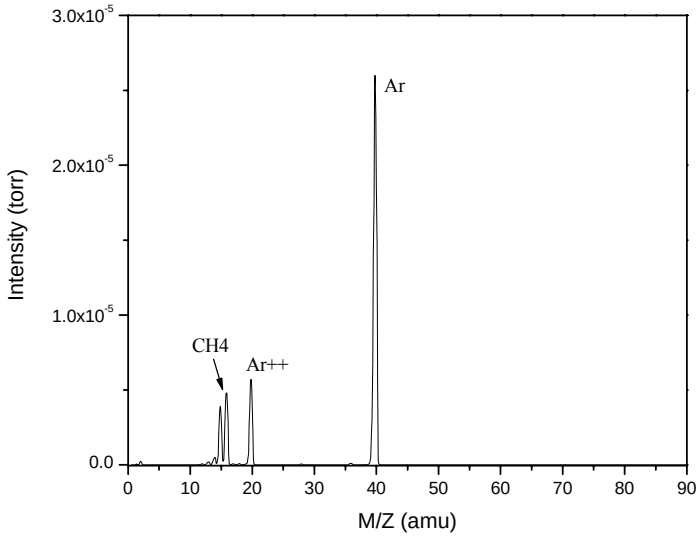

Figure 2. MS spectra of gas following the reaction. Methane is the minor component while Ar was the predominant component as the cell was loaded under argon in dry box.

X-ray diffraction (XRD)

In this part of the work, we have carried out several slow scans of post run products from the Technology Park in Rowan University. The samples were loaded in hermetically sealed sample holders (Bruker Model #A100B37) in a glove box under argon and wax sealed. Diffraction patterns were recorded using Scintag X2 Advanced Diffraction System with an operating voltage set to 40 kV and current of 30 mA. Patterns were recorded in a step mode [0.02 Deg/min] in the 2θ range 10-70 using a residence time of 8 seconds. The diffraction patterns of post reaction mixture of manganese iodide, potassium hydride, magnesium and titanium carbide recorded at Rowan are shown in Figure 3. The diffraction patterns from a library were matched to the diffraction pattern obtained from the post run samples. From the diffraction patterns potassium iodide, magnesium metal, manganese metal, titanium carbide, and magnesium hydride were observed. The diffraction patterns obtained at Rowan and at a commercial laboratory were similar.

Figure 4 shows the diffraction patterns obtained from the commercial laboratory. Quantitative XRD analysis from a commercial laboratory shows KH (2.6 $\pm$ 0.3 %), Mg (4.3 $\pm$ 0.4%), Mn (3.7$\pm$ 0.4%), KI (22.7 $\pm$ 0.3%), $KMgH_2$ (5.7 + 0.2%) and TiC (61.0 $\pm$ 0.8). Manganese iodide was absent from the reaction products suggesting that it may be the limiting reactant. This was the case based on the mole ratios of the reagents of the reaction mixture. Accordingly, all the energy calculations were based on the actual amount of MnI_2.

Figure 5 shows the XRD Diffraction patterns of post-reaction sample phase identification at Rowan. Reactants included potassium hydride, magnesium, titanium carbide and indium chloride. From the diffraction patterns we observe that there is no indium chloride in the post reaction mixture, indicating that it was consumed. The post reaction sample contains magnesium, traces of magnesium hydride, and magnesium chloride, and indium metal. There were other smaller peaks that could not be assigned and the phase identification is not conclusive.

XRD of post reaction mixtures containing (i) KH+Mg+SnI_2+TiC (ii) NaH+ MgH_2+ SF_6 +activated carbon, and (iii) KH+Mg+AgCl+activated carbon are given in the appendix section E. Although we were not able to establish the completion of the reaction, we however observe some magnesium hydride, in all cases. The XRD also suggests that all the initial halide salt used in the starting mixture was absent in the post reaction mixture.

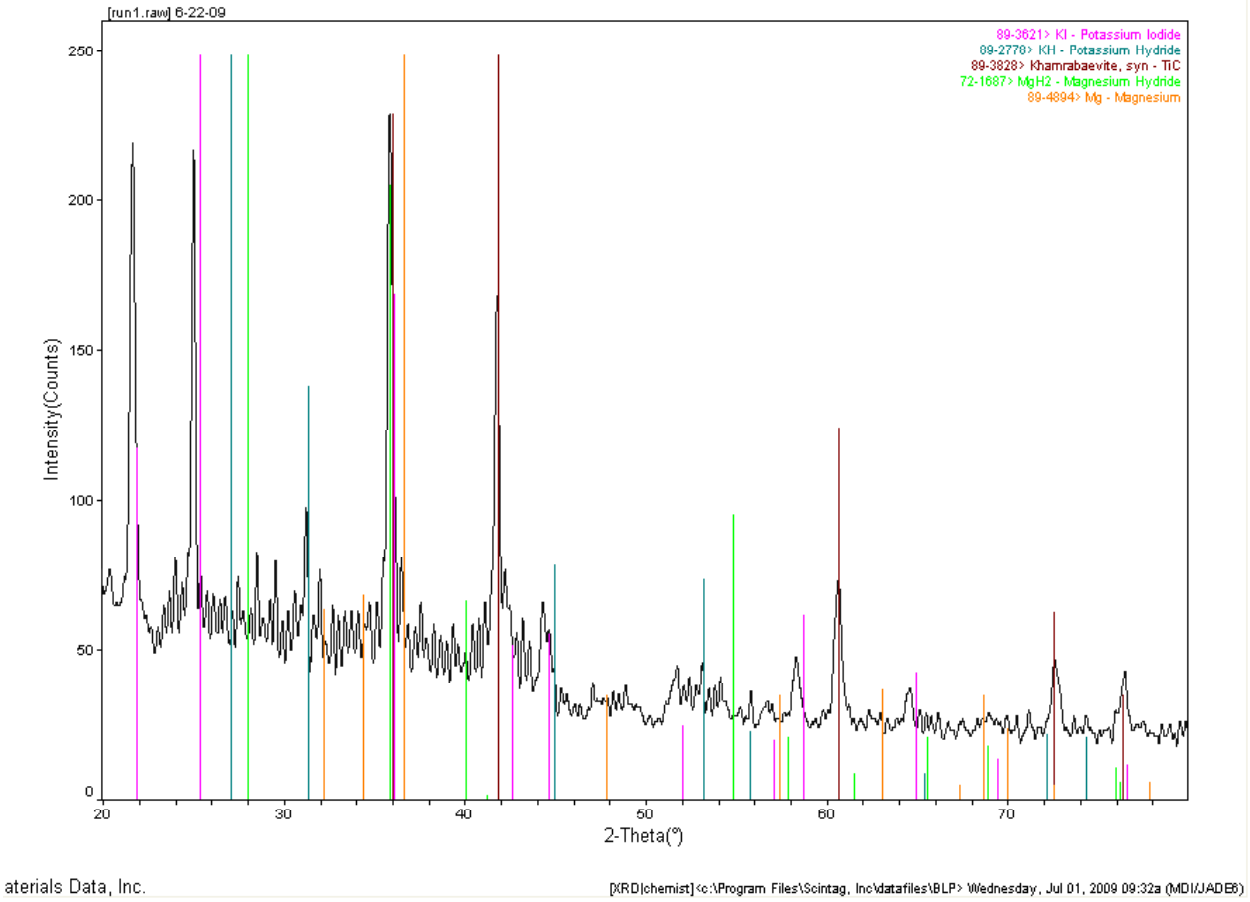

Figure 3. XRD Diffraction patterns of post-reaction sample phase identification at Rowan. Initial reactants included magnesium, manganese iodide, titanium carbide and potassium hydride.

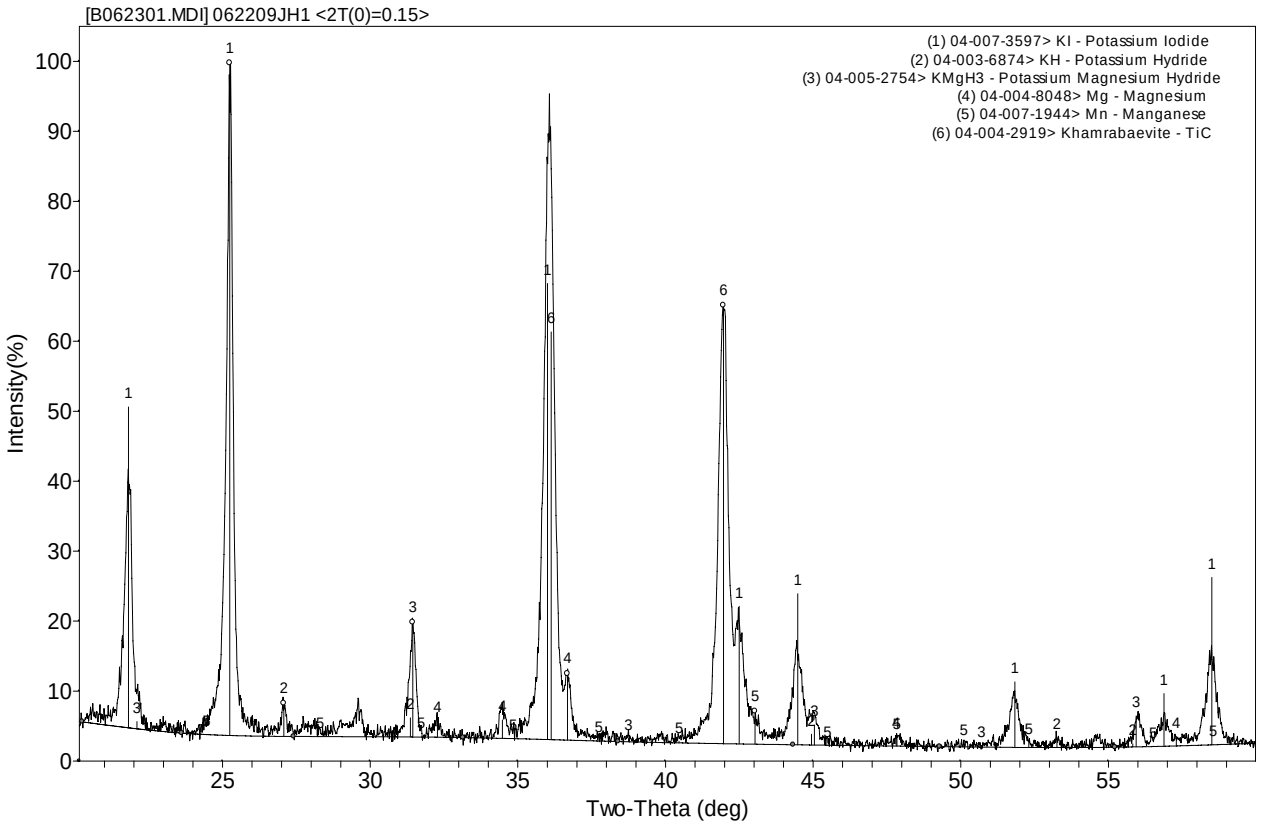

Figure 4. XRD Diffraction patterns of post-reaction sample phase identification at a commercial laboratory. Initial reactants included magnesium, manganese iodide, titanium carbide and potassium hydride.

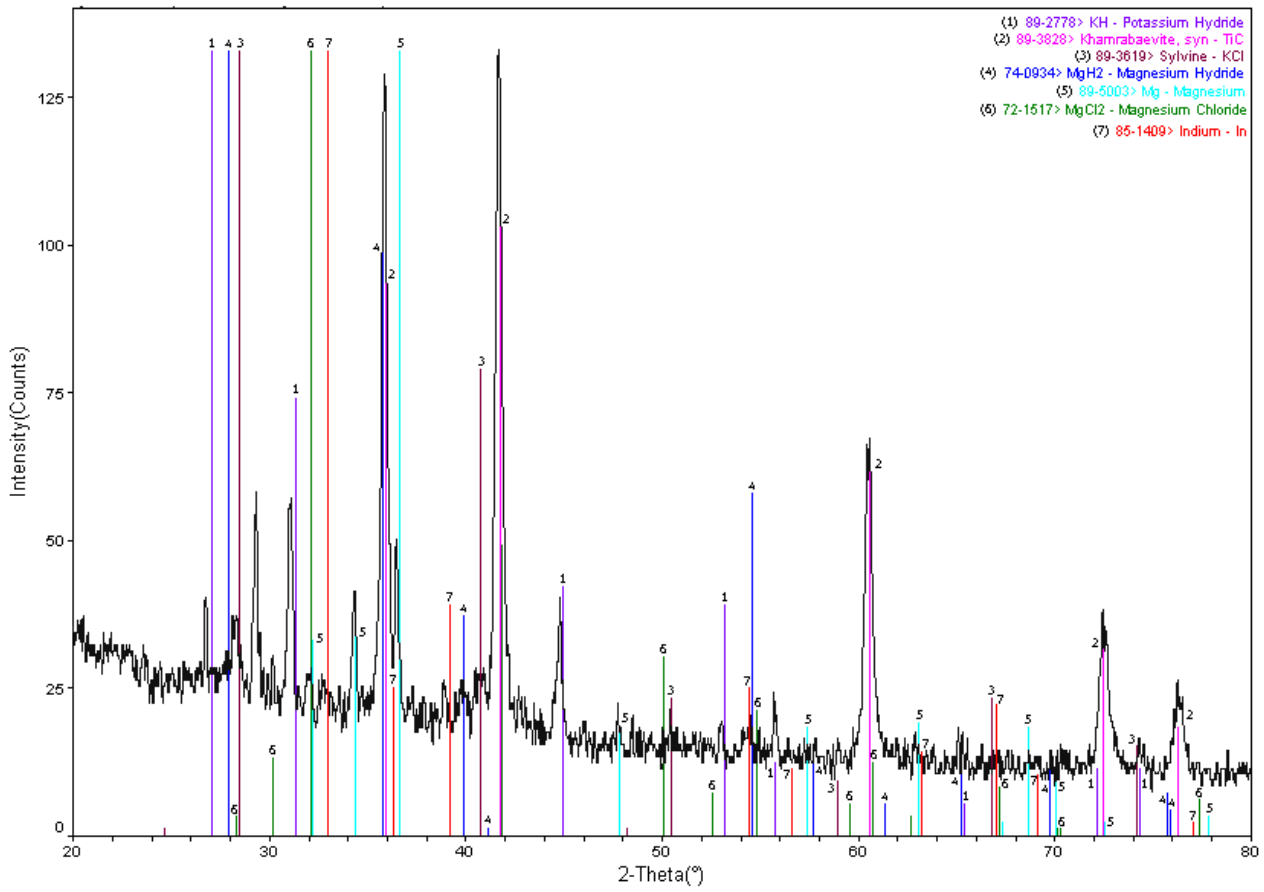

Figure 5. XRD Diffraction patterns of post-reaction sample phase identification at Rowan. Initialreactants included, KH, Mg, TiC and InCl.

Solution ^{1}H NMR characterization of post reaction products

Solution ^{1}H NMR spectrum of post reaction product involving sodium hydride, magnesium, activated carbon and SF_6 gas was extracted in DMF-d_7 solvent for at least 12 hours. Figure 6 shows the ^{1}H NMR spectra of the solution obtained. A singlet at 8.03 ppm and two quintets centered at 2.92 ppm, and 2.74 ppm are from the solvent. There was a clear additional large upfield shifted peak at -3.85 ppm, which was not due to the solvent. BLP has previously attributed the upfield shifted peaks at -3.85 ppm to $H^-(1/4)$. This upfield shifted NMR peak had been observed by us, in our compounds in reactions involving hydrogen gas in presence of catalyst and an alkaline salt at high temperature. BLP has attributed this ^{1}H NMR peak to the formation of hydrino hydride, $H^-(1/4)$ in the reaction.

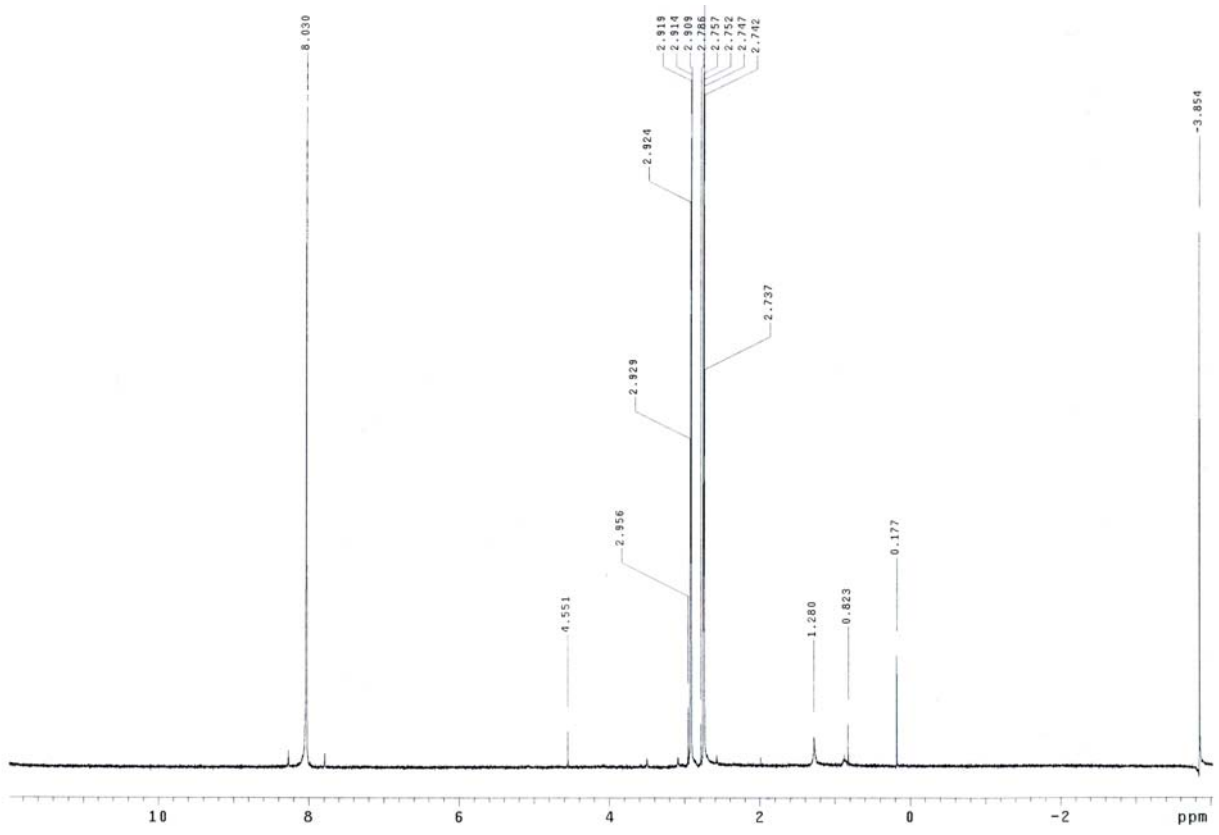

Figure 6. Liquid ^{1}H NMR spectrum of an extract of a post reaction sample containing $NaH+MgH_2+SF_6$+activated carbon in DMF-d_7 solvent.

Energy related discussions

Reactions involving manganese iodide, potassium hydride, magnesium and titanium carbide conducted at Rowan.

XRD of the chemical reactions above can help to propose the most probable reaction occuring. It is also possible to estimate the energy accompanying the reaction based on the products observed. The reaction below is the most exothermic known reaction possible.

$MnI_2(c) + 2KH(c) + Mg(c) = 2KI(c) + Mn(c) + MgH_2(c)$, ΔH = -373.00kJ/mole MnI_2.

The theoretical maximum conventional chemical reaction energy expected is -373.00 kJ per mole of MnI_2[MnI_2 is the limiting reagent in our trials].

For a 50X reactor, the calorimetric data (061809) showed that 0.5 moles of MnI_2 used generated 336 kJ of energy. This indicates that the energy observed was 1.8 times that theoretically possible by the conventional reaction above.

Three 5X reactors generated 45.0 kJ (062309), 46.8 kJ (062909) and 43.0 kJ (063009) excess energy which translated to 900 kJ/mole, 936 kJ/mole and 860 kJ/mole of MnI_2 respectively. This output is about 2.5 times more than that expected for known reactions. BLP has reported a value of 2.6 times more energy than that from known reactions. To rule out the presence of any oxide/carbonate, careful TPD studies were conducted on MnI_2 andTiC. From the TPD results the amount of water/CO_2/CO responsible for the formation of oxide/carbonate is negligible (see Appendix C).

Reactions involving 99% pure nickel bromide (109.5g), sodium hydride (50.0g), magnesium (50.0g) and carbon support (200g) performed at BLP.

The reaction conducted by BLP-personnel in presence of Rowan staff. For the 50X reaction and based on the products observed, the most exothermic reaction is given below.

$NiBr_2(c) + 2NaH(c) + 3Mg(c) = 2NaBr(c) + Mg_2Ni(c) + MgH_2(c)$ ΔH= -524.70kJ/mol $NiBr_2$

The calorimetric data (052909) also showed the energy generated during the reaction was 2.2 times that expected theoretically.

Reactions involving silver chloride (7.2g), potassium hydride (8.3g), magnesium (5.0g) and activated carbon (20.0g) conducted at Rowan.

The most exothermic reaction for the 5X reaction based on the products observed, is given below (XRD spectra in Appendix E).

$AgCl(c) + KH(c) + 0.5Mg(c) = KCl(c) + Ag(c) + 0.5MgH_2(c)$ ΔH= -289.44kJ/mol AgCl

The calorimetric data (070809) also showed that an average of 2.3 times the expected energy was generated.

Reactions involving sulphur hexaflouride (0.03 mol), sodium hydride (5.0g), magnesium hydride (5.0g) and activated carbon (20.0 g) conducted at Rowan.

The most exothermic reaction for the 5X reaction based on the products observed, is given below (XRD spectra in Appendix E) .

$SF_6(g) + 2NaH(c) + 3MgH_2(c) + 2C(s) = 2NaMgF_3(c) + 2CH_4(g) + MgS(c)$ ΔH= -2,369.22 kJ/mol SF_6

The calorimetric data also showed that an average of 1.2–1.5 times the expected energy was generated.

Reactions involving potassium hydride (8.3g), magnesium (5.0g), titanium carbide (20g) and indium chloride (7.5g) conducted at Rowan.

The most exothermic reaction for the 5X reaction based on the products observed, is given below (XRD spectra in Appendix E).

$InCl(c) + KH(c) + 0.5Mg(c) = KCl(c) + In(c) + 0.5MgH_2(c)$ ΔH= -230.15 kJ/mol InCl

The average calorimetric data showed that an average of 2.05 times the expected energy was generated.

Reactions involving potassium hydride (7.47g), magnesium (4.5g), titanium carbide (18g) and europium bromide (14.04g) conducted at Rowan.

The most exothermic reaction for the 5X reaction based on the products observed, is given below (XRD spectra in Appendix E).

$EuBr_2(c) + 2KH(c) = 2KBr(c) + EuH_2(c)$ ΔH= -136.55 kJ/mol $EuBr_2$

The average calorimetric data showed that an average of 6.5 times the expected energy was generated. Based on the XRD results, the corresponding reaction was endothermic, indicating an infinite gain relative to the observed chemical reactions.

Reactions involving potassium hydride (8.3g), magnesium (5.0g), titanium carbide (20g) and iron bromide (10.8 g) conducted at BLP in the presence of Dr. Peter Jansen.

For the 5X reaction and based on the products observed, the most exothermic reaction is given below.

$FeBr_2(c) + 2KH(c) + Mg(c) = 2KBr(c) + Fe(c) + MgH_2(c)$ ΔH= -497.7 kJ/mol $FeBr_2$

The average calorimetric data (062309) showed that an average of 1.84 times more energy than expected was generated.

Reactions involving potassium hydride (8.3g), magnesium (5.0g), titanium carbide (20g) and cobalt iodide (15.65 g) conducted at Rowan.

For the 5X reaction and based on the products observed, the most exothermic reaction is given below.

$CoI_2(c) + 2KH(c) + Mg(c) = 2KI(c) + Co(c) + MgH_2(c)$ ΔH= -527.0 kJ/mol CoI_2

The average calorimetric data (070609) showed that an average of 1.58 times more energy than expected was generated.

Reactions involving potassium hydride (8.3g), magnesium (5.0g), titanium carbide (20g) and tin iodide (18.5 g) conducted at Rowan.

For the 5X reaction and based on the products observed, the most exothermic reaction is given below

$SnI_2(c) + 2KH(c) + 3Mg(c) = 2KI(c) + Mg_2Sn(c) + MgH_2(c)$ ΔH= -552.8 kJ/mol SnI_2

The average calorimetric data (071609) showed that an average of 1.66 times more energy than expected was generated.

Reactions involving sodium hydride (5.0g), calcium (5.0g), activated carbon carbide (20g) and manganese iodide (15.45 g) conducted at Rowan.

For the 5X reaction and based on the products observed, the most exothermic reaction is given below:

$MnI_2(c) + Ca(c) + 2NaH(c) = 2NaI(c) + CaH_2(c) + Mn(c)$ ΔH= -402.0 kJ/mol MnI_2

The average calorimetric data (072409) showed that an average of 1.74 times more energy than expected was generated.

Summary

During the current reporting period we have investigated the chemistry and thermodynamics of the reaction mixtures containing AH (A = Na or K), Mg and , several halides on various supports. The alkali metal hydrides served the dual role of catalyst and hydrogen source. Both metal halides such as, $NiBr_2$, MnI_2, AgCl, EuBr, $FeBr_2$, InCl and non-metal halide SF_6 were tested for the reaction. The presence of calcium or magnesium metal powder, the metal halide and a support material were essential for the progress of the reaction. Typically, the reaction mixtures were loaded and heated in a cell to initiate the reaction. All manipulations were carried out in the Ar-filled drybox. The reaction products were characterized initially using XRD. The chemical identity of the products from the XRD studies were used in writing the reaction scheme. In several of the runs the products were mainly magnesium hydride, the metal of the metal halide reactant, and an alkali halide salt. There was no evidence of crystalline metal halide in the final product, indicating its complete consumption. Calorimetric studies indicated the release of energy far in excess of what is predicted based on the elementary thermodynamic calculations. Products of the reaction mixture containing NaH, MgH_2, activated carbon, and SF_6 indicated the presence of "hydrino" species by use of liquid ^1H NMR.

TPD results on the starting materials indicate that there was no water or oxides of carbon present. The absence of detectable amount of metal oxides in the XRD patterns of the products further rules out the possibility of a reaction between water and reactive metals. Although we have not concluded our work in the area of characterization, the presence of the new forms of lower energy hydrogen "hydrino" observed in our previous report may be responsible for these higher than expected energy gains observed.

In conclusion, the experimental work carried out at Rowan University in the Departments of Engineering and Chemistry confirms independently the empirical findings of BLP with respect to anomalous heat generation and chemical analysis. BLP attributes the anomalous heat generated to the formation of an unusual state of hydrogen during these reactions, what they have named 'hydrinos'.

Appendix Section:

Appendix A

CH_4 Quantification

CH_4 Control			
Pressure (T)	Area		
8.3	22682.8		
15.6	44624.7		
20.3	59342.5		
28.1	87465.5		
		y=3267.1x - 5524.1	
	CH_4		
P (T)	Area	Calculated Area	%
13.8	6064.4	39561.88	15.33
20.8	10110	62431.58	16.19
		Av:	15.76

CH_4 content in the gas is about 16%.

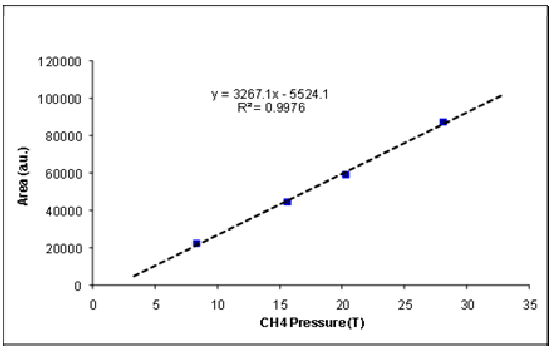

CH_4 calibration linear relationship of GC responding area vs pressure (with same sampling volume)

Appendix B

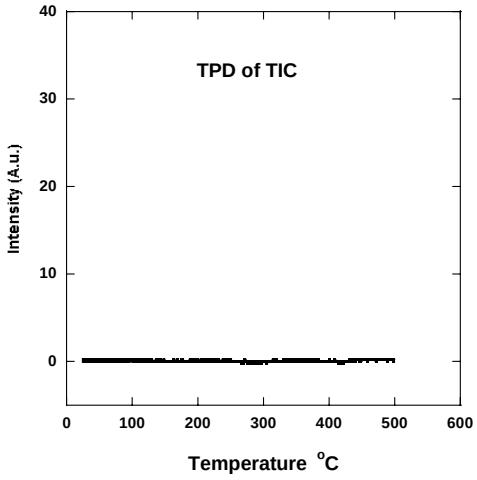

TPD (temperature-program desorption) of TiC

Appendix C

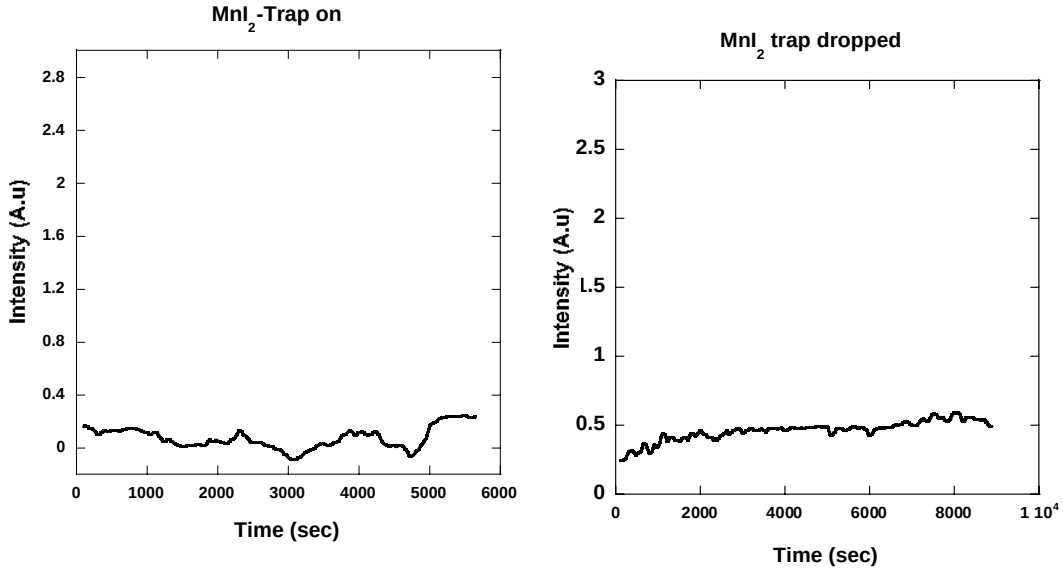

TPD (temperature-program desorption) was performed by trapping gases from heated MnI_2 using a cold trap and then dropping the trap to evaporate the condensed gas.

Appendix D

Sample	**RT** (oC)	**P** (T)	**Volume** (mL)	**Weight** (g)	**N (mole)**	**N (mole/g)**
TiC	23.61	2.37	314.3	0.508	4.025E-05	7.923E-05
MnI_2	23.4	1.5	314.3	0.54	2.549E-05	4.721E-05

Appendix E

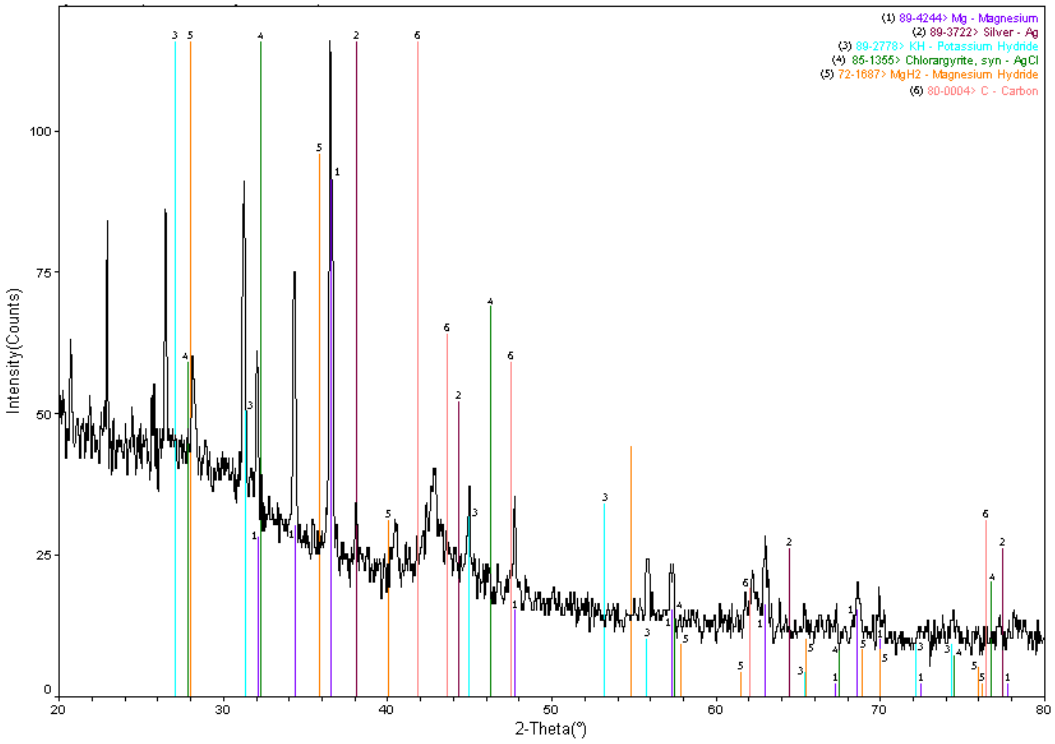

Initial reactants include potassium hydride, magnesium, activated carbon and silver chloride.

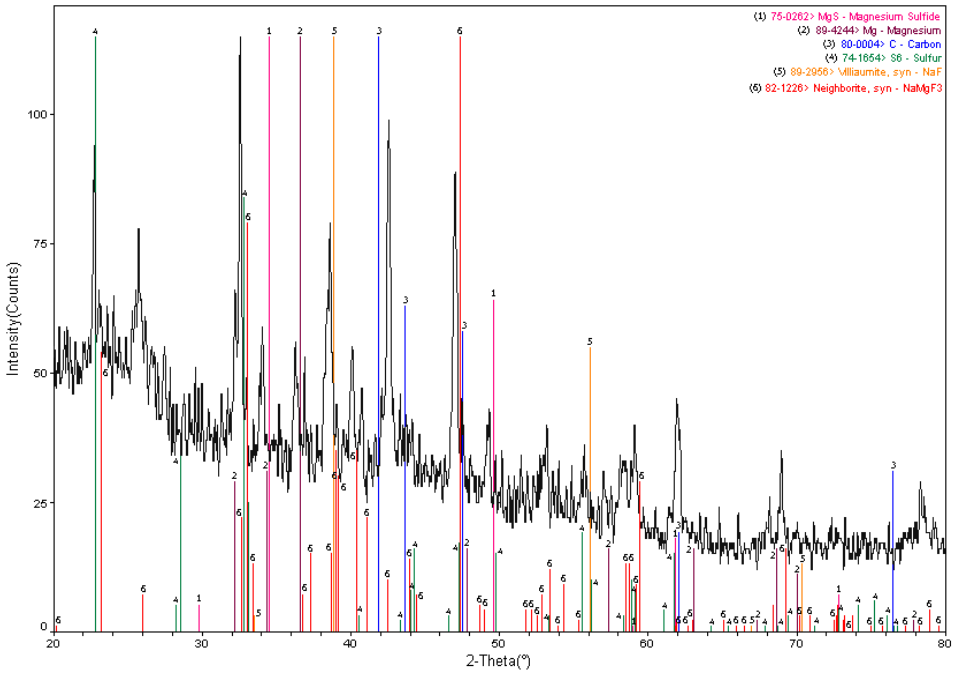

Initial reactants include sodium hydride, magnesium hydride, activated carbon and sulfur (VI) fluoride.

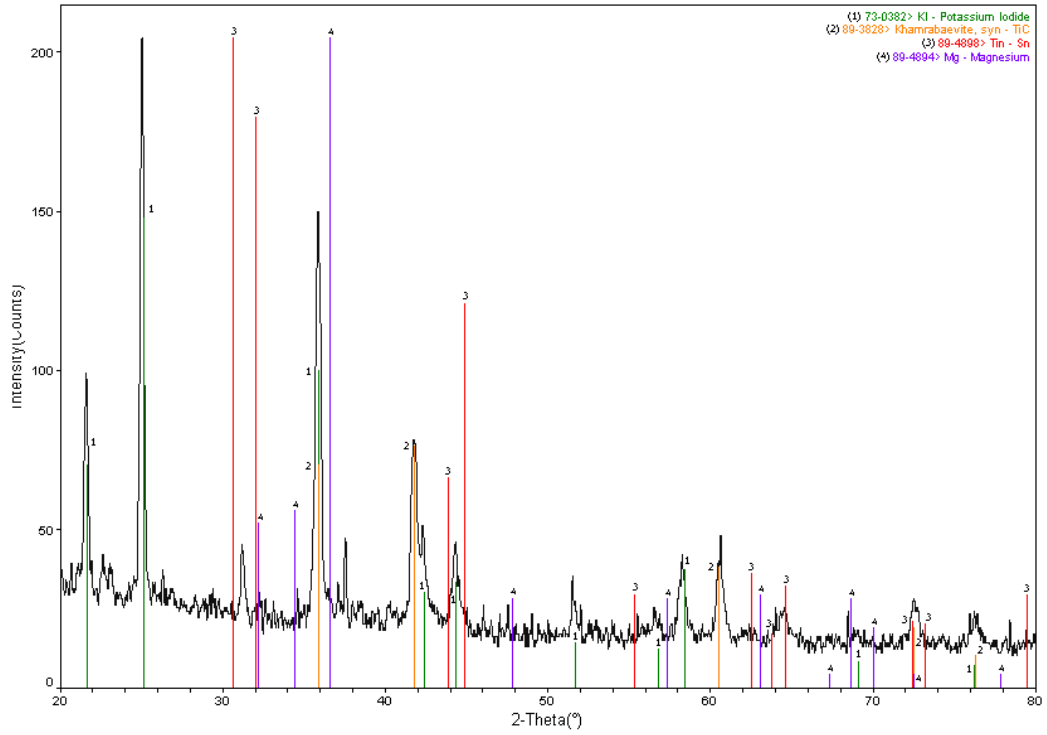

Initial reactants include potassium hydride, magnesium, titanium carbide and tin (II) iodide.

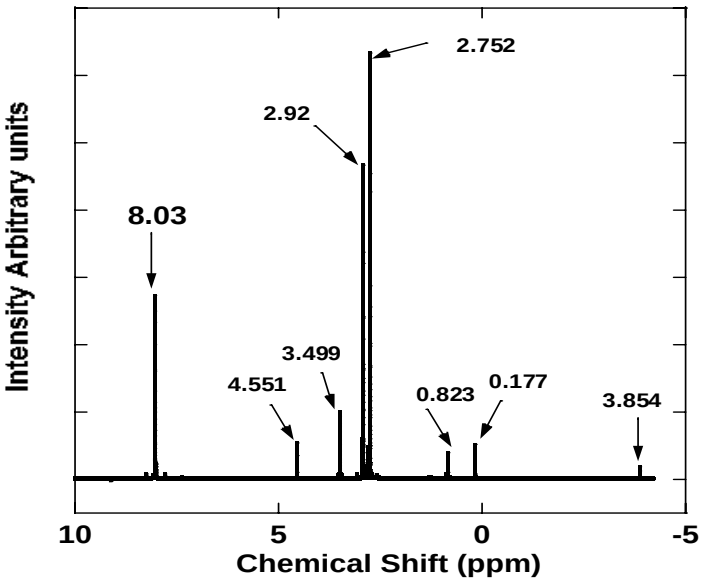

Liquid ^{1}H NMR spectrum of an extract of a post reaction sample containing $NaH+MgH_2+SF_6+$ activated carbon in DMF-d_7 solvent.

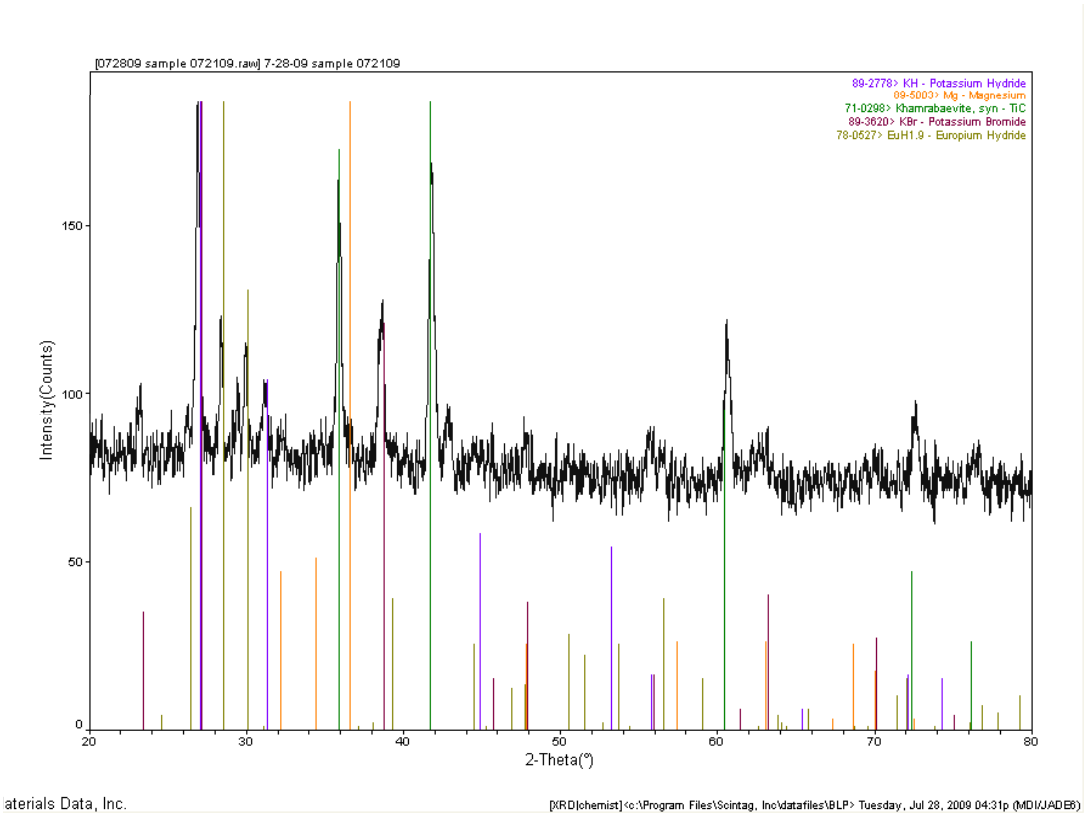

Initial reactants include potassium hydride, magnesium, activated carbon and europium bromide.

Anomalous Heat Gains from Multiple Chemical Mixtures:

Analytical Studies of "Generation 2" Chemistries of BlackLight Power Corporation

Rowan University Faculty & Staff:

Dr. Peter Mark Jansson, PP PE
Prof. Amos Mugweru
Prof. K.V. Ramanujachary
Heather Peterson, BSCh

Rowan University Students:

Ulrich K.W. Schwabe, BSECE
Kevin Bellomo-Whitten
Pavlo Kostetskyy
John Kong
Eric Smith

10 August 2009

Contents

Executive Summary

BlackLight Power (BLP) of Cranbury, NJ has been developing multiple chemical reactions that they believe create favorable conditions to provide catalysts and reaction conditions needed to relax the hydrogen atom below its widely accepted ground state. Through these reactions BLP claims they are capable of generating a significant quantity of heat from the energy released. In order to test and validate these claims, a team of engineering and chemistry professors and students at Rowan University have been independently conducting testing of the equipment and chemicals used by BLP in Rowan University laboratory facilities at Science Hall and the South Jersey Technology Park. This report specifically focuses on the details of the most recent testing (May – July 2009), which involves several different chemistries, performed in over 20 heat releasing runs during the three month period. The testing is a continuation of previous work commenced in the Spring of 2008 when Rowan University independently verified the calibration accuracy and testing protocols of the BLP measurement system and anomalous heat generation using BLP's proprietary catalysts. One 50X (0.5 moles) metal halide scale heat run and nearly 20 5X (0.05 moles) metal halide scale heat runs were performed using ten (10) different chemical mixtures. In addition, Rowan validators witnessed the loading and unloading of two additional 5X scale runs and a 50X scale run at BLP labs. The detailed chemical combinations are fully disclosed herein and include mixtures consisting of potassium hydride, sodium hydride, magnesium, calcium, titanium carbide, manganese iodide and other chemicals detailed in Table 1.

What is most significant about this new work is that our Rowan University (RU) team was able to consistently generate anomalous heat through these reactions in our South Jersey Technology Park calorimeter laboratory in quantities ranging from 1.2 times to 6.5 times the maximum theoretical heat available through known exothermic reactions. Also, we were able to procure the chemicals used in the reactions from normal chemical suppliers (e.g. Alfa Aesar and Sigma Aldrich). Of particular import is that the specific quantities and mixtures of reaction chemicals are fully disclosed in this document (See Tables 1 and 4). This significant disclosure by BLP now presented for the first time in this report makes it possible for any laboratory with a nominally accurate calorimetry system (1-3% error) to demonstrate the repeatability of these reactions which produce anomalous heat regularly in our university laboratory. Finally, the scientists of the Rowan University Chemistry and Biochemistry Department have analyzed the reaction products and are confident that the procedures we have followed and chemicals we have procured and reacted are not capable of generating the quantities of heat we have observed. They have also reproduced BLP tests which identify a novel form of hydrogen as a potential explanation of the additional heat evolved.

Introduction

The primary aim of this work was to reproduce synthesis experiments and conduct calorimetry studies of BLP 'generation 2' chemistry in a continuation of prior work that involved what BLP claims is 'lower energy' hydrogen. In this work potassium hydride, sodium hydride, magnesium metal powder, titanium carbide support material and several halide salts (See Table 4 for complete list of all chemicals involved in the numerous experiments) were loaded in a cell and heated to initiate a chemical reaction. The products of the reaction including the gases generated were collected and analyzed using gas chromatography and mass spectrometry. The solid samples were analyzed using XRD and showed the presence of magnesium hydride, the metal of the metal halide reactant and an alkali halide. A small amount of magnesium halide was also observed. However the starting halide salt was absent in the products. Liquid proton NMR showed the 'hydrino hydride ion $H^-(1/4)$' upfield at -3.85 ppm and the corresponding 'molecular hydrino $H_2(1/4)$' at 1.23 ppm as predicted by Mills [R. L. Mills, G. Zhao, K. Akhtar, Z. Chang, J. He, Y. Lu, W. Good, G. Chu, B. Dhandapani, "Commercializable Power Source from Forming New States of Hydrogen," Int. J. Hydrogen Energy, Vol. 34, (2009), 573–614.]. The heat generated during these many reaction experiments was determined by carrying out detailed calorimetric studies in the Department of Engineering at their South Jersey Technology Park calorimetry laboratory. These 20 experiments indicated an average energy of 1.95 and one as high as over 6.5 that of what would be expected for the most energetic conventional chemical reaction. Temperature programmed desorption studies were used to rule out the presence of water in the starting materials. In what follows, we present the results of some of the experimental studies that were carried out.

Background

In a prior report the Department of Chemistry and Biochemistry synthesized compounds using procedures provided by BLP in a search for potential causes of the anomalous heat being generated by the reactions. In that analysis, the RU Chemistry Department was able to confirm the presence of unusual hydrogen in the reaction products using both liquid ^{1}H NMR and MAS ^{1}H NMR studies. For that study, alkaline halides were heated in presence of hydrogen and a catalyst. According to BLP, the alkali metal halide is capable of trapping the 'lower energy' or 'hydrino' hydrogen as a high binding energy hydride ion called the 'hydrino hydride' ion and as the corresponding molecular hydrino. In this report our RU research team was to focus on BLP 'generation 2' chemistries. BLP has been conducting studies with a range of chemistries that they claim to represent a new energy source that is more easily verifiable. In the chemistry tests, which RU

personnel witnessed at BLP, potassium hydride, magnesium metal powder, a support material, and metal halide were mixed and heated to initiate the reaction. Calorimetric studies as well as chemical characterizations of the reaction products were done using XRD, TPD, GC/MS techniques. We report chemical test of reactions done at Rowan with our chemicals using both 5X and 50X scale reactors. We assess possible reactions occurring along with their enthalpies, and compare the enthalpies of the anticipated reaction with the actual heat observed for both the smaller 5X reactors and the larger 50X reactor.

Chemicals and Procedures

A number of components were used in preparation of reaction cells for heat runs conducted at Rowan University. Table 1 contains a summary of the components used along with purity and supplier information.

Table 1. Component Information

Component	Purity	Supplier	Formula
Titanium Carbide	n/a	Alfa Aesar	TiC
Tin Iodide	99%	Alfa Aesar	SnI_2
Iron Bromide	98+%	Alfa Aesar	$FeBr_2$
Magnesium Metal	99.80%	Alfa Aesar	Mg
Potassium Hydride (in mineral oil)	n/a	Alfa Aesar	KH
Manganese Iodide	98%	Strem Chemicals	MnI_2
Anhydrous Hexane	≥99%	Sigma Aldrich	$CH_3(CH_2)_4CH_3$
Indium Chloride	99.995%	Alfa Aesar	InCl
Cobalt Iodide	99.5%	Alfa Aesar	CoI_2
Europium Bromide	99.99%	Alfa Aesar	$EuBr_2$
Silver Chloride	99.9%	Alfa Aesar	AgCl
Sulfur Hexafluoride	99.9%	GTS–Welco	SF_6
Calcium	98.8%	Alfa Aesar	Ca

The following is an example of how RU prepared to perform one of these studies (conducted on 18 June 2009): In preparation for the reaction, titanium carbide was first dried in a flask under a vacuum of approximately 50 mTorr at 200 ^{o}C for 14 hours and then transferred to a glove box. The potassium hydride was washed inside the glove box with anhydrous hexane four times after decanting the mineral oil. Potassium hydride was further dried in the anti-chamber of the glove box for 4 hours to remove residual hexane and other organic residues, and afterwards placed in a sealed container.

In preparation for the experiment, 83.0 grams of KH, 50.0 grams of Mg, 200.0 grams of TiC and 154.0 grams of MnI_2 were weighed and thoroughly mixed in a large beaker inside the glove box. A 2.0 liter cell was placed in a glove box, the reaction mixture was quantitatively poured into it, after which the cell was sealed in the controlled environment. The loaded cell was then taken to SJTP where the calorimetric test was performed. For a 5X cell the weight of each individual component of reaction mixture was reduced by a factor of ten. The reaction was repeated with MnI_2 replaced by $FeBr_2$, InCl, CoI_2, SnI_2 and $EuBr_2$. In further reaction mixtures activated carbon (AC) replaced TiC and AgCl or SF_6 replaced MnI_2.

Temperature programmed desorption studies (TPD)

The analysis was performed using a Chembet 3000 chemisorption unit of Quantchrome corporation with a Thermal conductivity detector (TCD). The initial task of this phase of analysis was to quantify the water present, if any, in the starting materials. Argon was used as a carrier gas and dry ice was used for the separation of water [by condensation] during the course of desorption experiments. Approximately 0.1 grams of the sample was loaded into a TPD cell in an argon environment, the cell was then placed in a thermal heater and connected to a gas line (including stainless steel tubing and reservoir). Any condensed water would be carried into the TCD analyzer when the dry ice dewar was removed and the trap was warmed to room temperature. Appendix A shows the TPD trace for the starting materials (TiC and MnI_2) suggesting a negligible amount of condensable gas such as water and CO_2 present in the materials.

An independent TPD analysis was also performed using the ideal gas law. Approximately 0.1 grams of the starting chemical sample was loaded into a TPD cell under argon, the cell was then placed in a thermal heater and connected to a gas line (including stainless steel tubing and reservoir). Before heating, the sample and gas lines were evacuated to ~10^{-5} Torr of pressure. The cell was then heated slowly to roughly 500 ^{o}C in order to desorb all of the water present in the sample. The evolved gas was expanded into a reservoir of known volume. The gas line was then submerged into a liquid nitrogen dewar in order to condense any water vapor or other gas(es) present from the thermal desorption. After evacuating the noncondensable gases, the cold trap was removed to allow the reservoir to reach room temperature and evaporate any condensed gas with temperature increases. In the experiment, cell temperature, room temperature, and gas pressure were monitored and recorded by the Labview program.

The quantity of gas obtained was calculated using the ideal gas law (Equation 1) using the measured pressure, temperature and volume.

$$PV = nRT \quad (1)$$

The results of the TPD of the TiC and MnI_2 starting materials are given in Appendix A. Since liquid nitrogen was used as the cold trap, any gas with a boiling point temperature above -196 ^{o}C would have been condensed. As shown, the total condensable gas was negligible; thus, the material contained minute quantities of H_2O (and/or CO_2 and CO) from both TiC and MnI_2. Their contribution to the heat energy of the reaction was considered to be small enough to be negligible in the heat balance calculations.

Analysis of reaction products

Before collecting the gas for MS and GC analysis, the pressure and volume of the gas in the reactor was measured by connecting the reactor to a pre-evacuated reservoir of known volume that had a pressure gauge. Using the known combined volume, measured pressure and temperature, the moles of gas were determined using the ideal gas law. Room temperature was also recorded. The gas from the reaction was then collected in an empty cell for mass spectroscopic identification and quantitative gas chromatography. Gas chromatography (GC) showed that most of the gas generated during the reaction was methane. Figure 1 below shows a GC chromatogram of the gases generated during the reaction. Argon is present due to cell loading being done in an argon environment of a glove box. The gas was directly injected into a GC via a six-port rotary valve, which was connected to the gas line right before the injector. Prior to the gas sample addition, the sample loop (~3 ml) in the six-port rotary valve was sufficiently evacuated (~10E-5 Torr) to remove any residual gases and contaminants. The oven temperature was set to 80 ^{o}C, the injector to 100 ^{o}C, and the detector to 120 ^{o}C. Helium at a flow rate of 43.4 ml/min was chosen as a carrier gas. Calibrations using pure H_2, CH_4, CO, and CO_2 were performed prior to testing. Figure 2 shows an MS spectrum of gas generated during the reaction. To quantify the amount of methane found in the gaseous phase, a calibration curve of methane gas was obtained (Appendix A). In the case of the reaction mixture 83g KH +50g Mg + 200g TiC + 154.5g MnI_2, a quantitative analysis of the gaseous phase indicated that 16.0% of volume of the gas produced was methane. Since the total gas pressure was about 1 atm and the volume of methane was 384 ml (2400 ml × 16%), the moles of methane in the product was 0.0158 mole (at a room temperature of 24 ^{o}C).

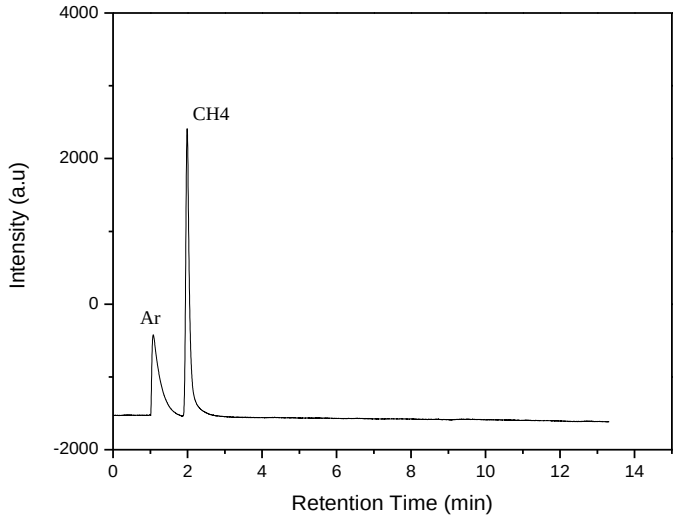

Figure 1. Gas Chromatograph of contents of gas phase generated during the reaction

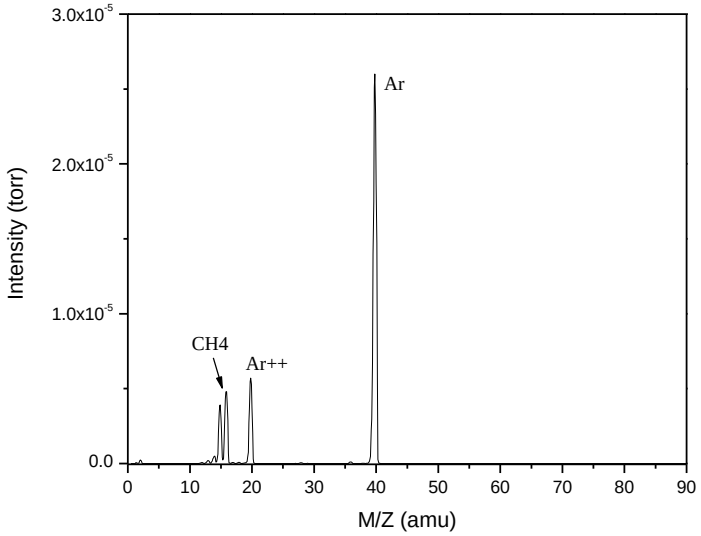

Figure 2. MS spectra of gas generated in the reaction.
Methane shows as the minor component due to cell loading in an Argon filled dry-box.

X-ray diffraction (XRD)

In this part of the work, the Department of Chemistry carried out several slow scans of post run samples from the Tech Park at RU. Diffraction patterns were recorded using the Scintag X2 Advanced Diffraction System with an operating voltage set to 40 kV and current of 30 mA. Patterns were recorded in a step mode [0.02 Deg/min] at a diffraction angle of 2θ in the range of 10-70 using a residence time of 8 seconds. The

diffraction patterns of the post reaction product of manganese iodide, potassium hydride, magnesium and titanium carbide done at Rowan is shown in Figure 3. The diffraction patterns from the library were matched to those obtained from the post-run samples. From the diffraction patterns potassium iodide, magnesium metal, manganese metal, titanium carbide and magnesium hydride were observed. The diffraction patterns obtained at Rowan and independently at a commercial testing laboratory (CTL) were similar. Figure 4 shows the diffraction patterns obtained from the CTL. Quantitative XRD from the CTL shows KH (2.6 $\pm$ 0.3 %), Mg (4.3 $\pm$ 0.4%), Mn (3.7$\pm$ 0.4%), KI (22.7 $\pm$ 0.3%), $KMgH_2$ (5.7 + 0.2%) and TiC (61.0 $\pm$ 0.8). Manganese iodide was absent from the reaction products indicating it may have been the limiting reactant. Energy calculations performed were thus based on MnI_2.

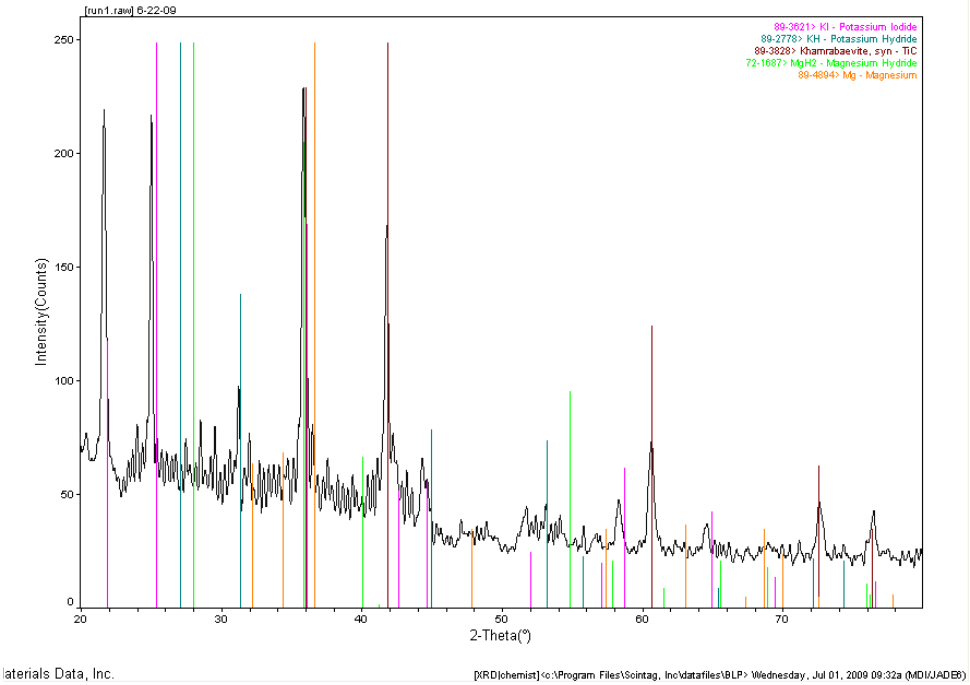

Figure 3. XRD Diffraction patterns of post-reaction sample phase identification at RU. Initial reactants included magnesium, manganese iodide, titanium carbide, and potassium hydride.

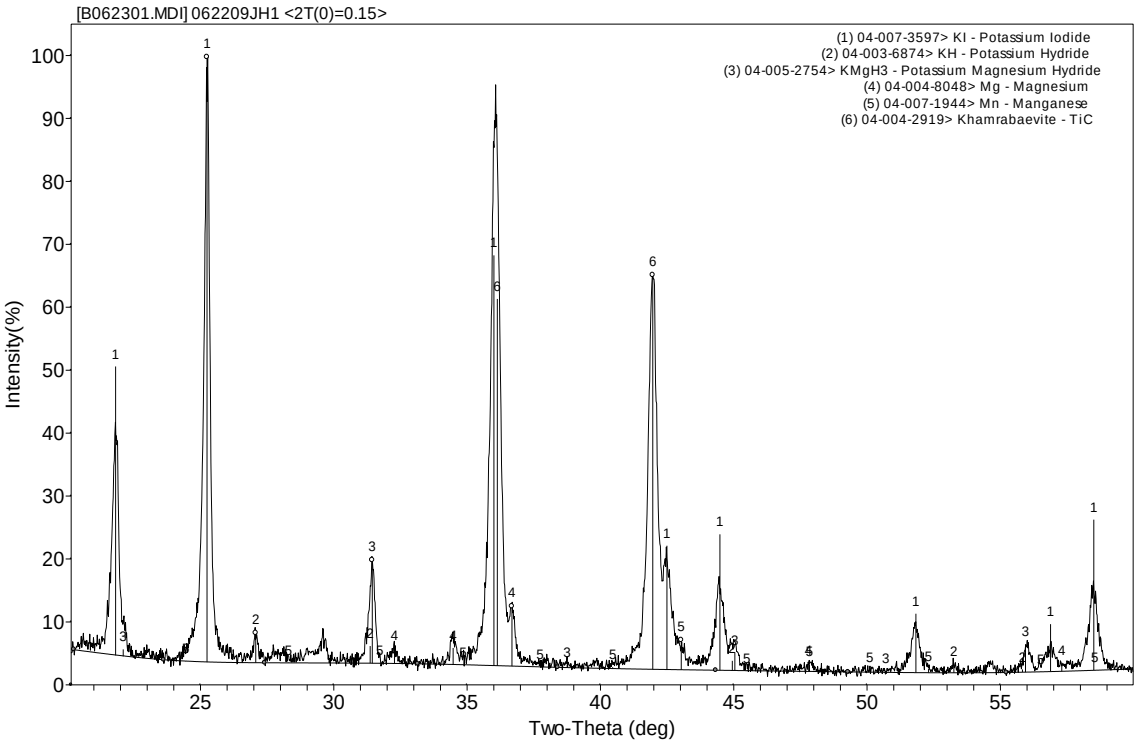

Figure 4. XRD Diffraction patterns of post-reaction sample phase identification at the CTL. Initial reactants included magnesium, manganese iodide, titanium carbide, and potassium hydride.

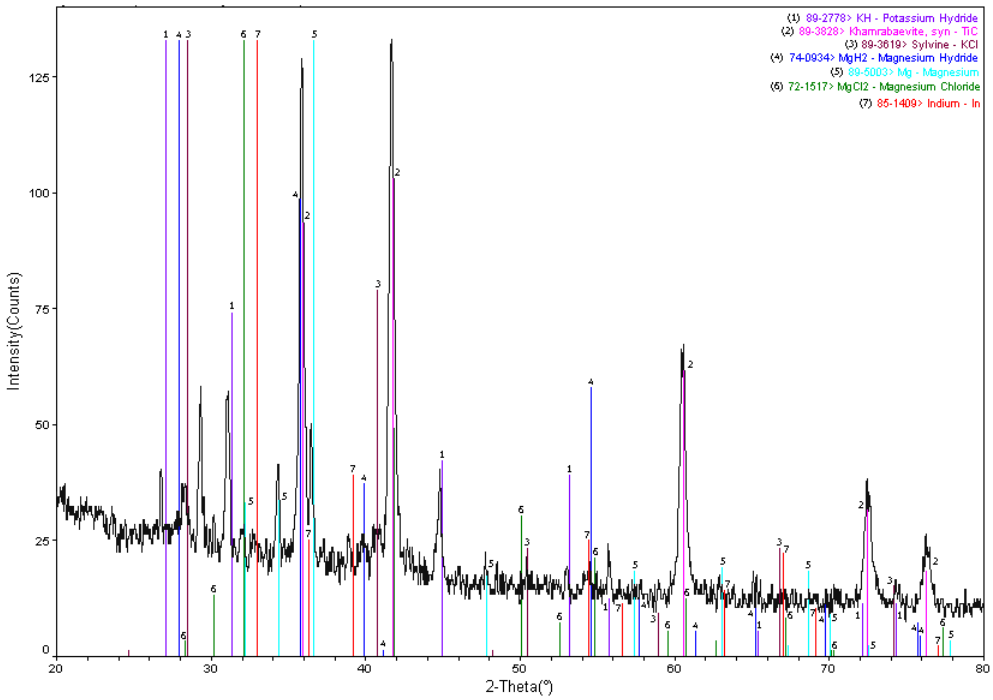

Figure 5. XRD Diffraction patterns of post-reaction sample phase identification at Rowan. Initial reactants included, KH, Mg, TiC, and InCl.

Energy related discussion

Reactions involving manganese iodide, potassium hydride, magnesium and titanium carbide conducted at Rowan.

XRD of the chemical reactions above can help to propose the most probable reactions occurring. It is also possible to estimate the energy accompanying the reaction based on the products observed. The reaction below is the most exothermic known reaction possible.

$MnI_2(c) + 2KH(c) + Mg(c) = 2KI(c) + Mn(c) + MgH_2(c)$, $\Delta H = -373.00 kJ/mole\ MnI_2$

The theoretical maximum conventional chemical reaction energy expected is -373.00 kJ per mole of MnI_2. MnI_2 is the only reactant not found in the products.

For a 50X reactor, the calorimetric data (061809) showed that 0.5 moles of MnI_2 used generated 336 kJ of energy. This indicates that the energy observed was 1.8 times that theoretically possible by the conventional reaction above.

Three 5X reactors generated 45.0 kJ (062309), 46.8 kJ (062909) and 43.0 kJ (063009) excess energy, which translated to 900 kJ/mole, 936 kJ/mole and 860 kJ/mole of MnI_2 respectively. This output is about 2.5 times more than that expected for known reactions. BLP has reported a value of 2.6 times more energy than that from known reactions. To rule out any oxide formation TPD was carried out on MnI_2 and also TiC to check the amount of H_2O, CO_2 and CO by thermal desorption. From the TPD results the amount of water/CO_2/CO present is negligible (Appendix C).

Reactions involving nickel bromide (109.5g), sodium hydride (50.0g), magnesium (50.0g) and carbon support (200g) performed at BLP.

The reaction of reagents above were conducted by BLP in presence of Rowan staff. For the 50X reaction and based on the products observed, the most exothermic reaction is given below.

$NiBr_2(c) + 2NaH(c) + 3Mg(c) = 2NaBr(c) + Mg_2Ni(c) + MgH_2(c)$ $\Delta H = -524.70 kJ/mol\ NiBr_2$

The calorimetric data (052909) also showed the energy generated during the reaction was 2.2 times that expected theoretically.

Reactions involving silver chloride (7.2g), potassium hydride (8.3g), magnesium (5.0g) and activated carbon (20.0g) conducted at Rowan.

The most exothermic reaction for the 5X reaction based on the products observed, is given below (XRD spectra in appendix E).

$AgCl(c) + KH(c) + 0.5Mg(c) = KCl(c) + Ag(c) + 0.5MgH_2(c)$ ΔH= -289.44kJ/mol AgCl

The calorimetric data (070809) also showed that an average of 2.3 times the expected energy was generated.

Reactions involving sulfur hexafluoride (0.03 mol), sodium hydride (5.0g), magnesium hydride (5.0g) and activated carbon (20.0 g) conducted at Rowan.

The most exothermic reaction for the 5X reaction based on the products observed, is given below (XRD spectra in appendix E) .

$SF_6(g) + 2NaH(c) + 3MgH_2(c) + 2C(s) = 2NaMgF_3(c) + 2CH_4(g) + MgS(c)$ ΔH= -2,369.22 kJ/mol SF_6

The calorimetric data also showed that an average of 1.2–1.5 times the expected energy was generated.

Reactions involving potassium hydride (8.3g), magnesium (5.0g) and titanium carbide (20g) and indium chloride (7.5g) conducted at Rowan.

The most exothermic reaction for the 5X reaction based on the products observed, is given below (XRD spectra in appendix E).

$InCl(c) + KH(c) + 0.5Mg(c) = KCl(c) + In(c) + 0.5MgH_2(c)$ ΔH= -230.15 kJ/mol InCl

The average calorimetric data showed that an average of 2.05 times the expected energy was generated.

Reactions involving potassium hydride (7.47g), magnesium (4.5g) and titanium carbide (18g) and europium bromide (14.04g) conducted at Rowan.

The most exothermic reaction for the 5X reaction based on the products observed, is given below (XRD spectra in appendix E).

$EuBr_2(c) + 2KH(c) = 2KBr(c) + EuH_2(c)$ $\Delta H = -136.55$ kJ/mol $EuBr_2$

The average calorimetric data showed that an average of 6.5 times the expected energy was generated. Based on the XRD results, the corresponding reaction was endothermic, indicating an infinite gain relative to the observed chemical reactions.

Reactions involving potassium hydride (8.3g), magnesium (5.0g), titanium carbide (20g) and iron bromide (10.8 g) conducted at BLP in the presence of Dr. Peter Jansen.

For the 5X reaction and based on the products observed, the most exothermic reaction is given below.

$FeBr_2(c) + 2KH(c) + Mg(c) = 2KBr(c) + Fe(c) + MgH_2(c)$ $\Delta H = -497.7$ kJ/mol $FeBr_2$

The average calorimetric data (062309) showed that an average of 1.84 times more energy than expected was generated.

Reactions involving potassium hydride (8.3g), magnesium (5.0g), titanium carbide (20g) and cobalt iodide (15.65 g) conducted at Rowan.

For the 5X reaction and based on the products observed, the most exothermic reaction is given below.

$CoI_2(c) + 2KH(c) + Mg(c) = 2KI(c) + Co(c) + MgH_2(c)$ $\Delta H = -527.0$ kJ/mol CoI_2

The average calorimetric data (070609) showed that an average of 1.58 times more energy than expected was generated.

Reactions involving potassium hydride (8.3g), magnesium (5.0g), titanium carbide (20g) and tin iodide (18.5 g) conducted at Rowan.

For the 5X reaction and based on the products observed, the most exothermic reaction is given below

$SnI_2(c) + 2KH(c) + 3Mg(c) = 2KI(c) + Mg_2Sn(c) + MgH_2(c)$ $\Delta H = -552.8$ kJ/mol SnI_2

The average calorimetric data (071609) showed that an average of 1.66 times more energy than expected was generated.

Reactions involving sodium hydride (5.0g), calcium (5.0g), activated carbon carbide (20g) and manganese iodide (15.45 g) conducted at Rowan.

For the 5X reaction and based on the products observed, the most exothermic reaction is given below:

$MnI_2(c) + Ca(c) + 2NaH(c) = 2NaI(c) + CaH_2(c) + Mn(c)$ ΔH= -402.0 kJ/mol MnI_2

The average calorimetric data (072409) showed that an average of 1.74 times more energy than expected was generated.

Calorimetry

A continuous water flow calorimeter was used as part of the experimental setup. In order to ensure valid experimental results from exothermic heat runs a series of calibrations were conducted using both the 1kW and 50kW systems. All of the experiments performed strictly followed the experimental procedures written specifically for each cell type. A detailed procedure write-up can be found in previously submitted reports. A series of calibrations were performed for both cell types from early May 2009 through the present time. Nearly all of the results obtained were well within the accepted coupling range (1-3% error) with a few exceptions that could be attributed to equipment malfunction and errors in experimental procedure. A summary of these calibrations has been provided in Table 2.

Table 2. Summary of Small Cell Calibrations

Run	Date	Input	Output (kJ)	ΔE (kJ)	% Difference	Coupling
1	5/13/2009	149.52	147.56	-1.96	-1.31%	98.69%
2	5/20/2009	150.36	149.39	-0.98	-0.65%	99.35%
3	5/22/2009	200.50	197.16	-3.35	-1.67%	98.33%
4	5/26/2009	127.46	124.32	-3.15	-2.47%	97.53%
5	5/27/2009	240.73	239.28	-1.45	-0.60%	99.40%
6	5/28/2009	149.69	148.58	-1.12	-0.75%	99.25%
7	5/29/2009	152.57	151.72	-0.84	-0.55%	99.45%
8	6/2/2009	149.74	149.33	-0.41	-0.27%	99.73%
9	6/28/2009	120.17	119.29	-0.88	-0.73%	99.27%
10	7/1/2009	140.19	139.10	-1.09	-0.78%	99.22%
11	7/5/2009	179.44	179.07	-0.37	-0.21%	99.79%
12	7/14/2009	268.78	265.31	-3.48	-1.29%	98.71%
13	7/15/2009	230.66	228.13	-2.52	-1.09%	98.91%
14	7/20/2009	199.25	198.73	-0.52	-0.26%	99.74%
15	7/27/2009	199.67	198.49	-1.17	-0.59%	99.41%
16	7/28/2009	199.23	198.69	-0.55	-0.27%	99.73%

Calibrations were performed frequently and the results obtained can be observed in Appendices B and C. Detailed graphical analysis of the small cell calibrations can be seen in Appendix B.

A summary of large cell calibrations is contained in Table 3 below. The results obtained from data analysis using Matlab software were within acceptable ranges. The percent difference between input and output energies was between 1.0 and 3.0 percent. These calibrations were, on average, higher than their smaller cell counterparts, an anomaly which can be attributed to the necessity for significantly lengthier cool down periods that allowed for higher losses to the surroundings.

Table 3. Summary of Large Cell Calibrations

Run	Date	Input	Output (kJ)	ΔE (kJ)	% Difference	Coupling
1	6/10/2009	1452.59	1425.85	-26.74	-1.84%	98.20%
2	6/11/2009	899.03	888.22	-10.81	-1.20%	98.80%
3	6/12/2009	776.40	763.04	-13.36	-1.72%	98.28%
4	6/24/2009	1401.19	1360.74	-40.45	-2.89%	97.11%
5	6/26/2009	1203.16	1173.96	-29.20	-2.43%	97.57%

Several heat runs were also conducted using different component mixtures as reactants. The compositions and quantities of the reactant mixtures were discussed in further detail in the chemistry section. All of the heat runs conducted at SJTP coincided well with those obtained from heat runs conducted at BLP. A summary of the heat run results can be found in Table 4. Figures obtained from Matlab analysis of the heat run data can be found in Appendices D and E.

Table 4. Heat Run Summary

Date	Chemical Composition	Input (kJ)	Output (kJ)	ΔE (kJ)	Max Theoretical Energy (kJ)	Energy Gain (ΔE/Max. Theoretical Energy)
5/29/2009	50.0 g NaH + 50 g Mg + 200 g AC + 109.5 g $NiBr_2$ (BLP SITE) Amos/Chari	1990.00	2567.00	577.00	262	2.2
6/18/2009	83 g KH + 50.0 g Mg + 200.0 g TiC + 154.5 g MnI_2	715.28	1051.92	336.60	186	1.8
6/23/2009	8.3 g KH + 5.0 g Mg + 20.0 g TiC + 15.45 g MnI_2(BLP SITE) Peter/Kevin	292.00	337.00	45.00	18.6	2.4
6/23/2009	8.3 g KH + 5.0 g Mg + 20.0 g TiC + 10.8 g $FeBr_2$ (BLP SITE) Peter/Kevin	308.00	354.00	46.00	24.9	1.84
6/29/2009	8.3 g KH + 5.0 g Mg + 20.0 g TiC + 15.45 g MnI_2	252.74	299.63	46.89	18.6	2.52
6/30/2009	8.3 g KH + 5.0 g Mg + 20.0 g TiC + 15.45 g MnI_2	287.82	330.83	43.00	18.6	2.31
7/2/2009	8.3 g KH + 5.0 g Mg + 20.0 g TiC + 7.5 g InCl	243.94	266.98	23.04	11.5	2.0
7/3/2009	8.3 g KH + 5.0 g Mg + 20.0 g TiC + 7.5 g InCl	269.97	294.43	24.46	11.5	2.12
7/6/2009	8.3 g KH + 5.0 g Mg + 20.0 g TiC + 15.65 g CoI_2	240.11	281.93	41.81	26.35	1.58
7/8/2009	8.3 g KH + 5.0 g Mg + 20.0 g AC + 7.2 g AgCl	487.24	521.41	34.17	14.52	2.35
7/9/2009	8.3 g KH + 5.0 g Mg + 20.0 g AC + 7.2 g AgCl	357.07	382.56	25.48	14.52	1.75
7/10/2009	5.0 g NaH + 5.0 g MgH_2 + 20.0 g AC + 0.03 mole of SF_6 Online	217.06	301.46	84.40	71 (0.03 mole SF_6)	1.2
7/13/2009	5.0 g NaH + 5.0 g MgH_2 + 20.0 g AC + 0.03 mole of SF_6 Online	177.69	282.66	104.97	71 (0.03 mole SF_6)	1.5
7/16/2009	8.3 g KH + 5.0 g Mg + 20.0 g TiC + 18.5 g SnI_2	199.86	245.85	45.99	27.6	1.66
7/21/2009	7.47 g KH + 4.5 g Mg + 18.0 g TiC + 14.04 g $EuBr_2$	321.17	361.77	40.60	6.16	6.5
7/23/2009	5.0 g NaH + 5.0 g Ca + 20.0 g AC + 15.45 g MnI_2	336.56	388.61	52.05	29.5	1.76
7/24/2009	5.0 g NaH + 5.0 g Ca + 20.0 g AC + 15.45 g MnI_2	346.88	398.29	51.41	29.5	1.74
7/25/2009	5.0 g NaH + 5.0 g MgH_2 + 20.0 g AC + 0.03 mole of SF_6 Online	252.77	349.29	96.53	71 (0.03 mole SF_6)	1.37

Conclusion

The scientific investigations completed at Rowan University make it quite clear that there is a source of heat being generated in these numerous chemical reactions that cannot be explained in the confines of conventional modern chemistry. Dozens of calibrations on both the 5X and 50X calorimeter cells have given our research team confidence that there is but a small error in the water flow calorimetry, (having coupling efficiencies averaging above 98%). In all cases the heat gains observed are many multiples greater than any potential inaccuracies of our measurement system. The chemical analyses completed by RU chemists have been performed on all the heat runs reported herein for both 5X and 50X scale reactions. These studies show repeatedly that the amount of heat generated in the reactions exceed known conventional chemical reaction pathways. Many additional studies by the Department of Chemistry indicate that an anomalous signature of a novel form of hydrogen (called “hydrino” by BLP) has been observed during characterization of the products. In addition to the dozens of experiments completed to date on BLP technology at the South Jersey Technology Park, several validation runs have also been observed at BLP by Rowan University professors and students. From this plethora of data our conclusion is that some novel reaction is causing large releases of excess energy as BLP contends. It is the sincere hope of the research team at Rowan University that other research laboratories across the world will find confidence from our results to begin reproducing these experiments for themselves.

This report has revealed BLP proprietary recipes that demonstrate consistent heat gains from what their scientists state are the result of the formation of lower energy hydrogen. While this initial analysis is not intended to conclusively validate BLP’s lower energy hydrogen hypothesis our conclusions clearly are not in conflict with it. We encourage the scientific community to replicate our experiments and seek to understand with us if there are any alternative explanations for these consistent experimental results. This report (combined with others published in journals or on the web) provides sufficient detail to enable a reasonably equipped research lab to immediately validate and critique our findings.

Appendix A – Chemistry Information

CH_4 Quantification

CH_4 Control			
Pressure (T)	Area		
8.3	22682.8		
15.6	44624.7		
20.3	59342.5		
28.1	87465.5		
		y=3267.1x - 5524.1	
	CH_4		
P (T)	Area	Calculated Area	%
13.8	6064.4	39561.88	15.33
20.8	10110	62431.58	16.19
		Av:	15.76

CH_4 content in the gas is about 16%.

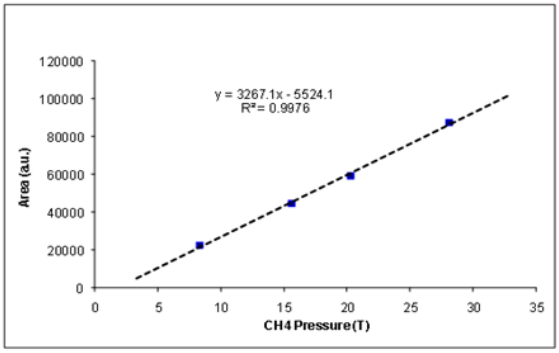

CH_4 calibration: linear relationship of GC responding area vs pressure (with same sampling volume)

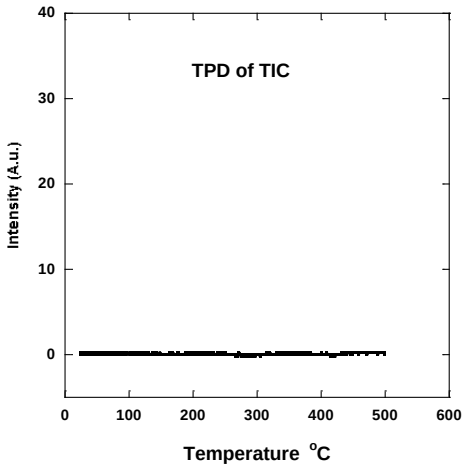

TPD (temperature-program desorption) of TiC

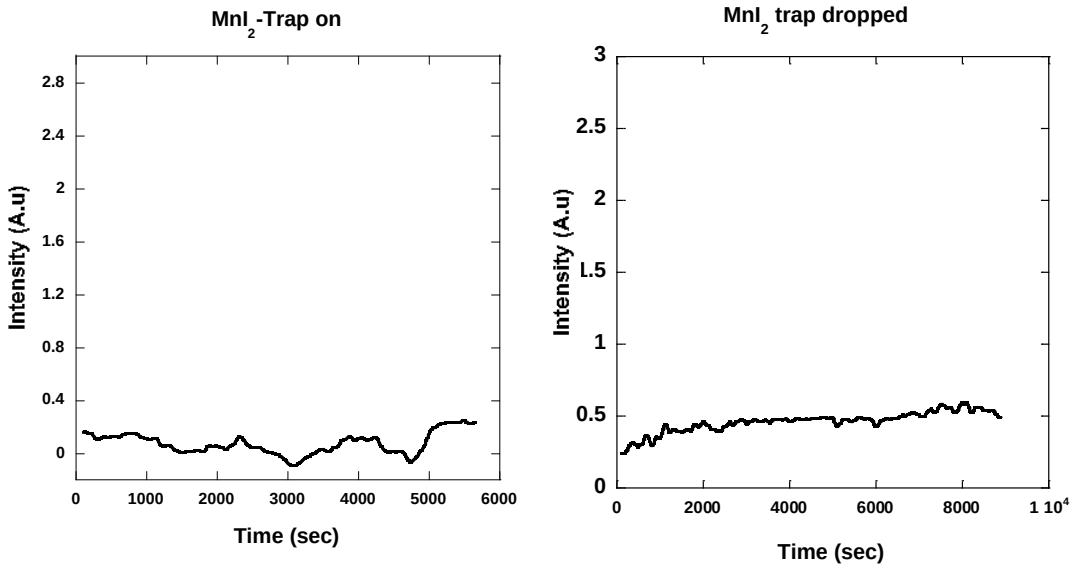

Trapping gases from heated MnI_2 using a cold trap and then dropping the trap to evaporate the condensed gas by use of TPD (temperature-program desorption)

Table 5. Content of Condensable Gas from TPD of Starting Chemicals

Sample	RT (°C)	P (T)	Volume (mL)	Weight (g)	N (mole)	N (mole/g)
TiC	23.61	2.37	314.3	0.508	4.025E-05	7.923E-05
MnI_2	23.4	1.5	314.3	0.54	2.549E-05	4.721E-05

Appendix B– Small Cell Calibrations

Small Cell calibration data for 5-13-2009

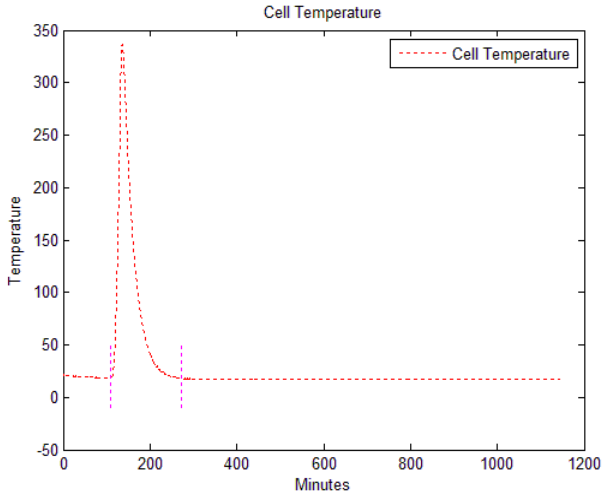

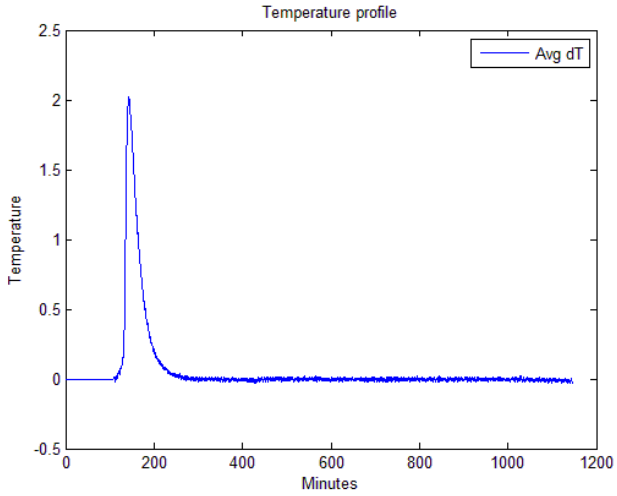

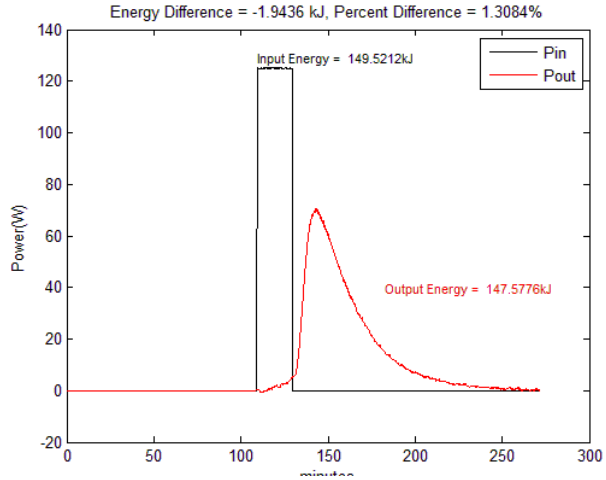

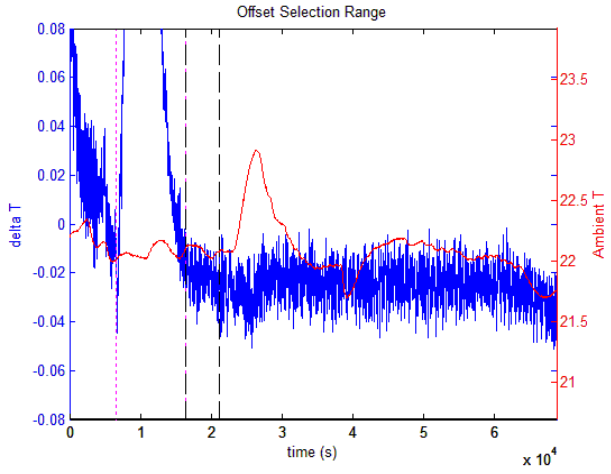

Small Cell calibration data for 5-20-2009

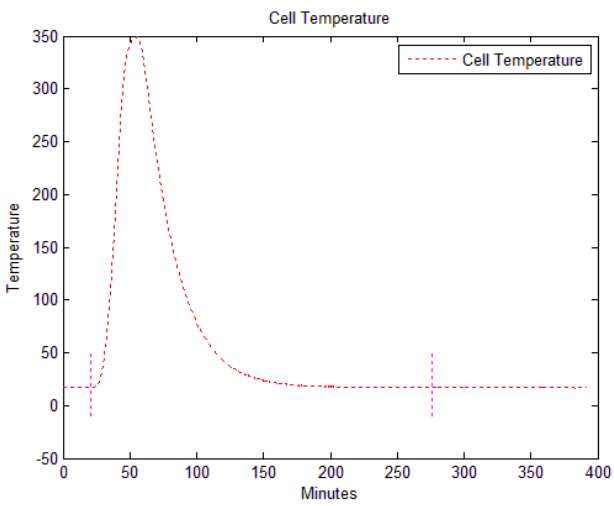

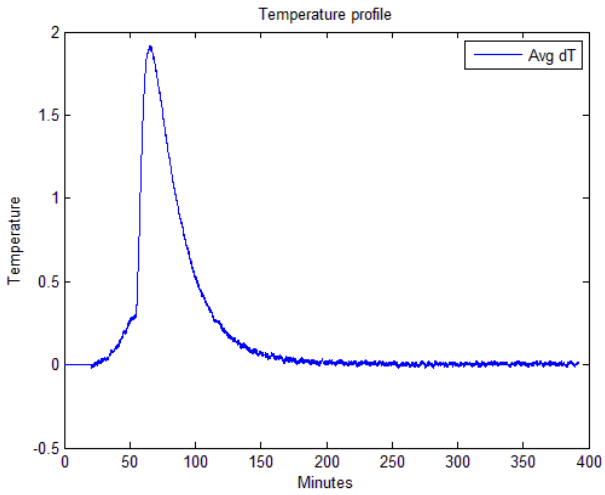

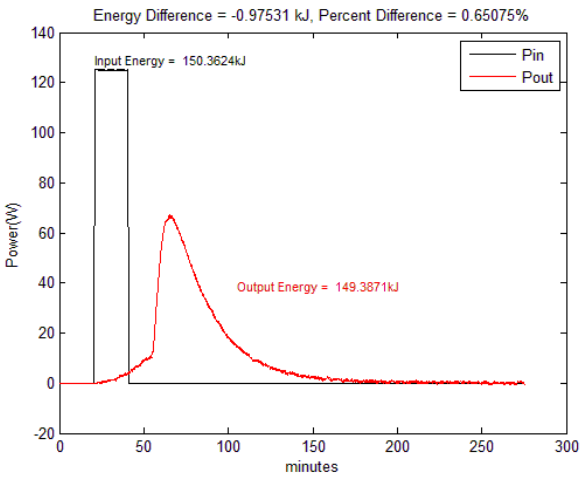

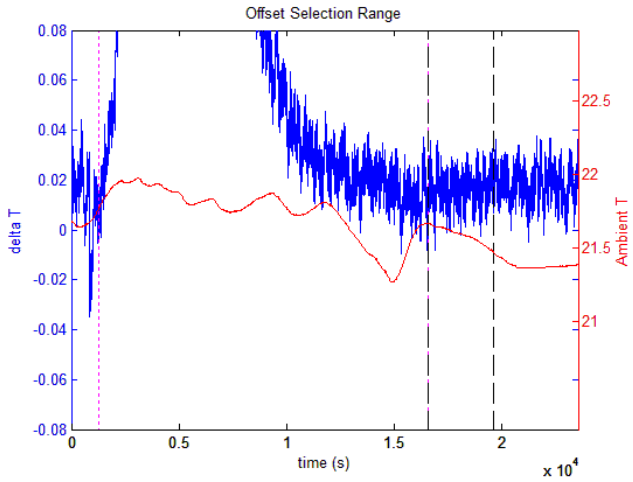

Small Cell calibration data for 5-22-2009

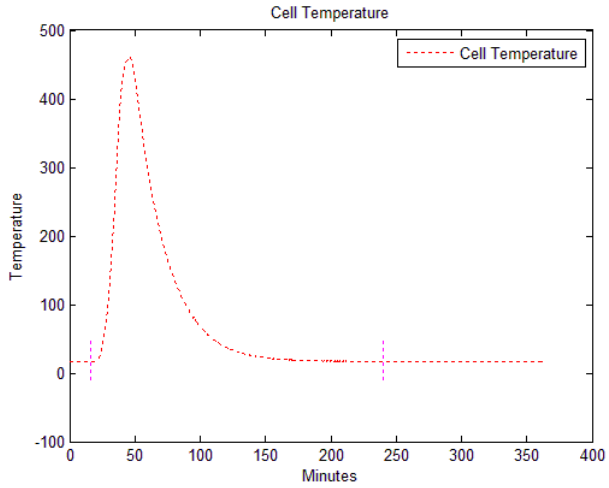

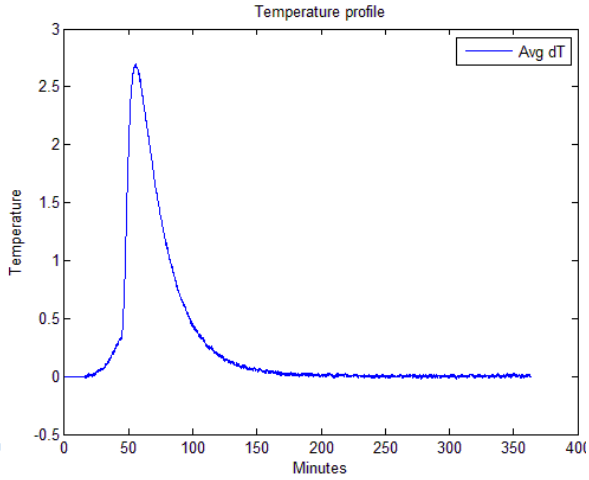

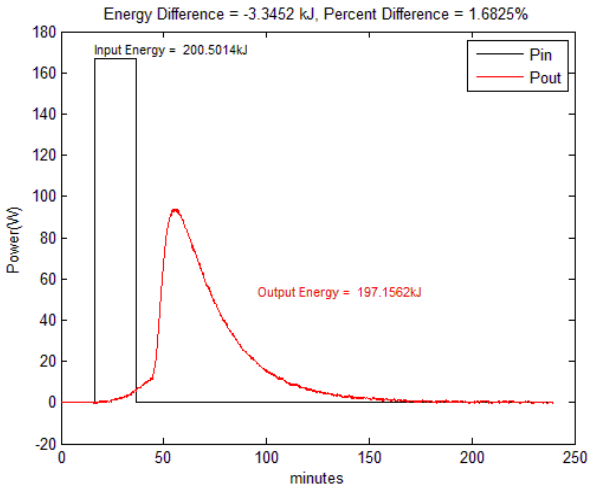

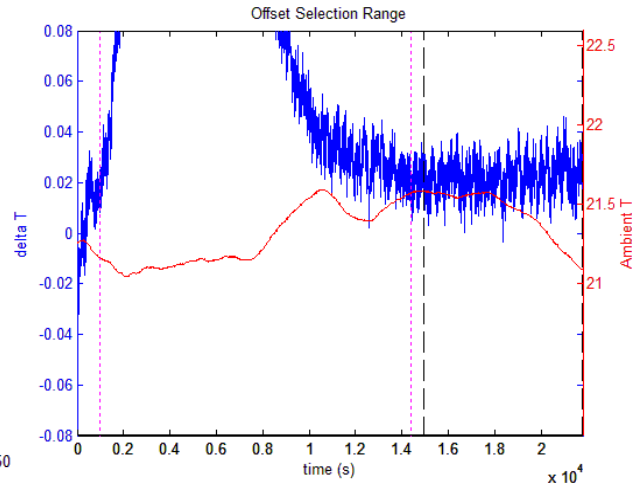

Small Cell calibration data for 5-26-2009

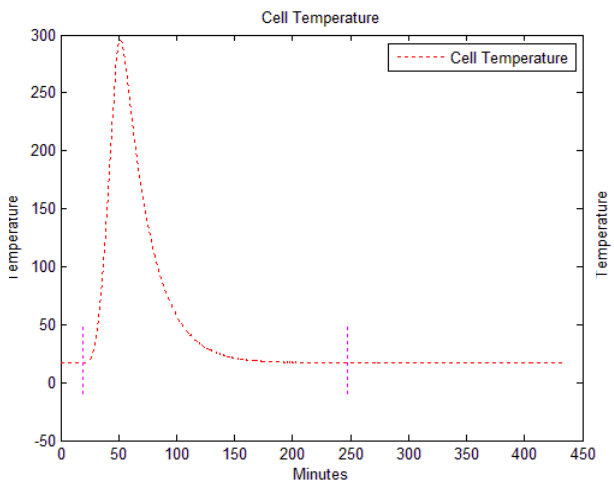

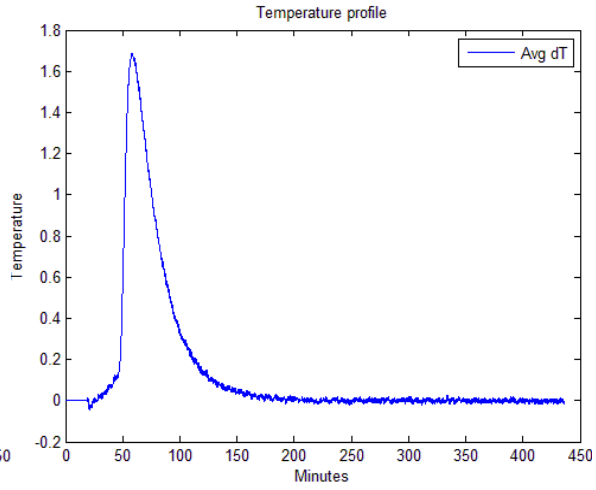

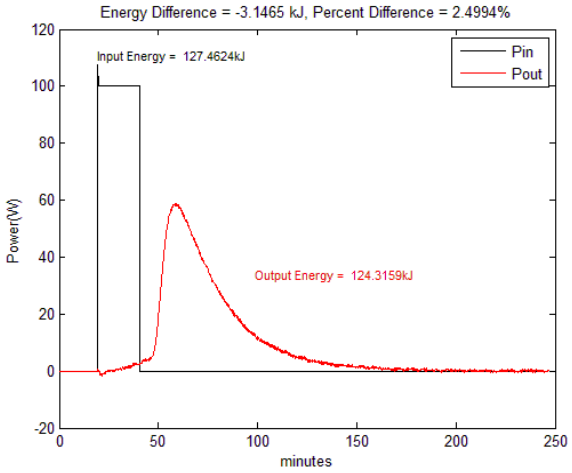

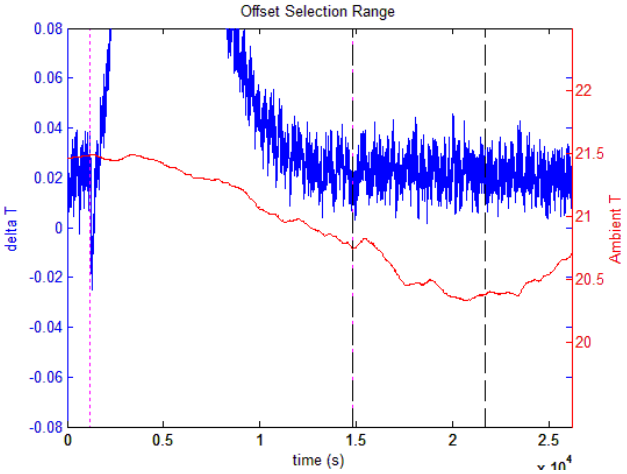

Small Cell calibration data for 5-27-2009

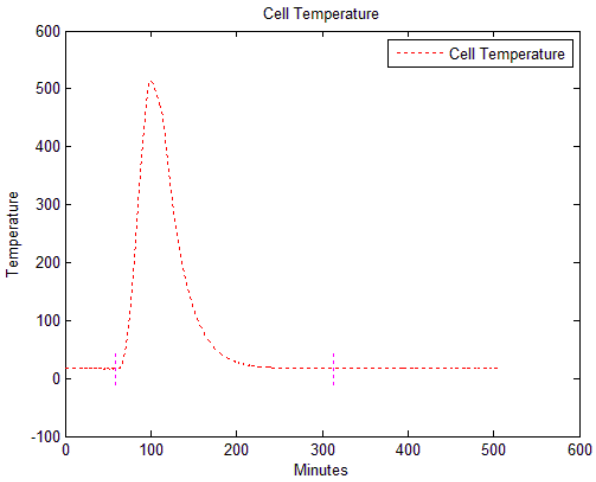

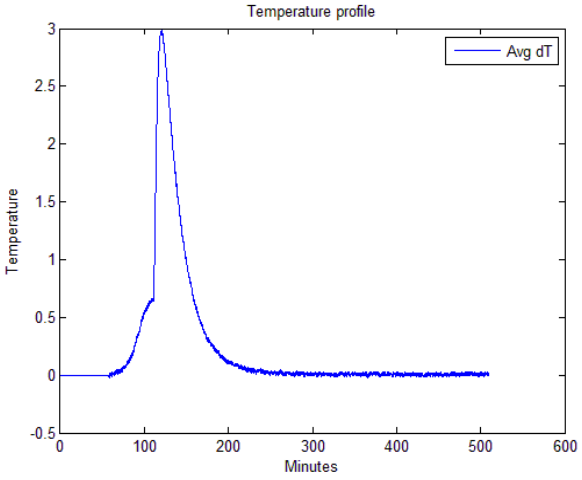

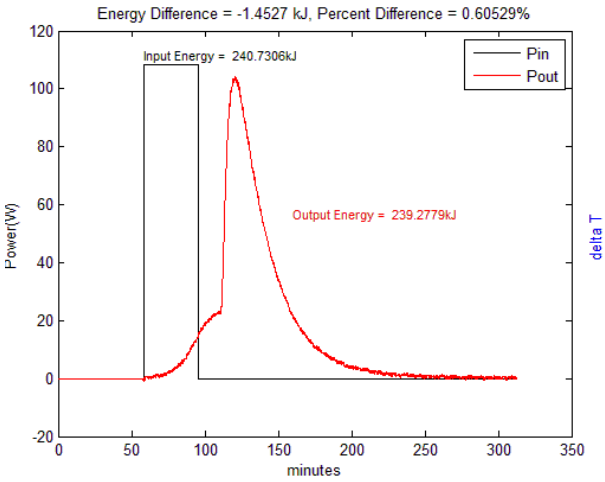

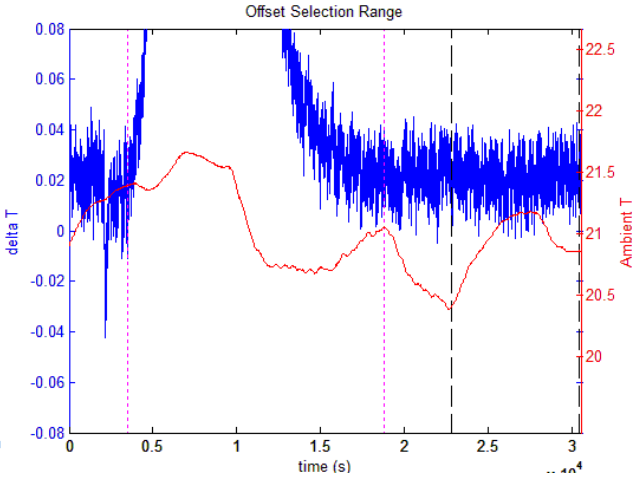

Small Cell calibration data for 5-28-2009

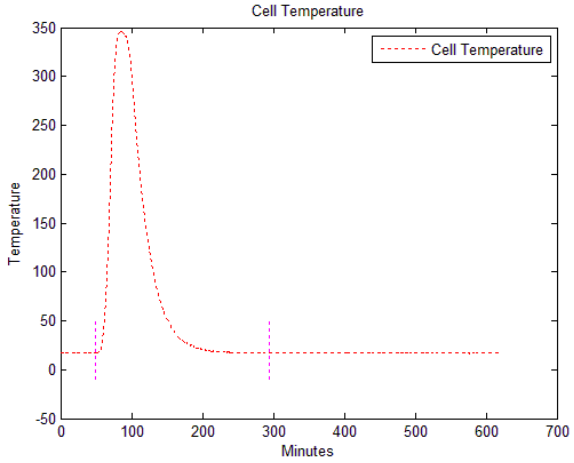

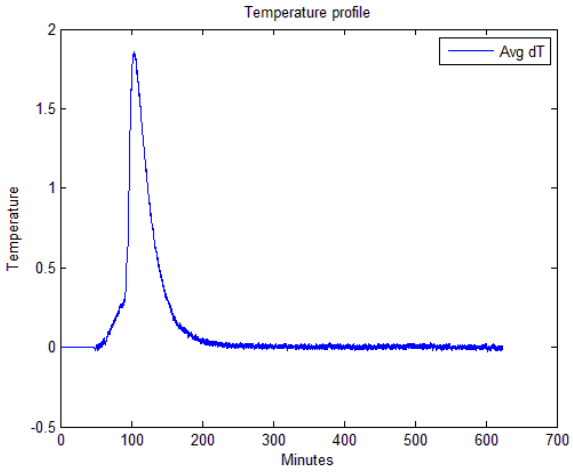

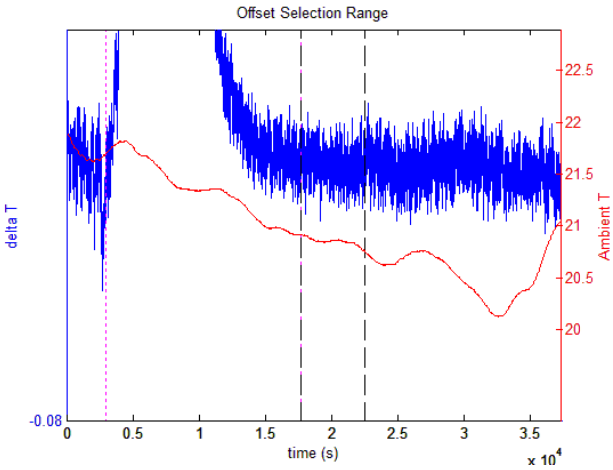

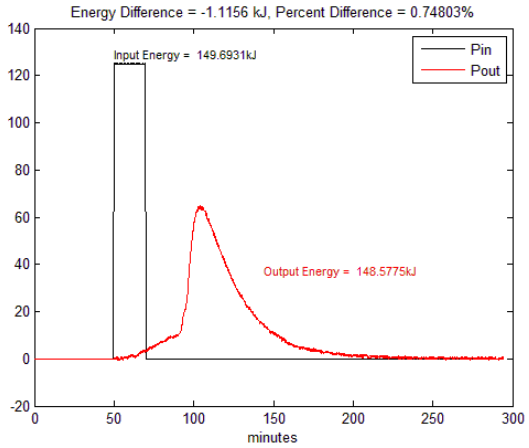

Small Cell calibration data for 5-29-2009

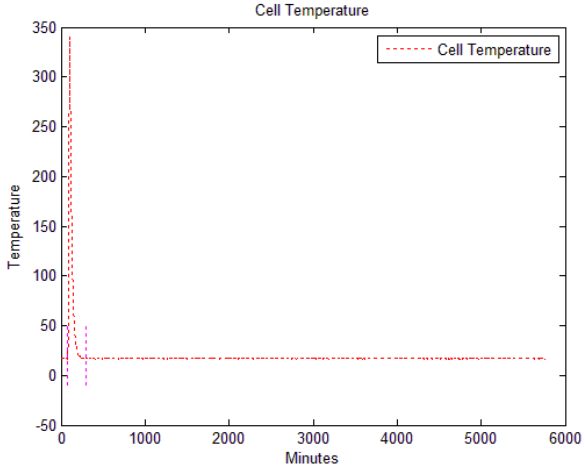

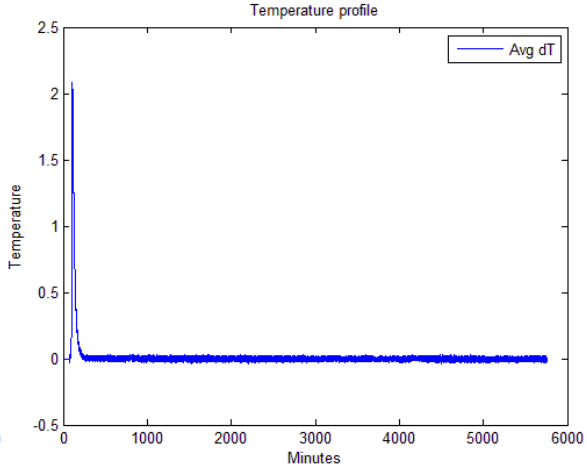

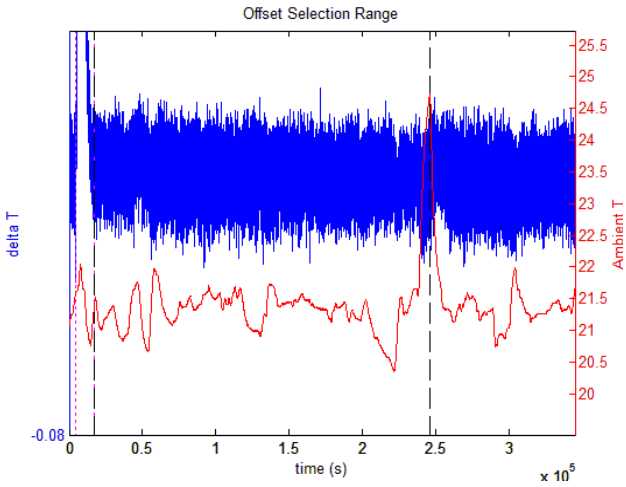

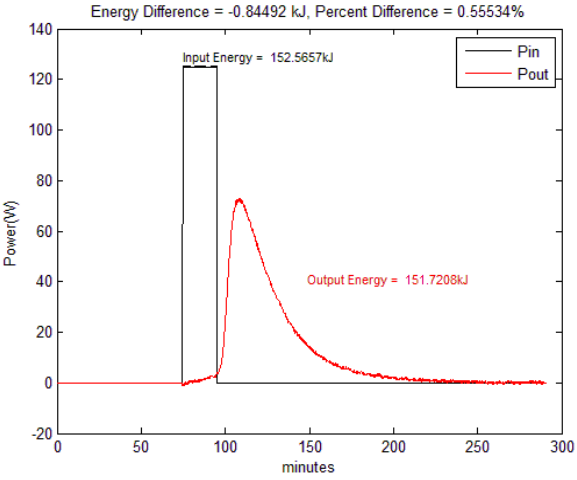

Small Cell calibration data for 6-2-2009

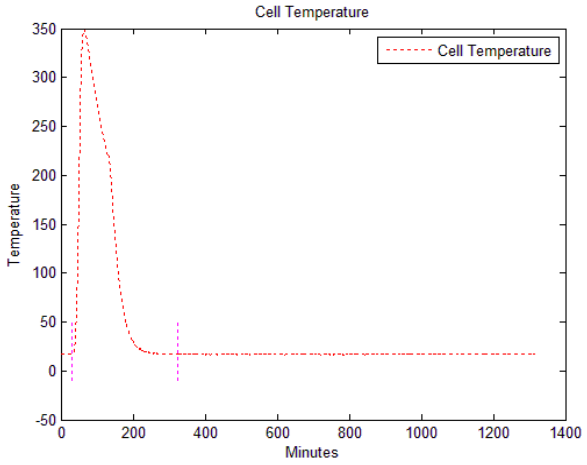

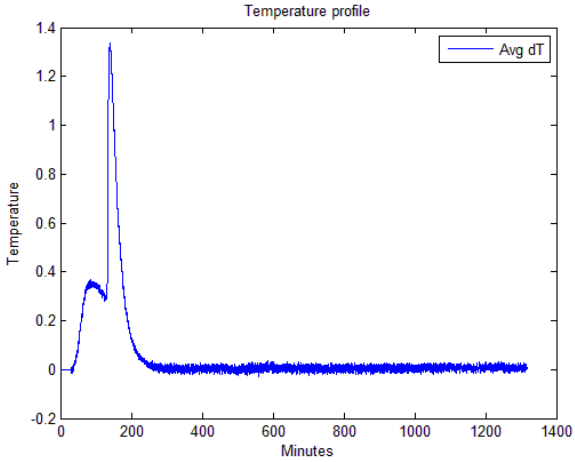

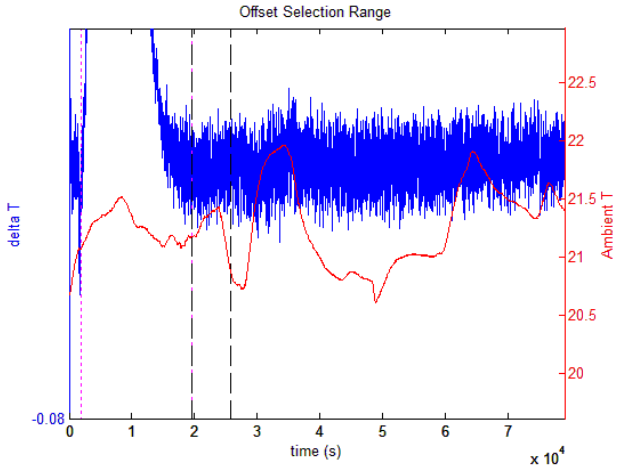

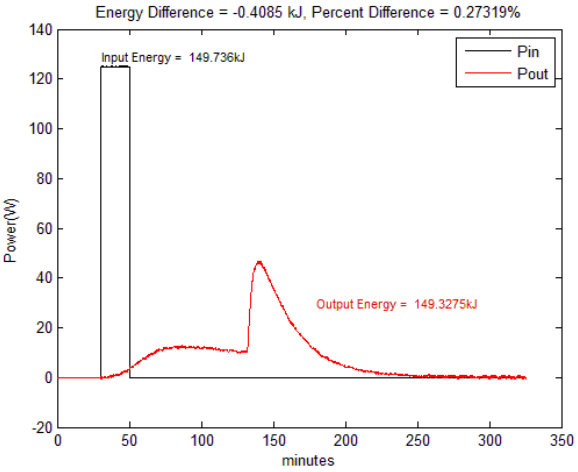

Small Cell calibration data for 6-28-2009

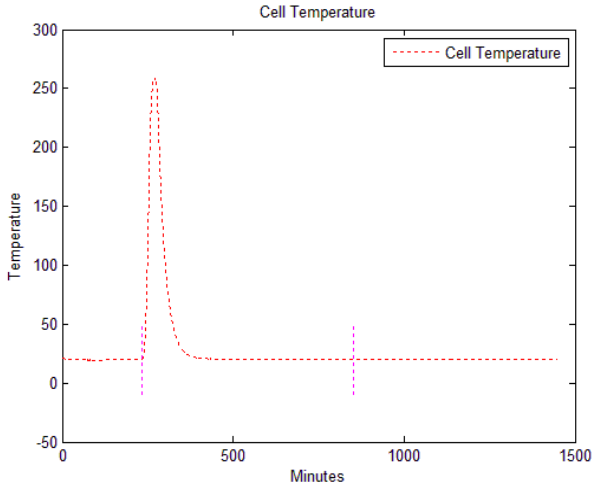

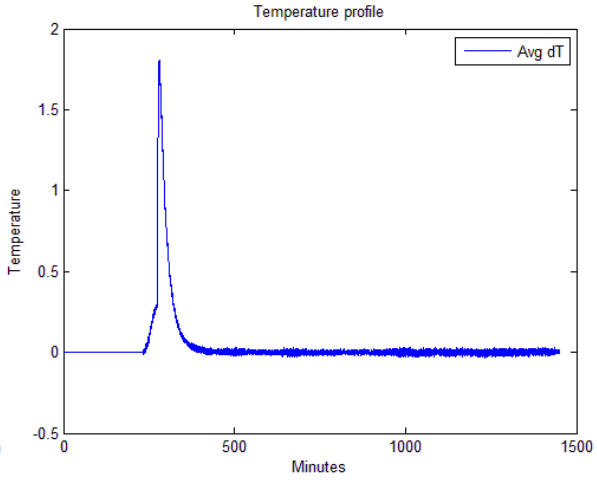

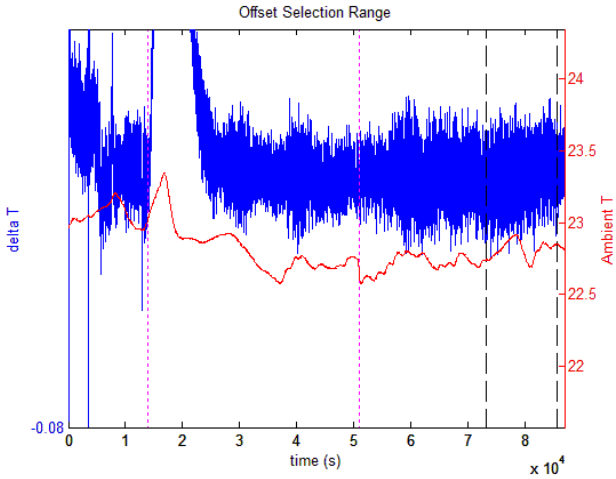

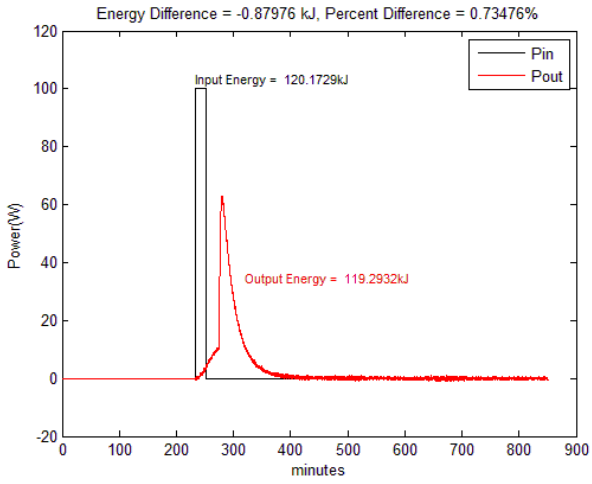

Small Cell calibration data for 7-1-2009

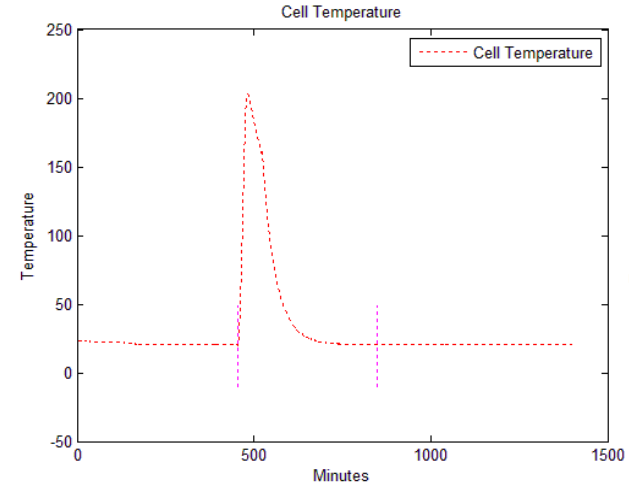

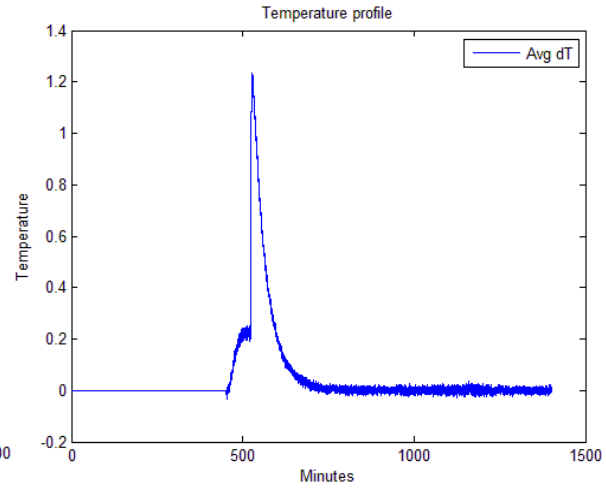

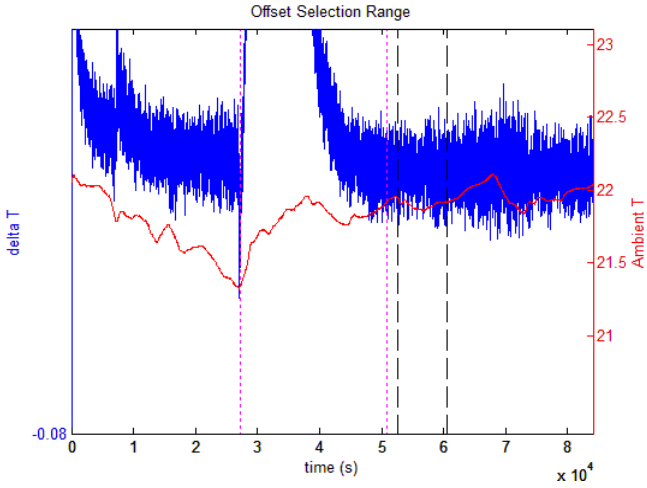

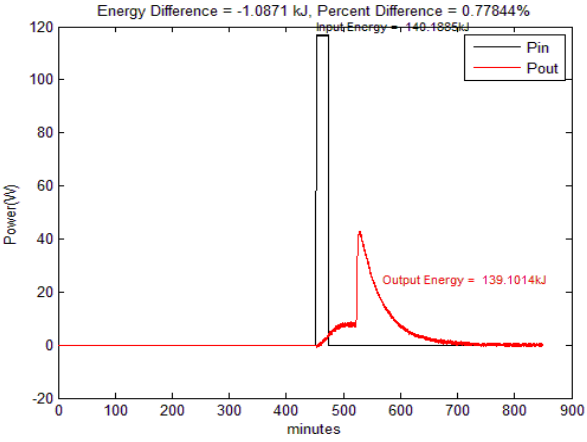

Small Cell calibration data for 7-5-2009

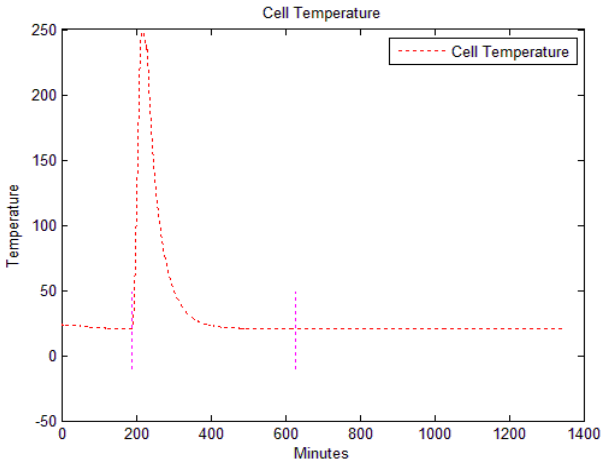

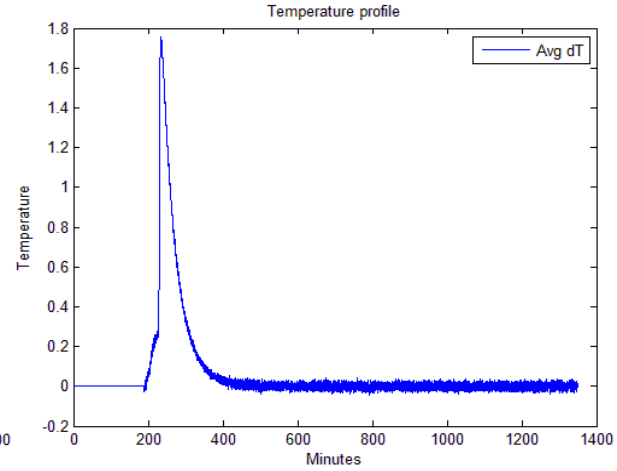

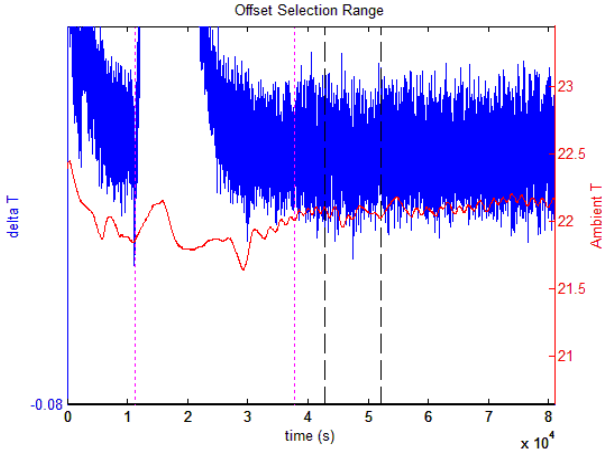

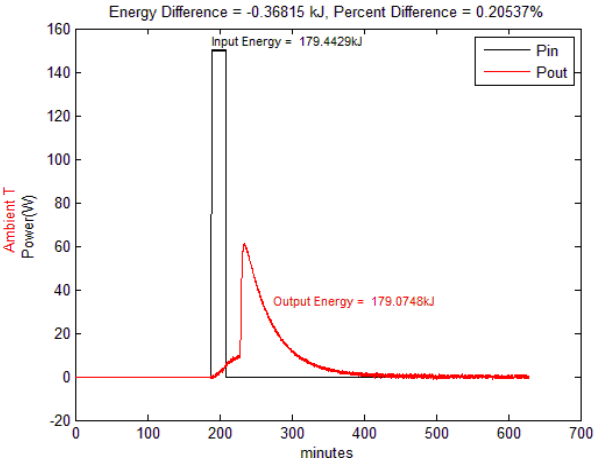

Small Cell calibration data for 7-14-2009

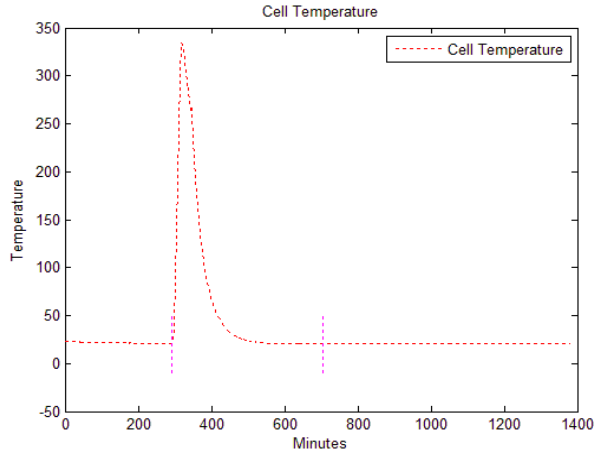

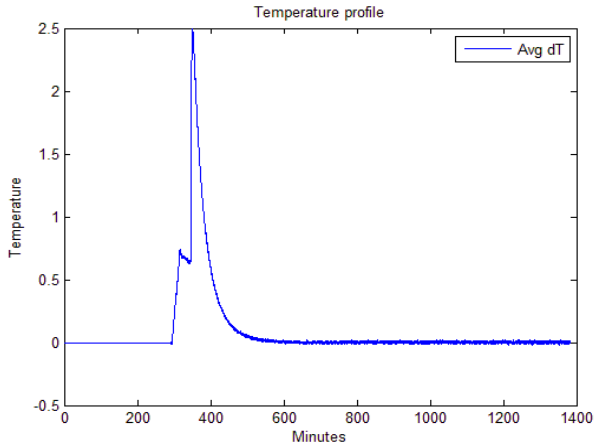

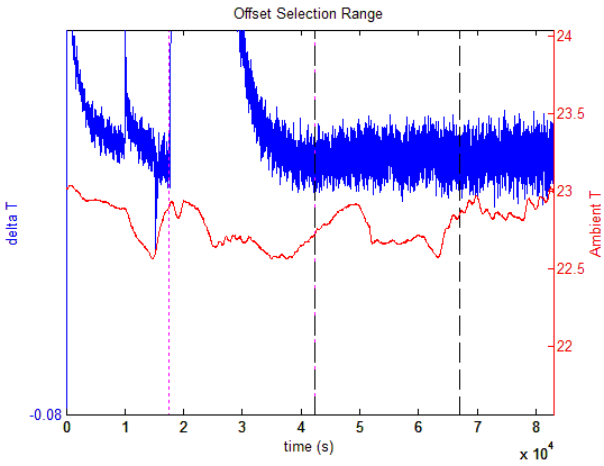

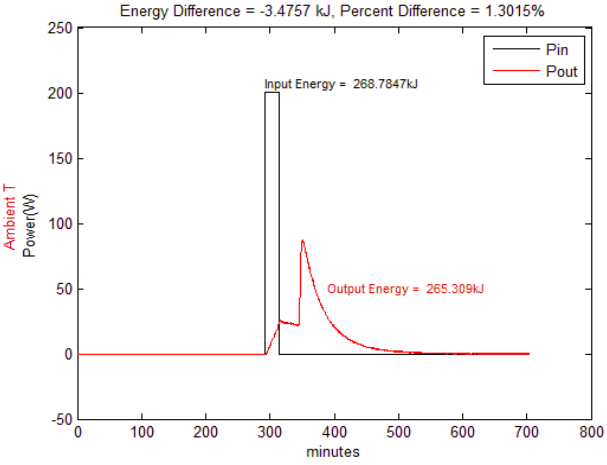

Small Cell calibration data for 7-15-2009

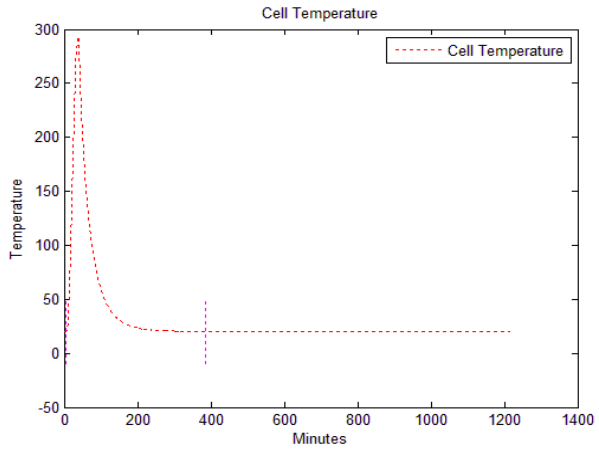

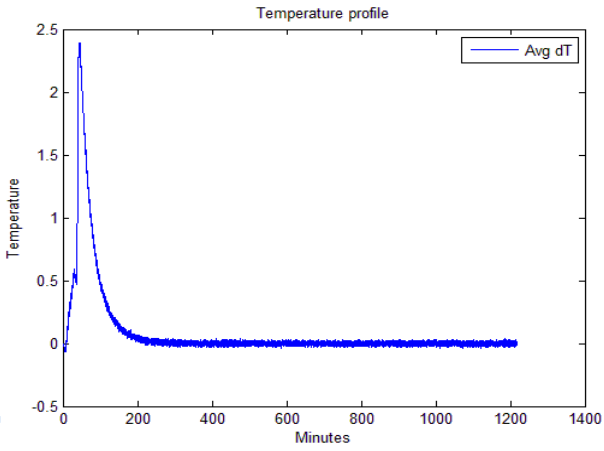

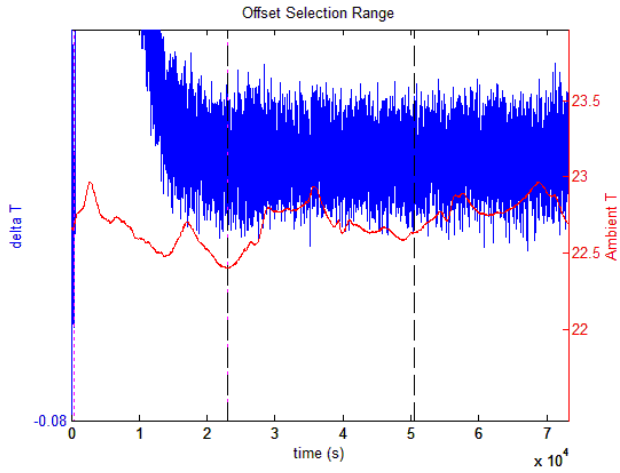

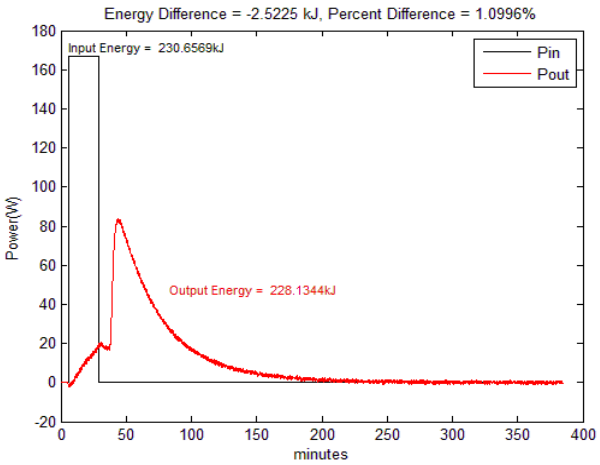

Small Cell calibration data for 7-20-2009

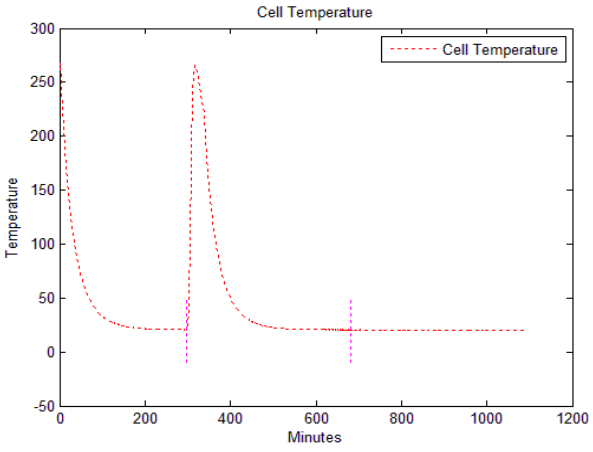

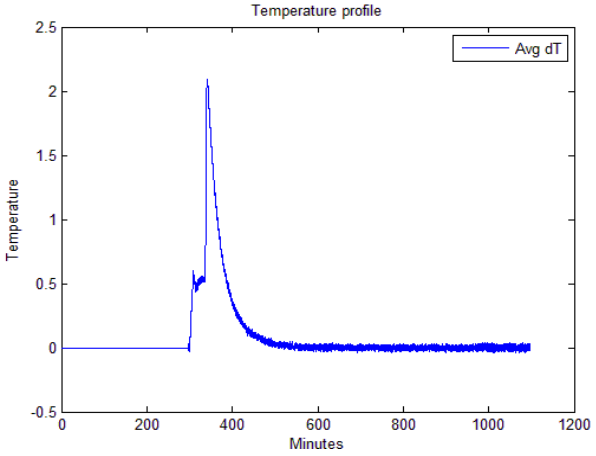

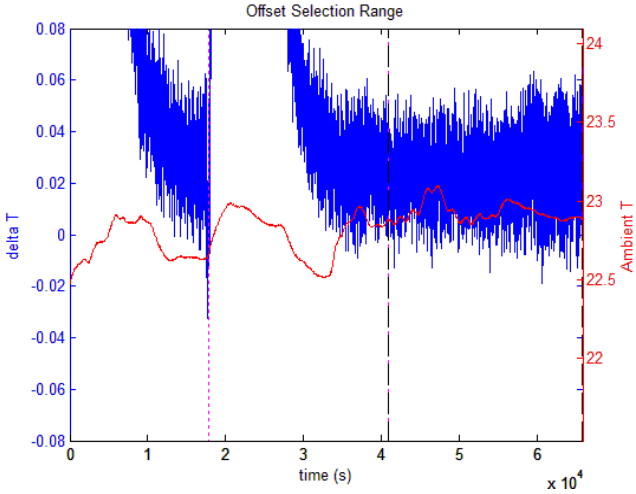

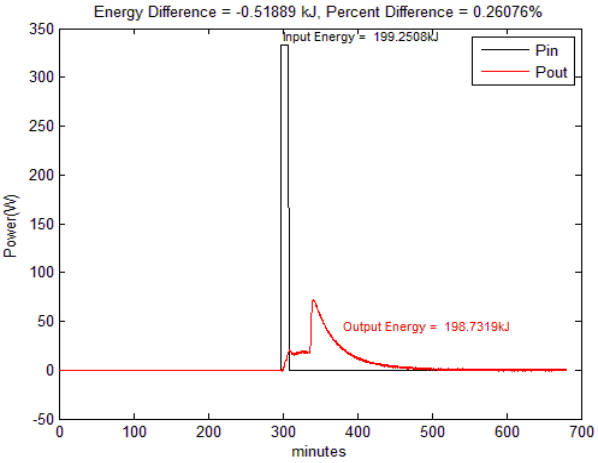

Small Cell calibration data for 7-27-2009

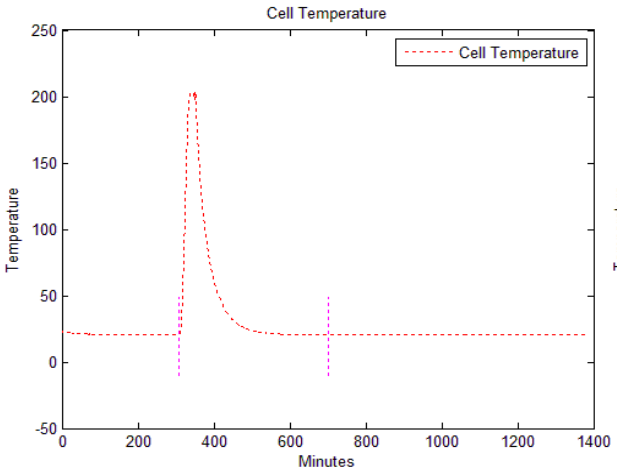

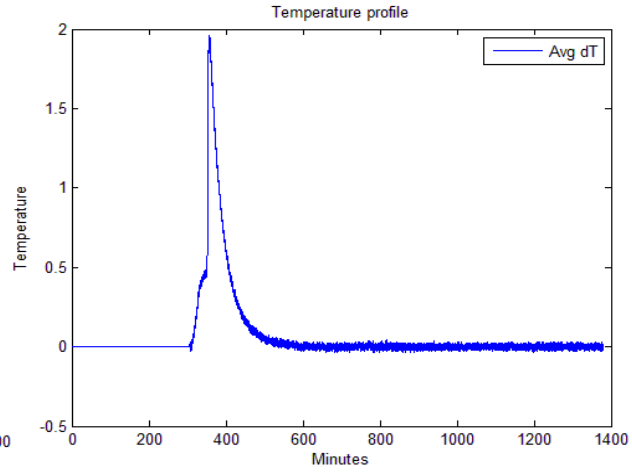

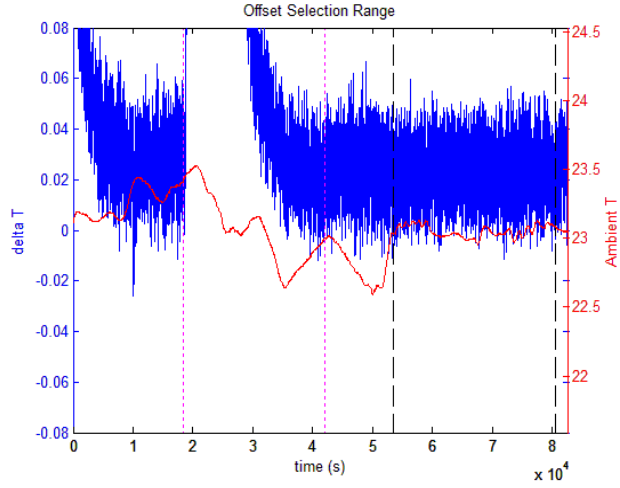

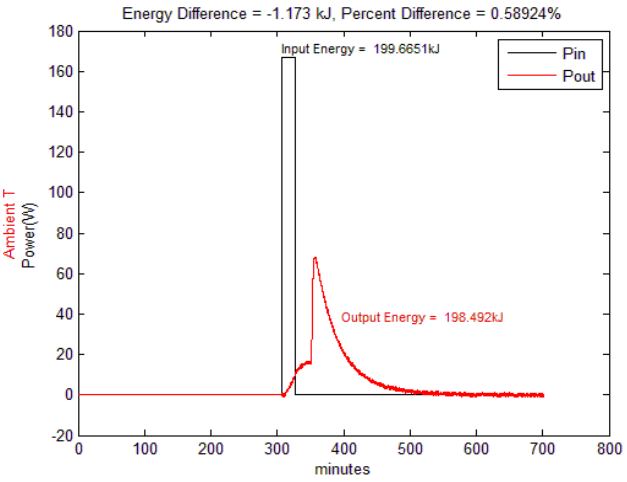

Small Cell calibration data for 7-28-2009

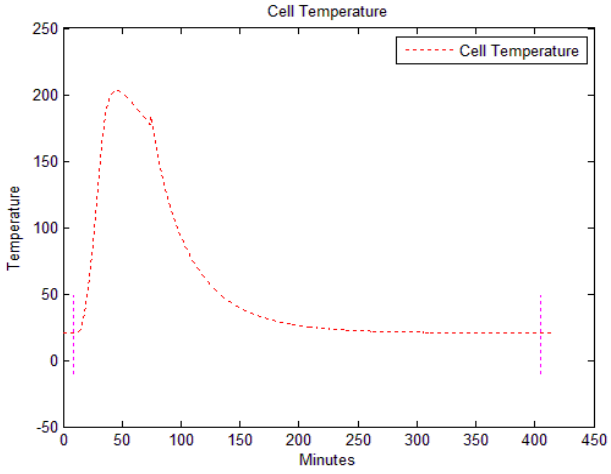

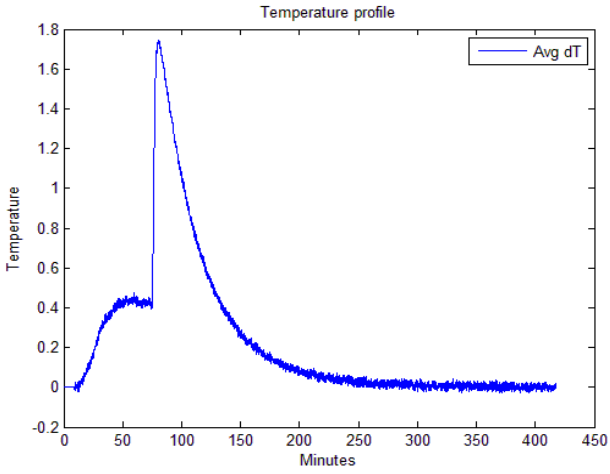

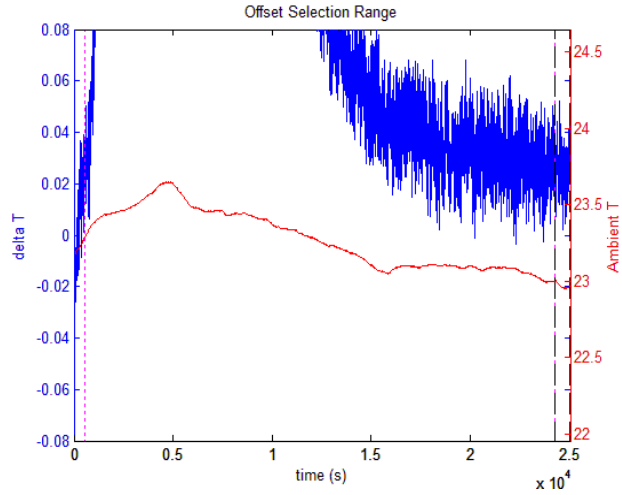

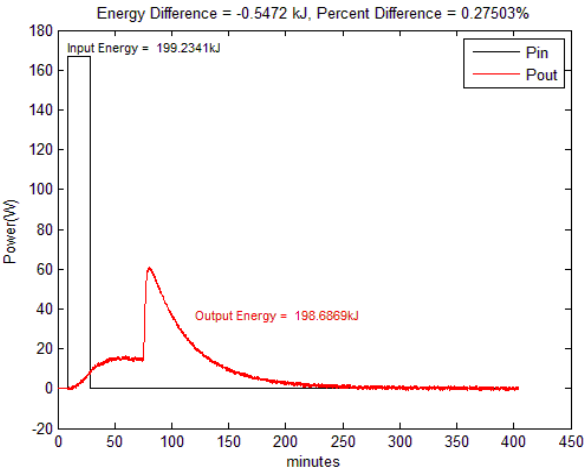

Appendix C – Large Cell Calibrations

Large Cell calibration data for 6-10-2009

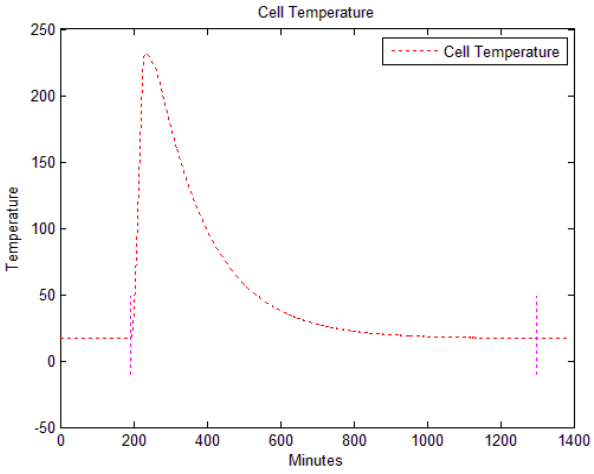

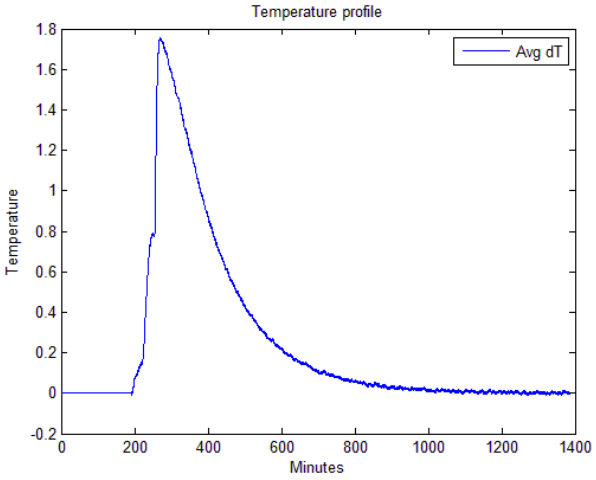

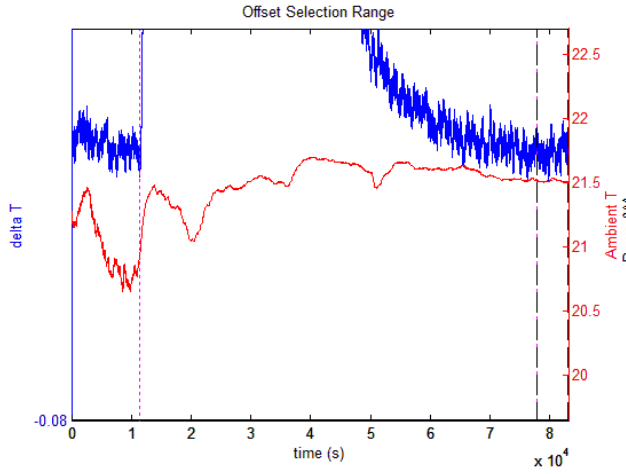

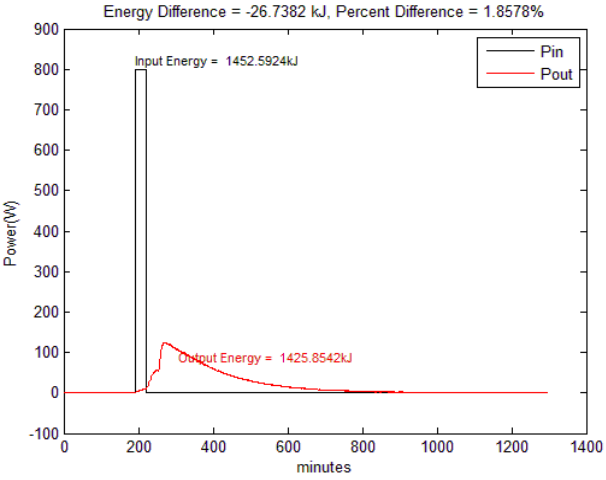

Large Cell calibration data for 6-11-2009

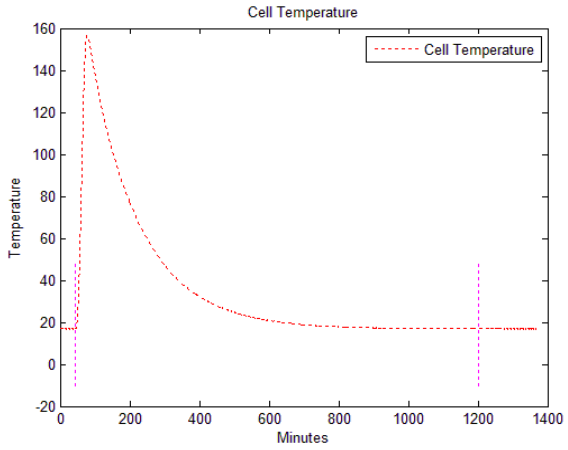

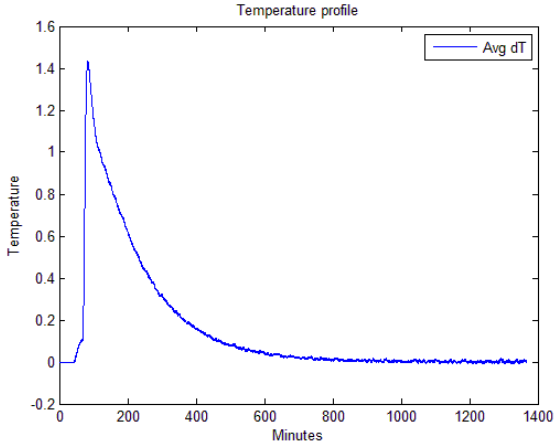

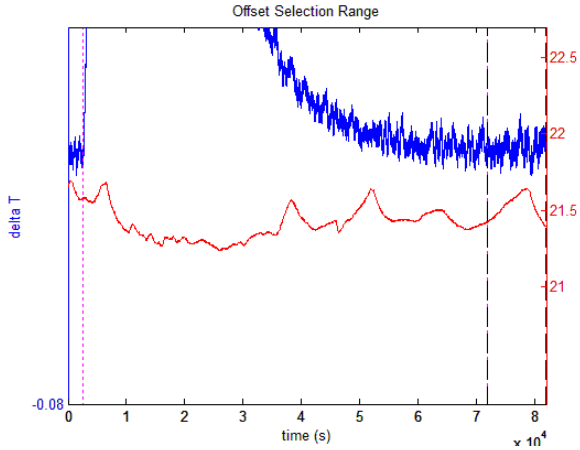

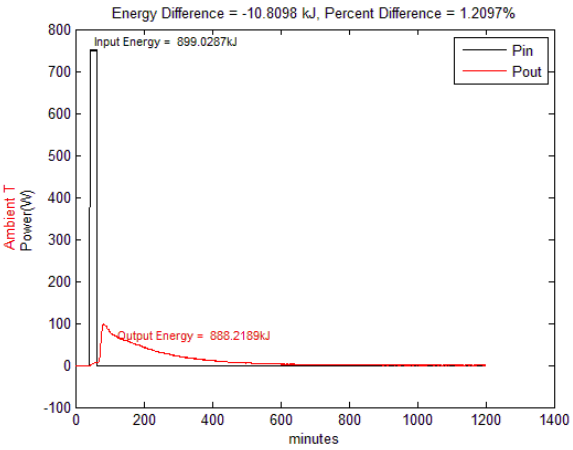

Large Cell calibration data for 6-12-2009

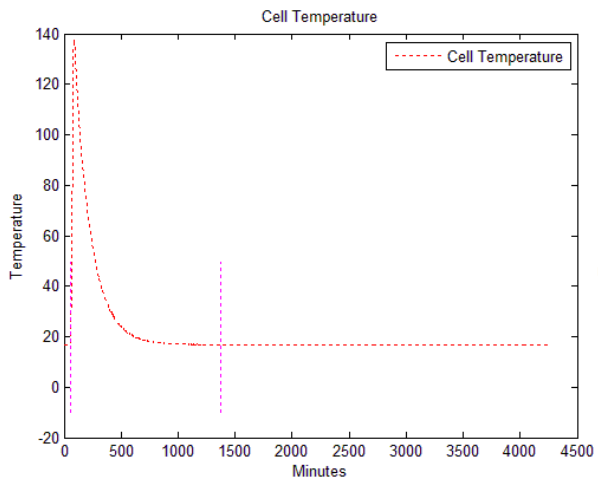

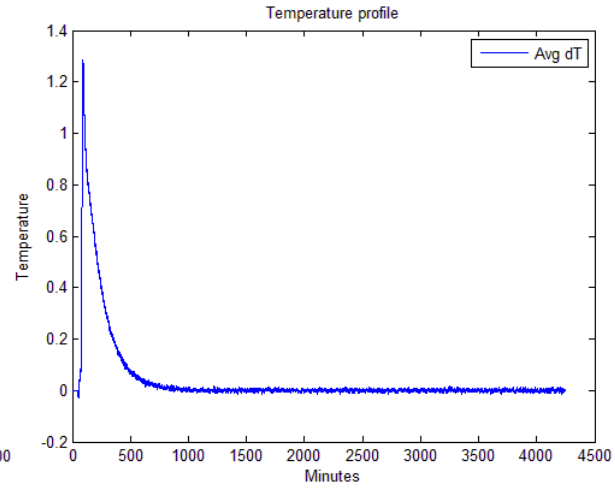

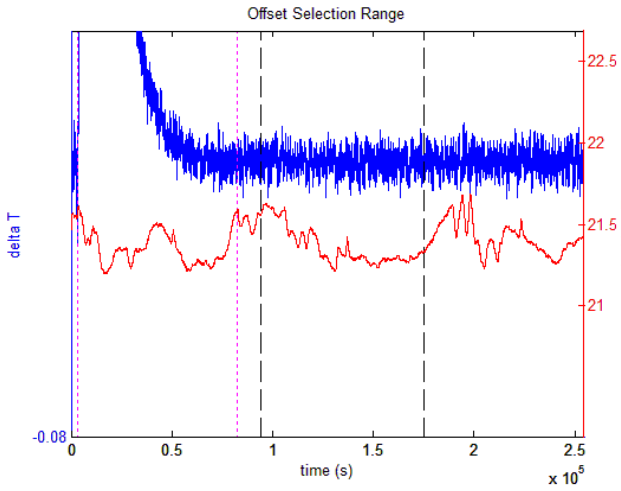

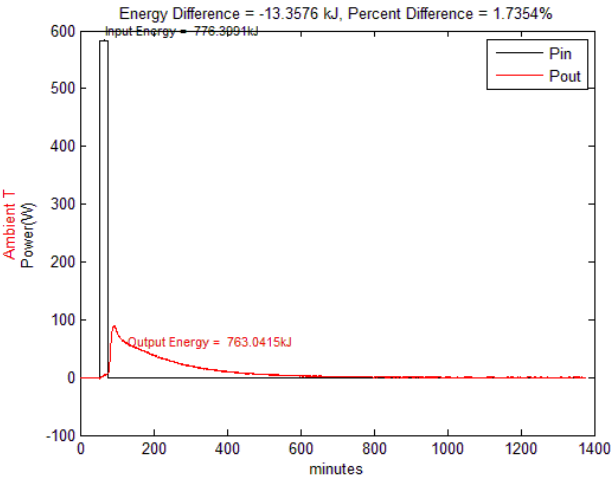

Large Cell calibration data for 6-24-2009

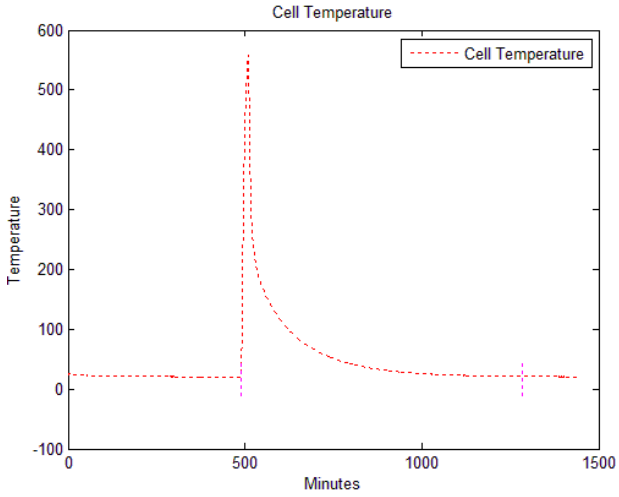

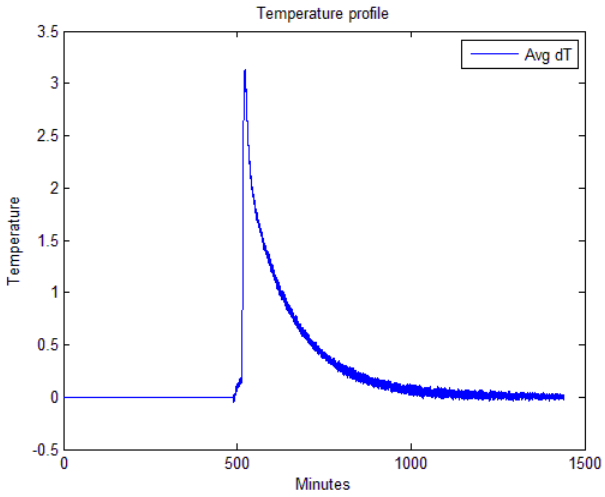

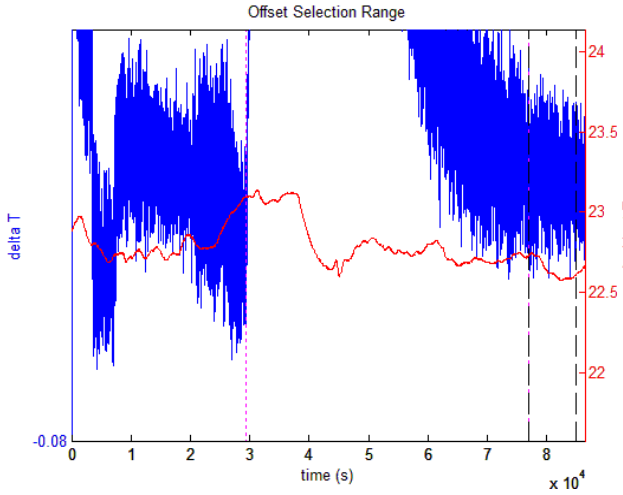

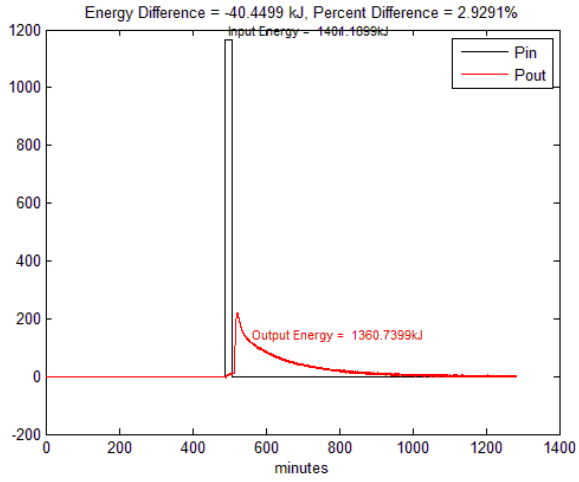

Large Cell calibration data for 6-26-2009

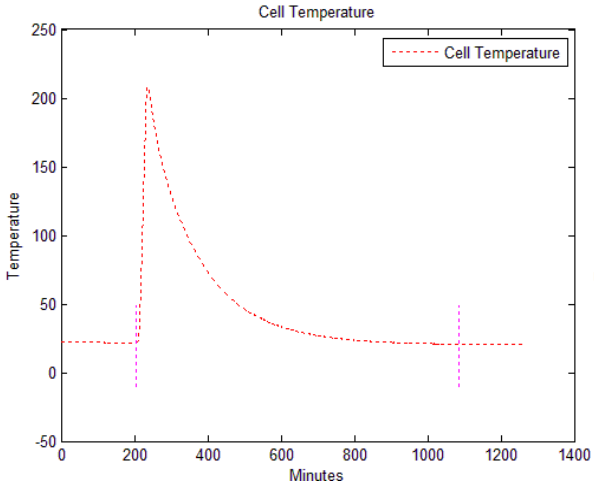

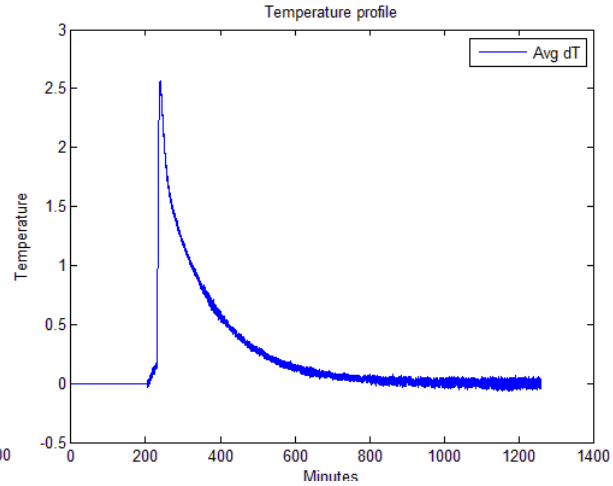

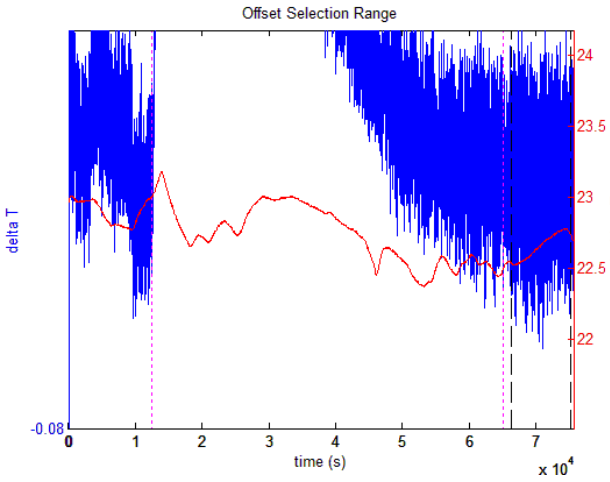

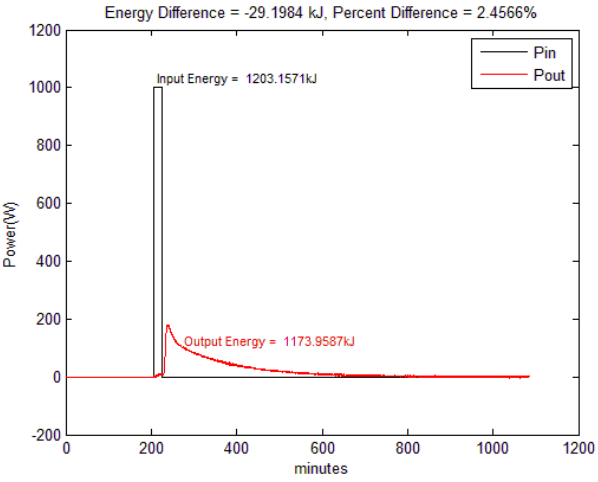

Appendix D – Small Cell Heat Runs 6-23-09

Observed by Dr.Jansson & Kevin at BLP

$FeBr_2$

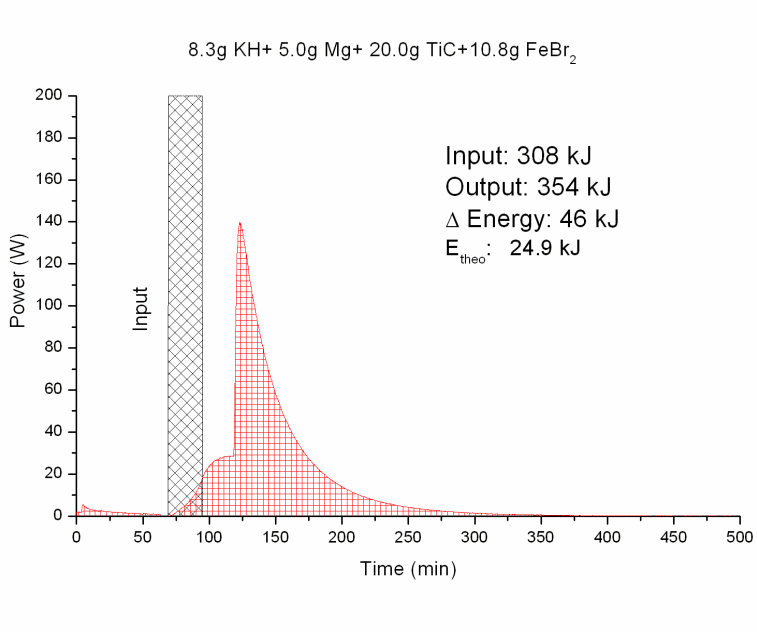

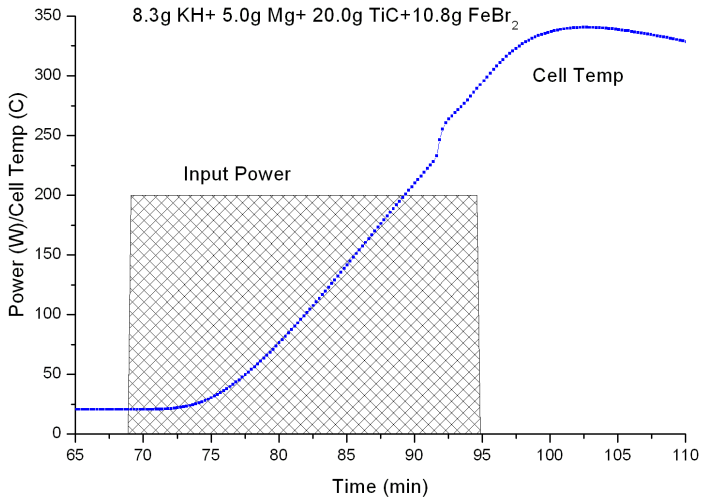

MnI_2

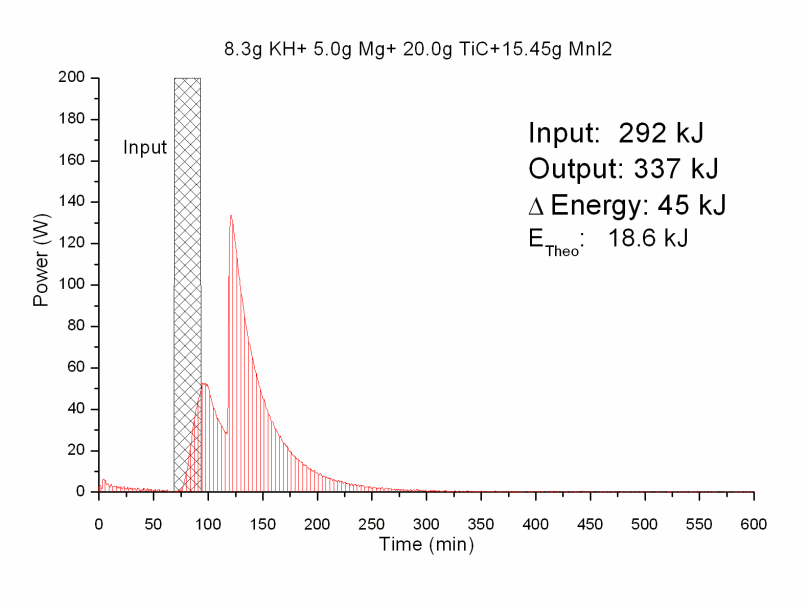
8.3g KH+ 5.0g Mg+ 20.0g TiC+15.45g MnI2
Input
Input: 292 kJ
Output: 337 kJ
Δ Energy: 45 kJ
E_Theo: 18.6 kJ
Power (W)
Time (min)

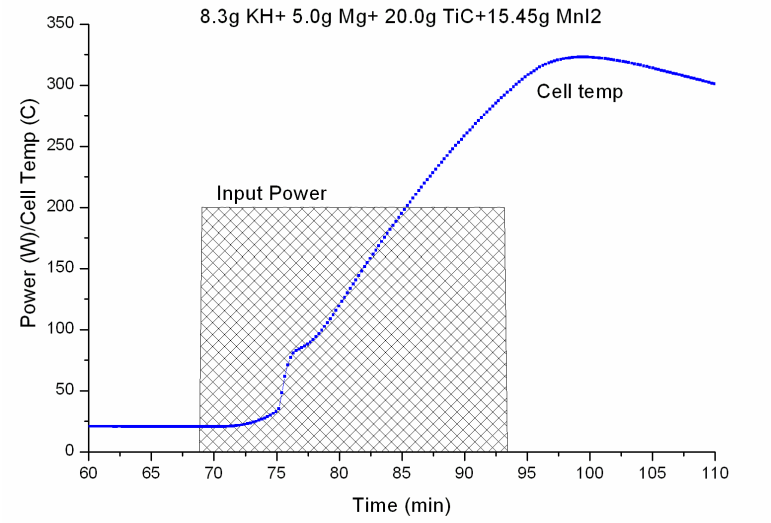
8.3g KH+ 5.0g Mg+ 20.0g TiC+15.45g MnI2
Cell temp
Input Power
Power (W)/Cell Temp (C)
Time (min)

Small Cell heat run data for 6-29-2009

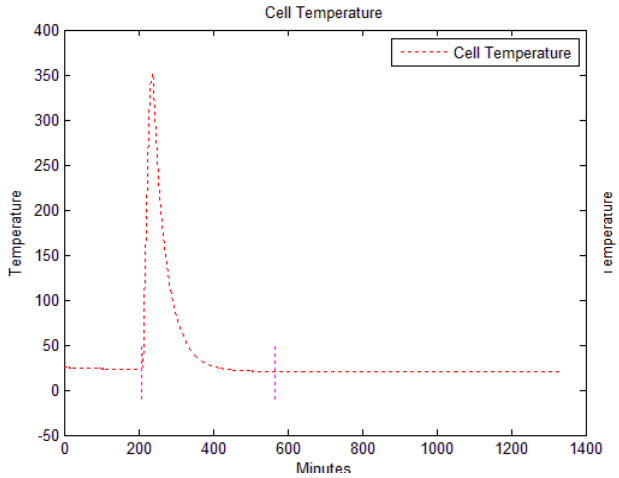

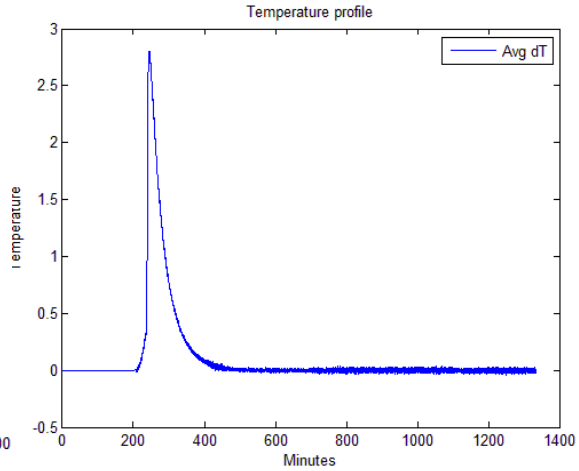

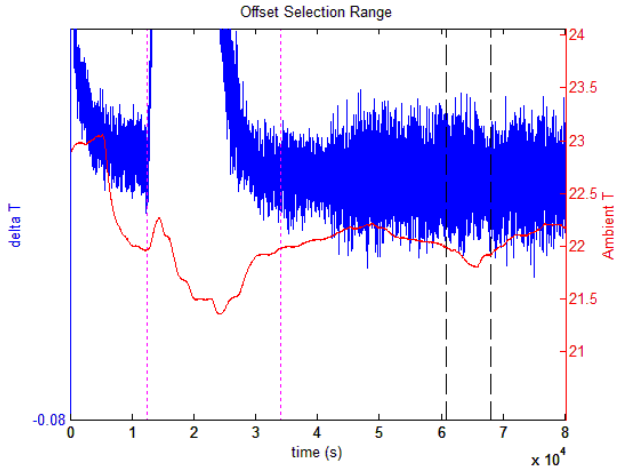

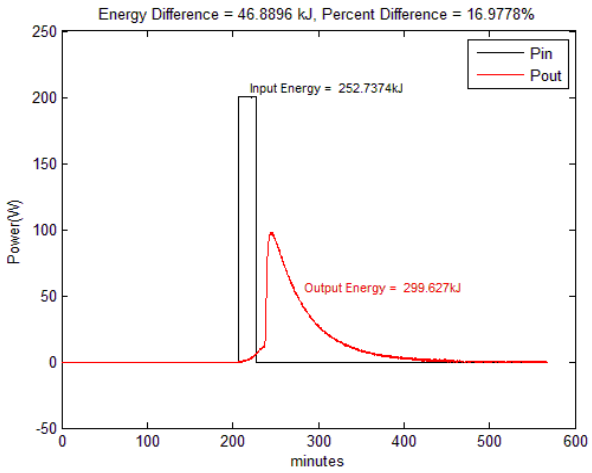

Small Cell heat run data for 6-30-2009

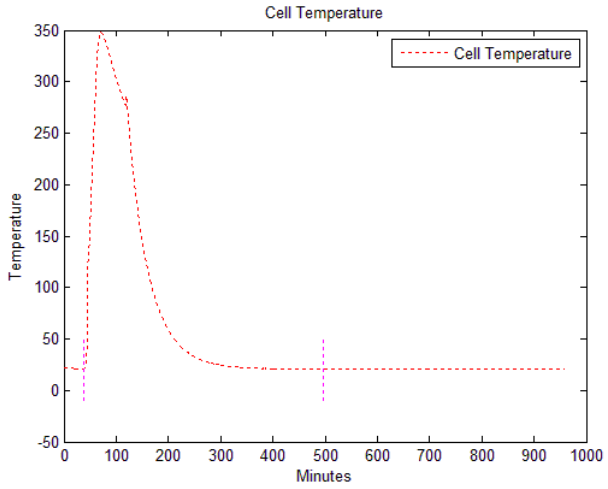

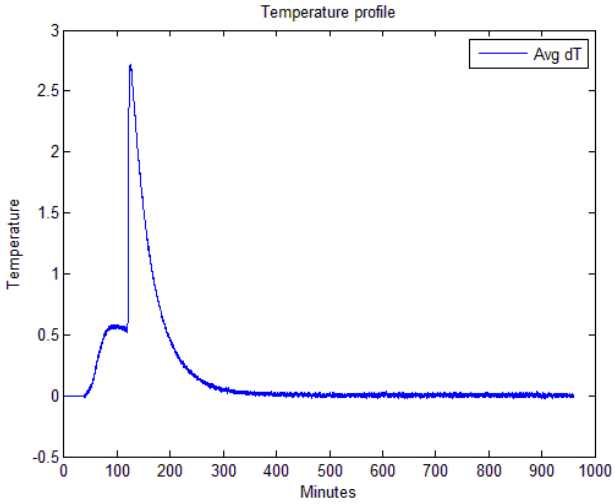

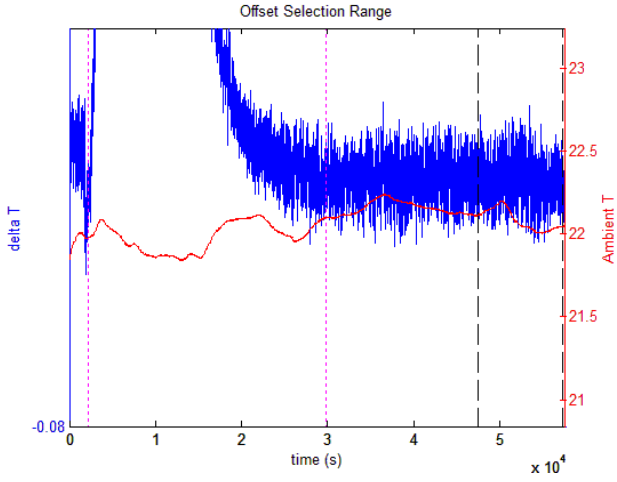

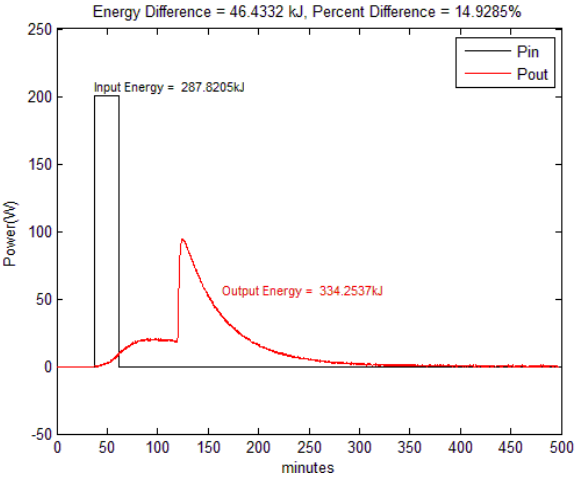

Small Cell heat run data for 7-2-2009

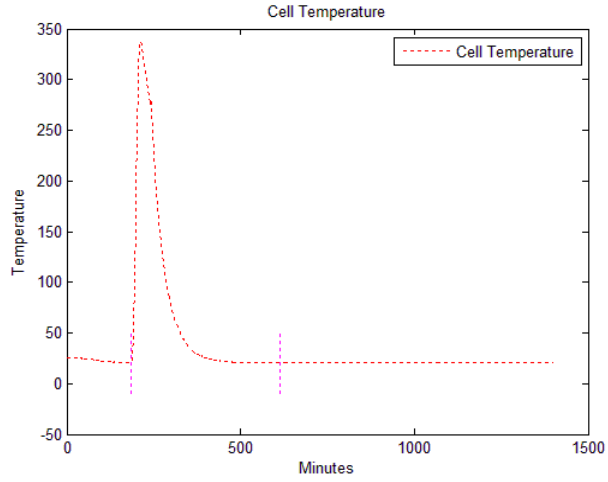

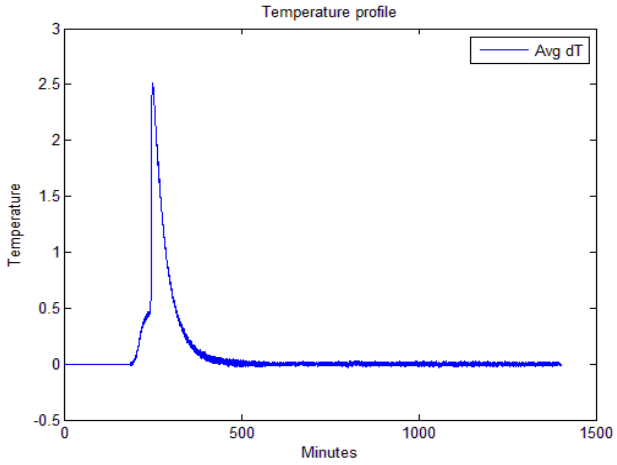

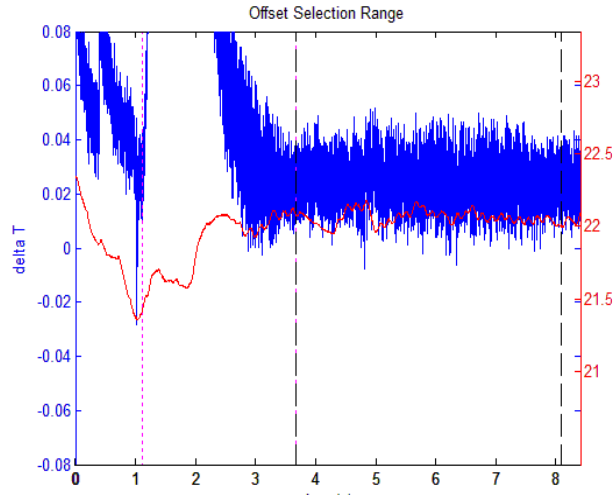

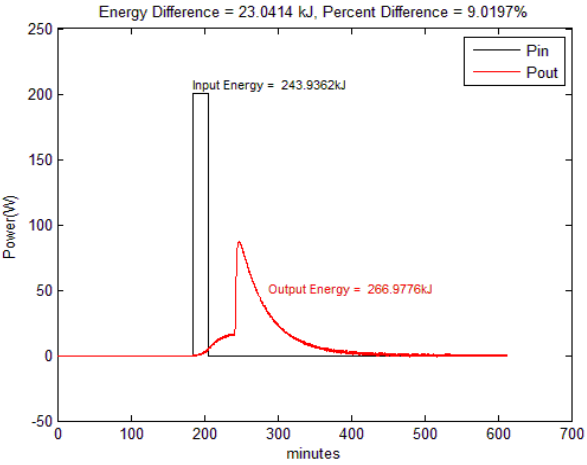

Small Cell heat run data for 7-3-20093

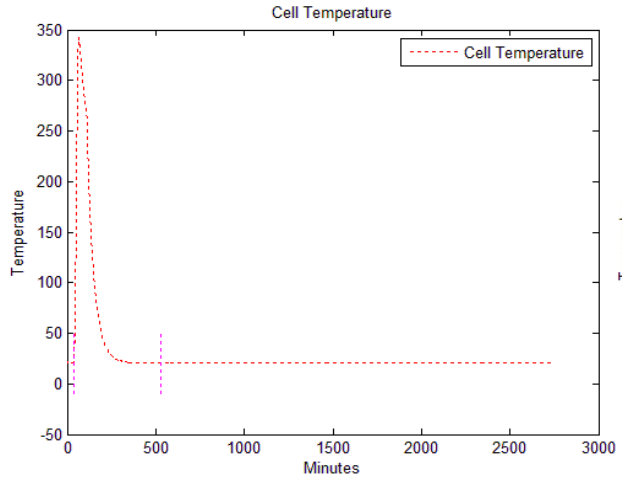

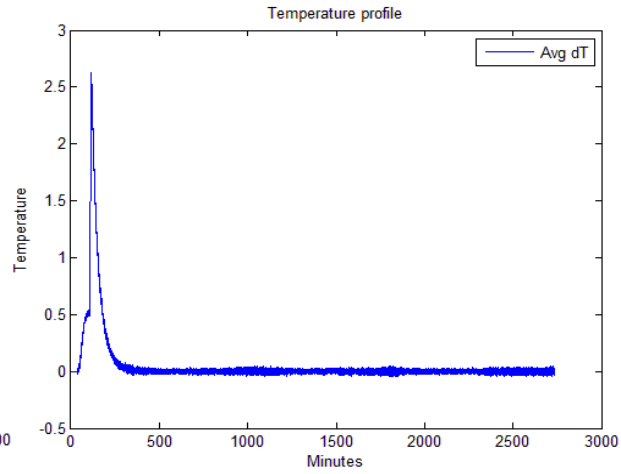

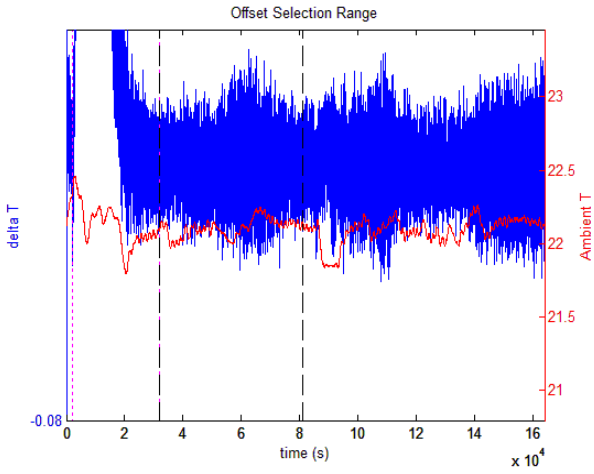

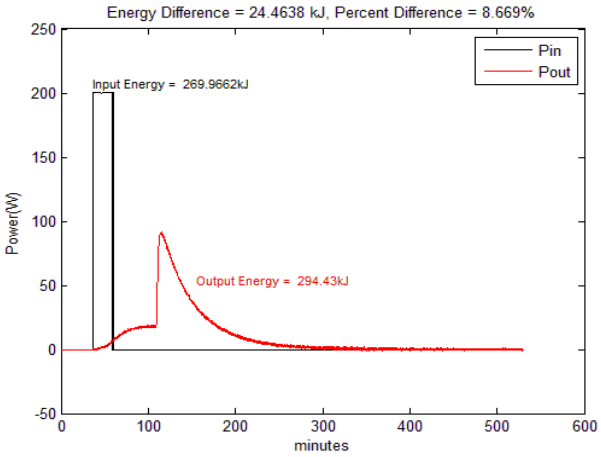

Small Cell heat run data for 7-6-2009

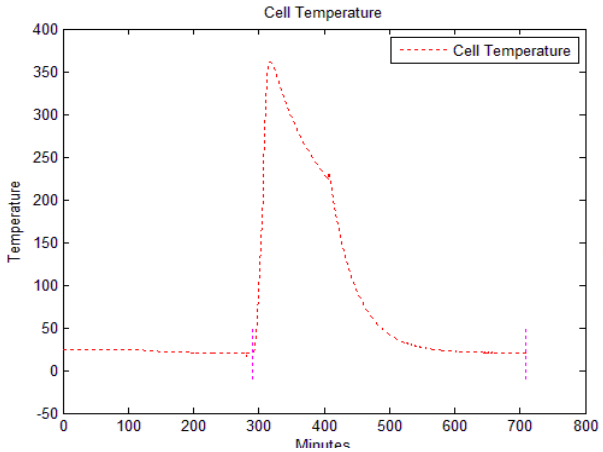

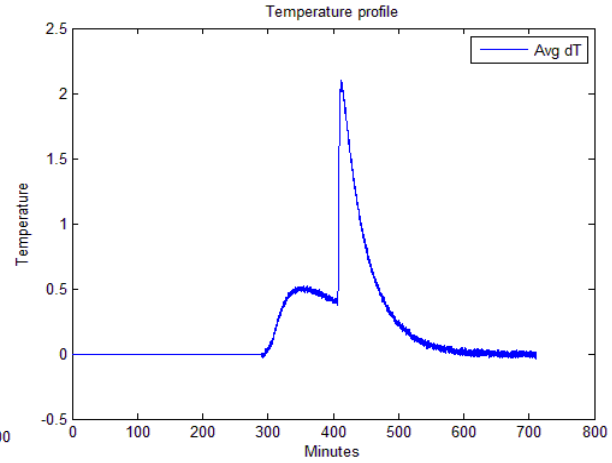

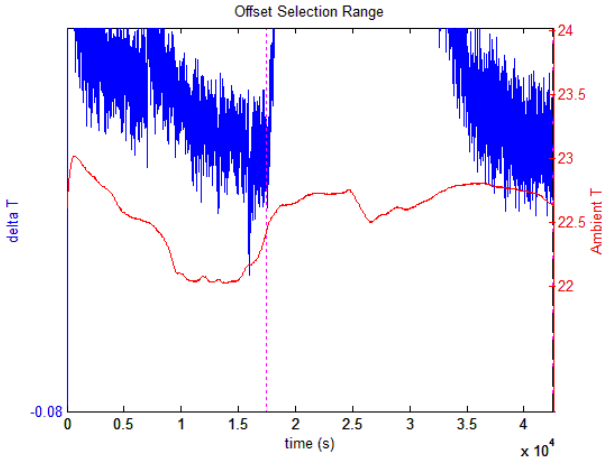

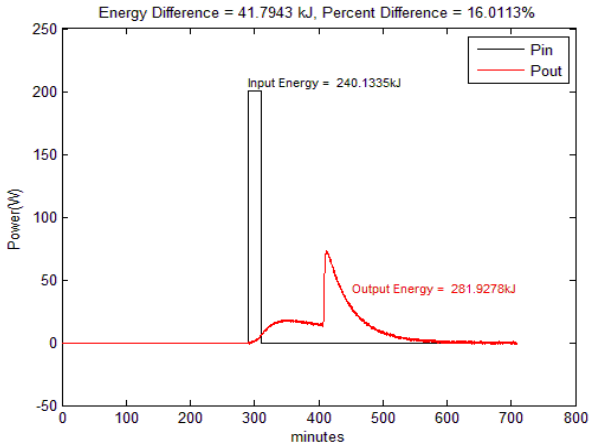

Small Cell heat run data for 7-8-2009

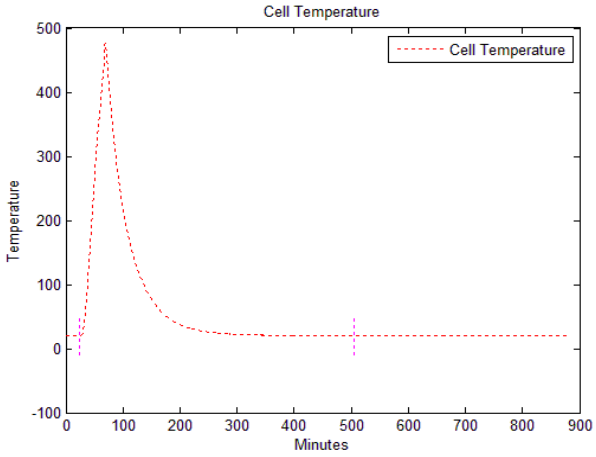

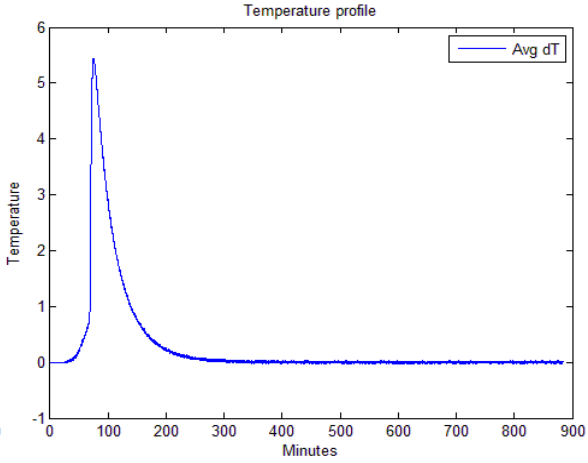

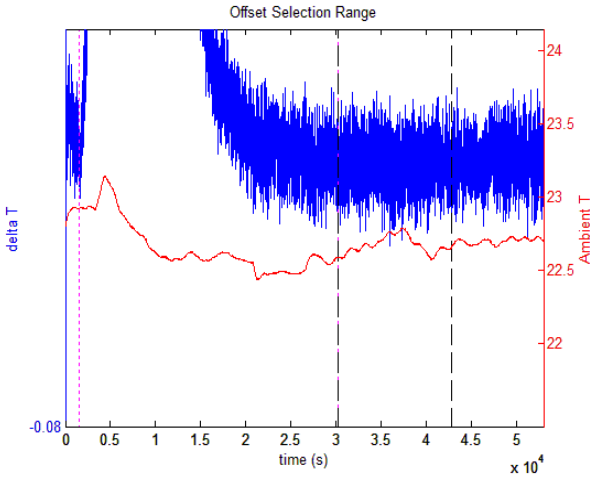

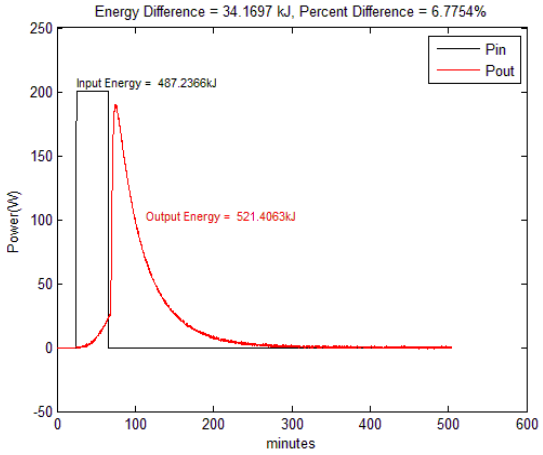

Small Cell heat run data for 7-9-2009

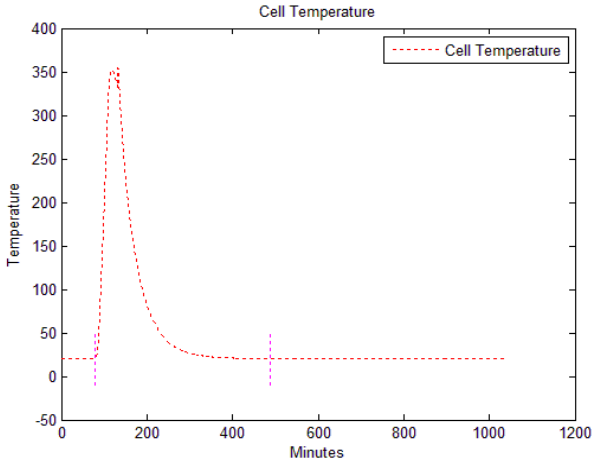

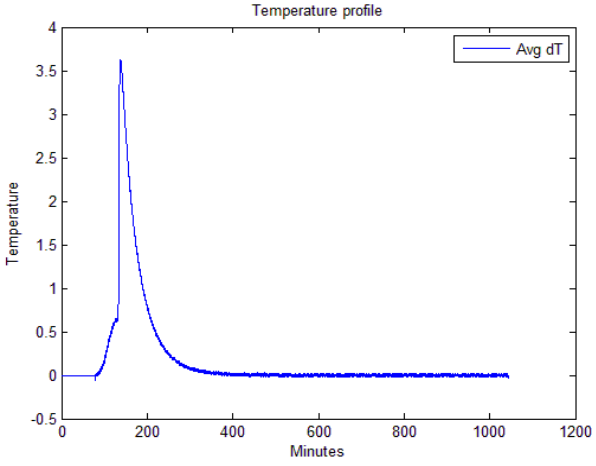

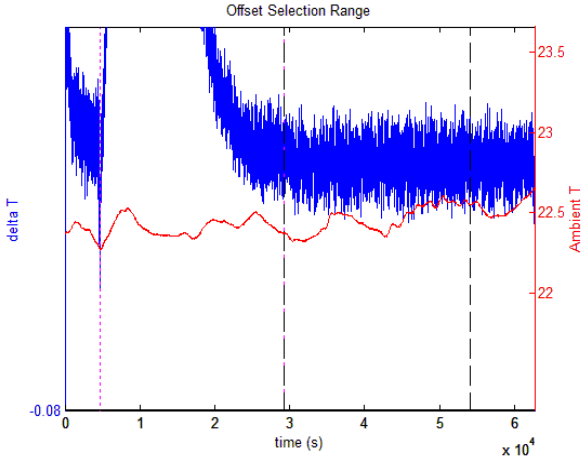

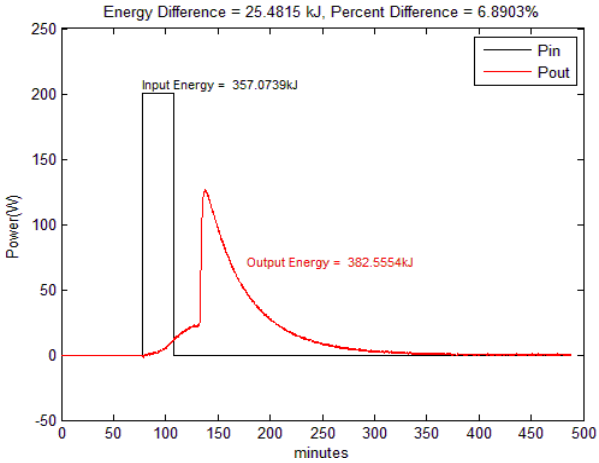

Small Cell heat run data for 7-10-2009

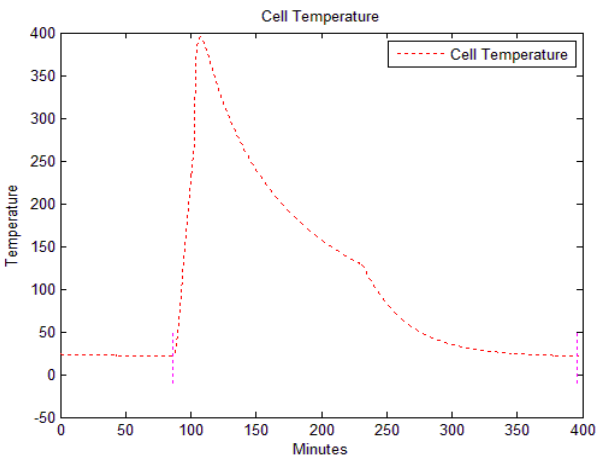

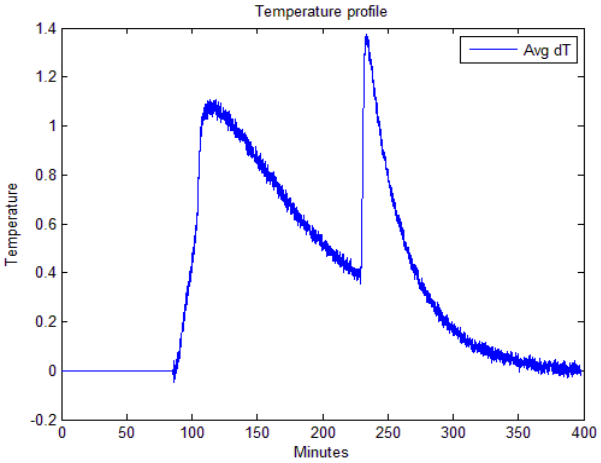

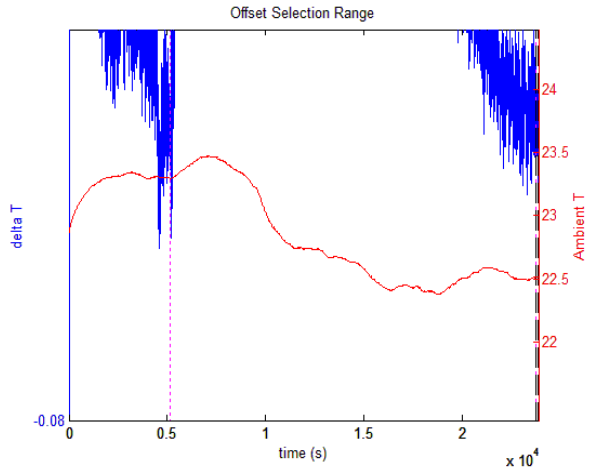

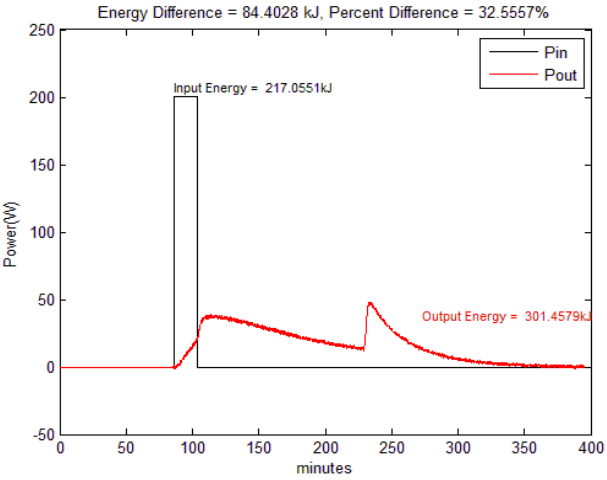

Small Cell heat run data for 7-13-2009

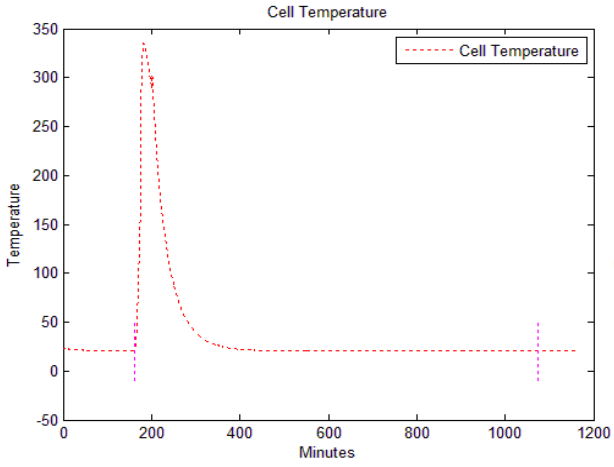

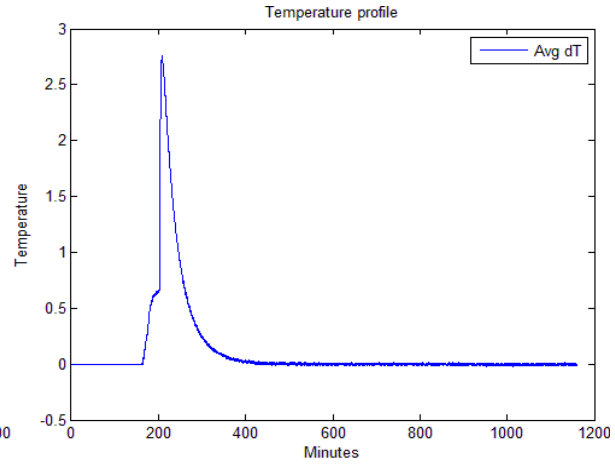

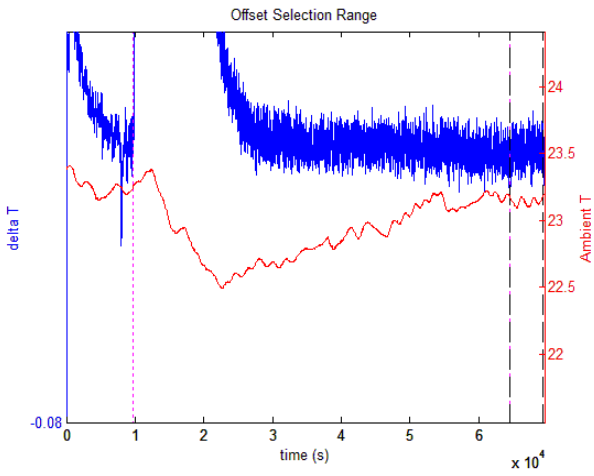

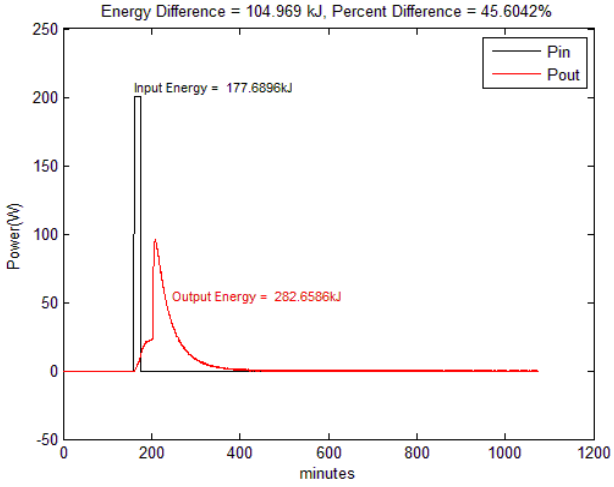

Small Cell heat run data for 7-16-2009

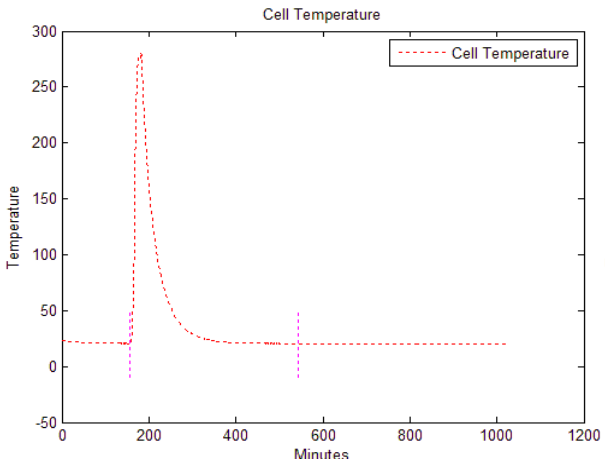

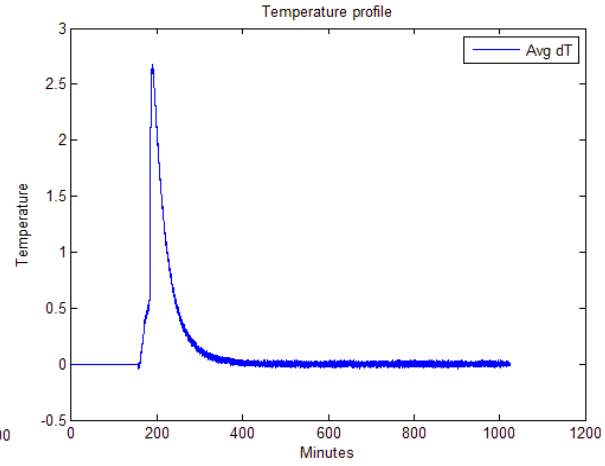

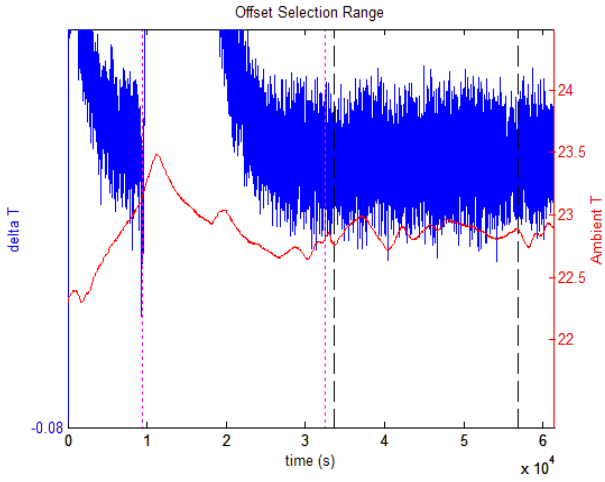

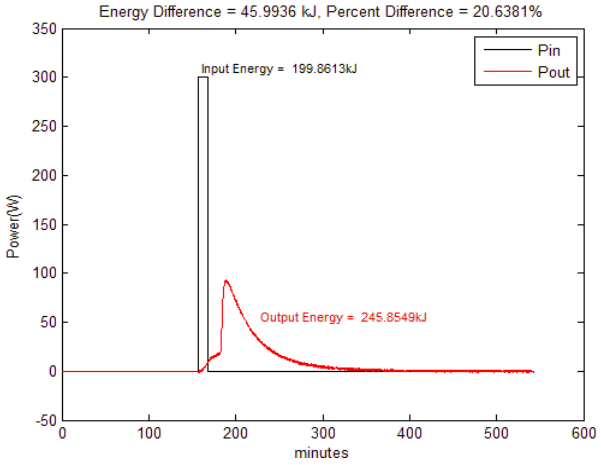

Small Cell heat run data for 7-21-2009

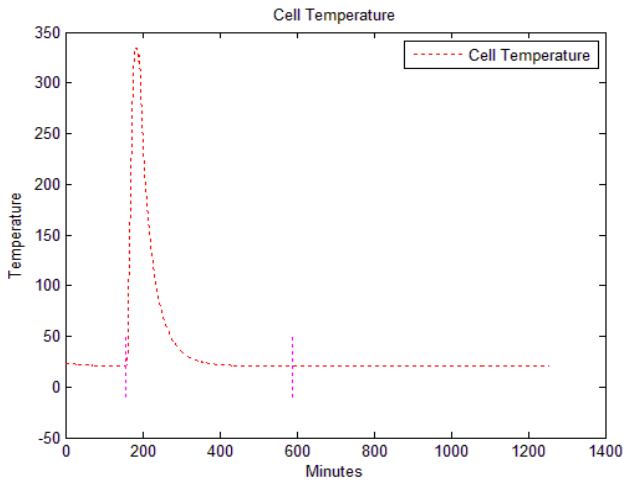

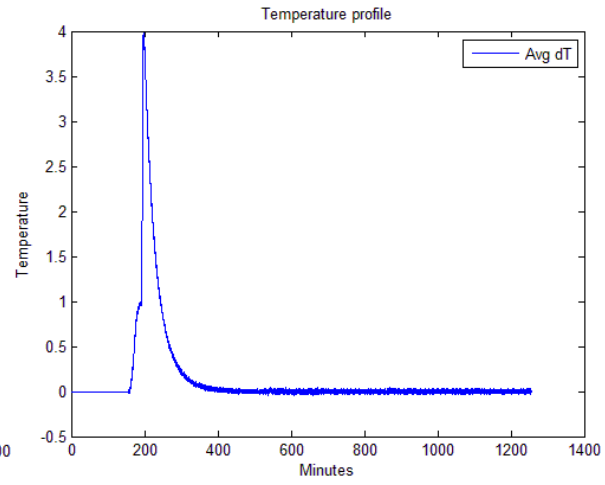

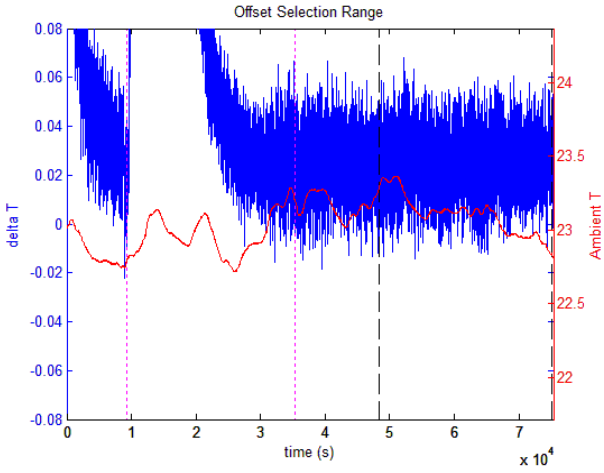

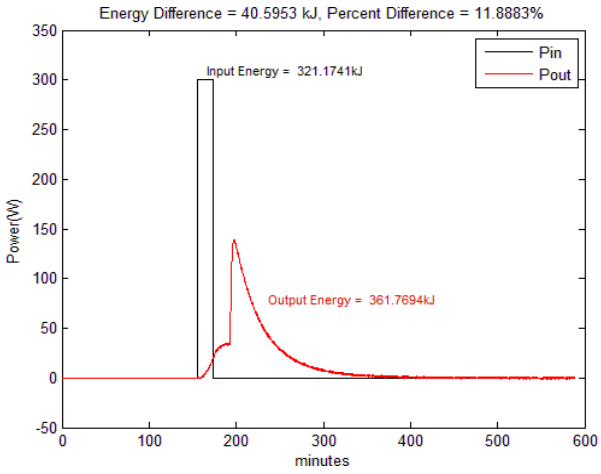

Small Cell heat run data for 7-23-2009

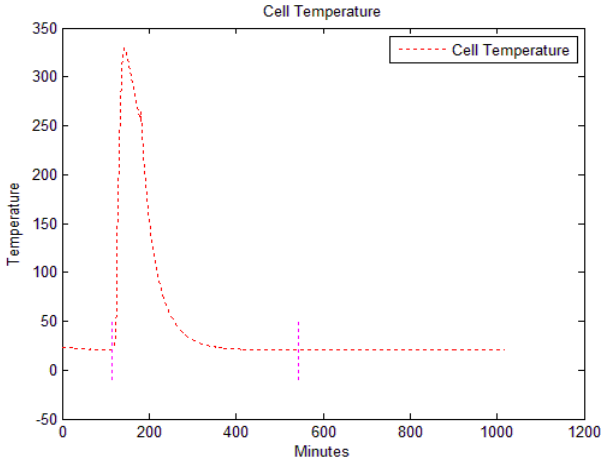

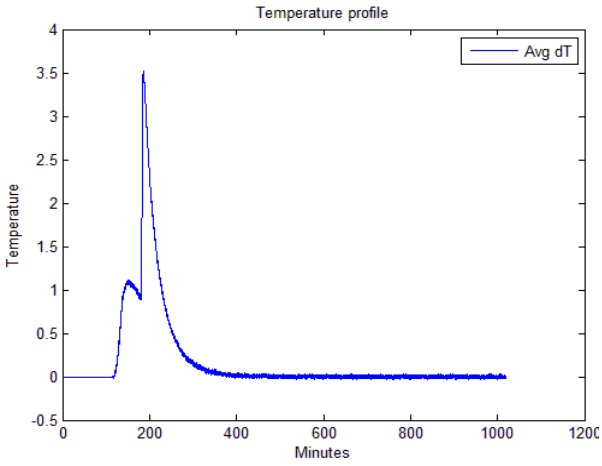

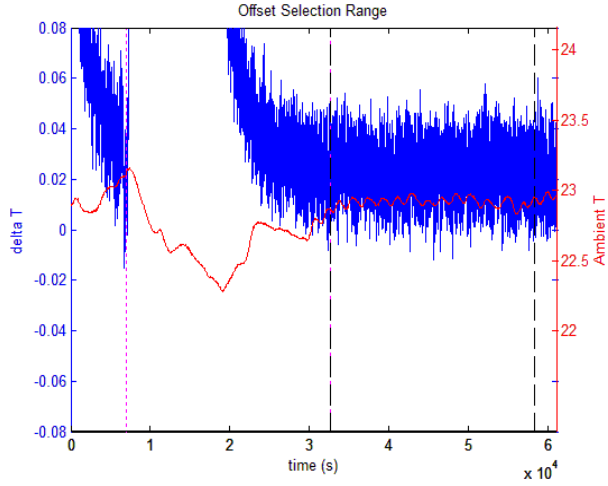

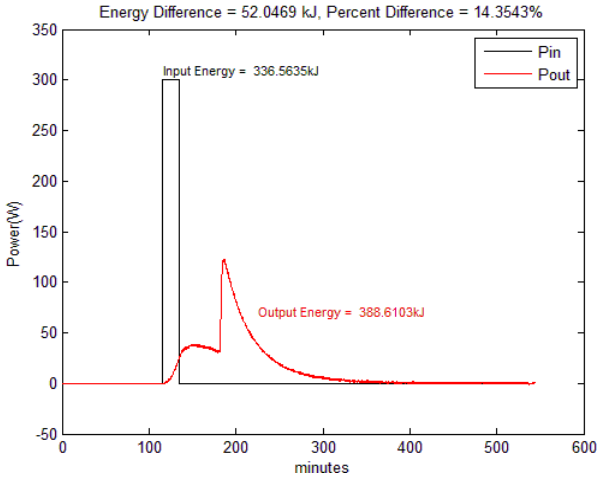

Small Cell heat run data for 7-24-2009

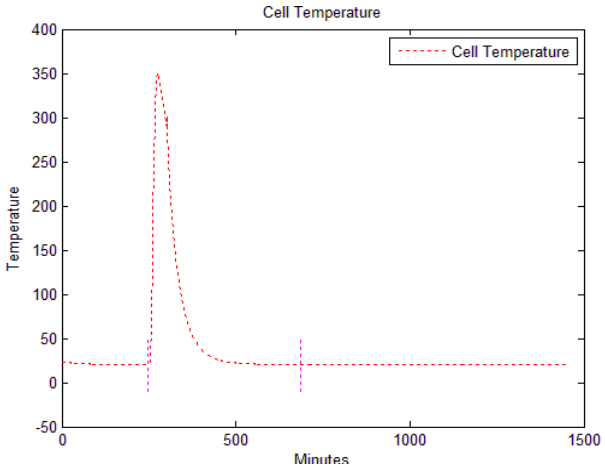

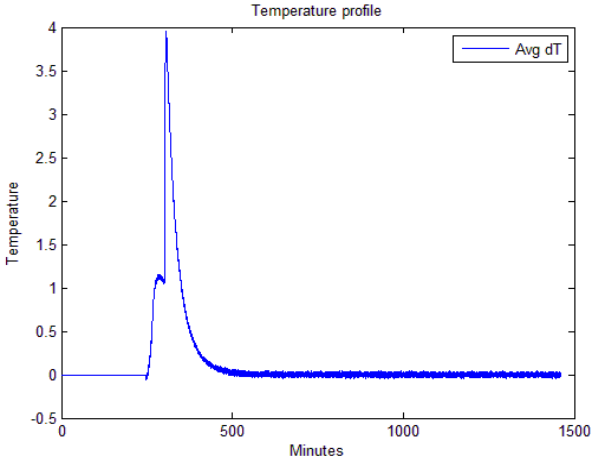

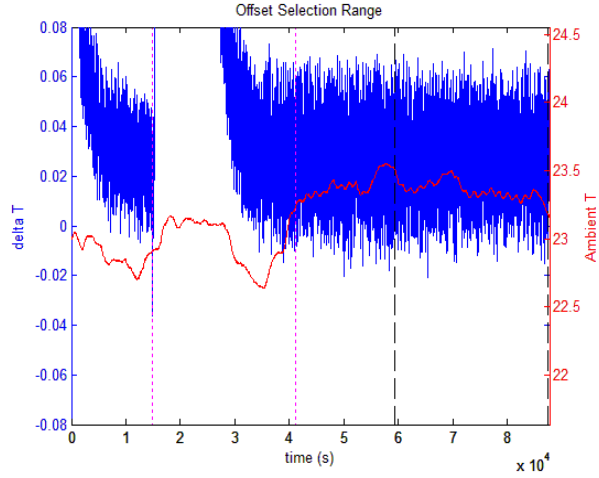

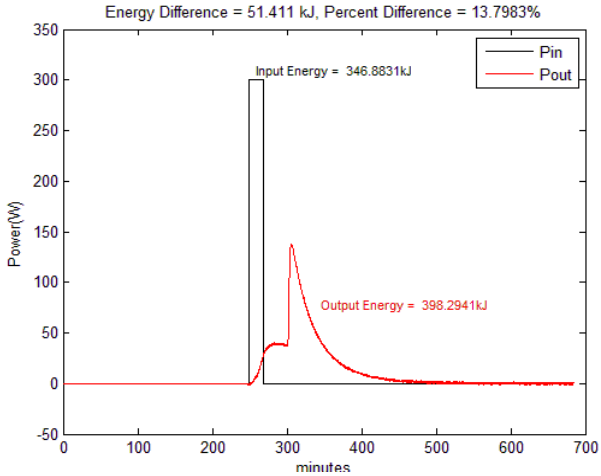

Small Cell heat run data for 7-25-2009

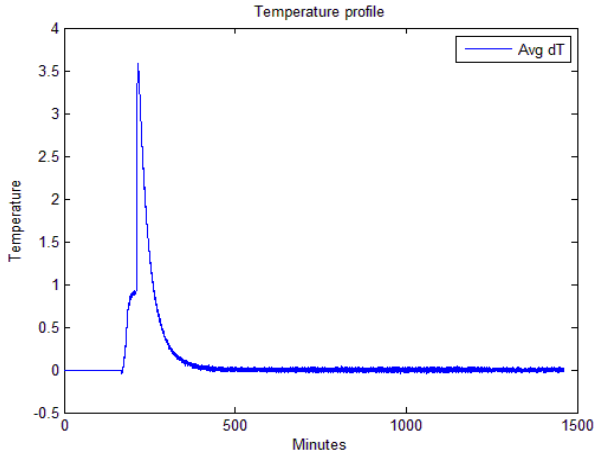

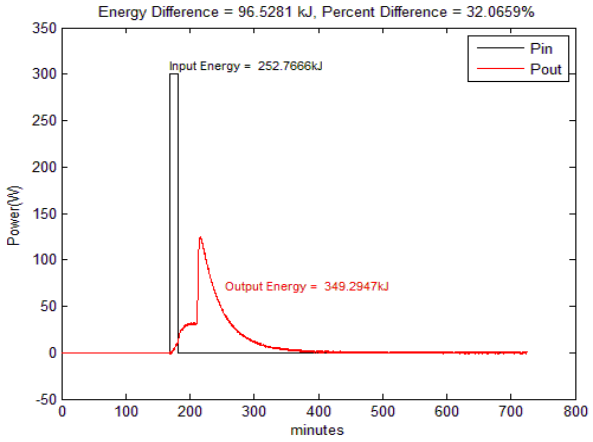

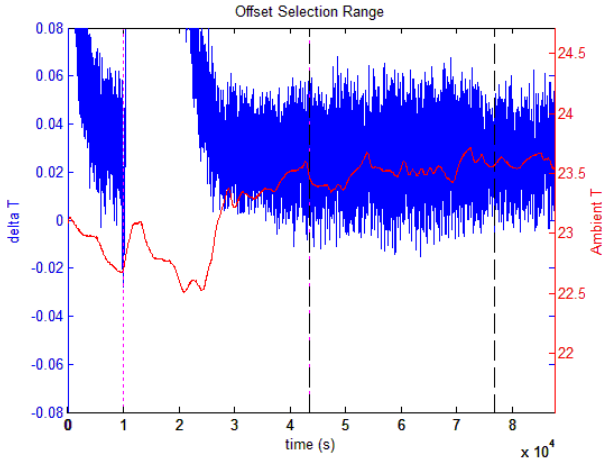

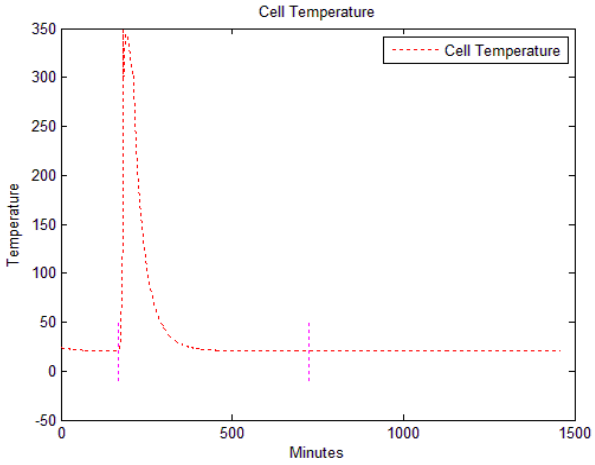

Appendix E – Large Cell Heat Runs

Large Cell heat run data for 6-18-2009

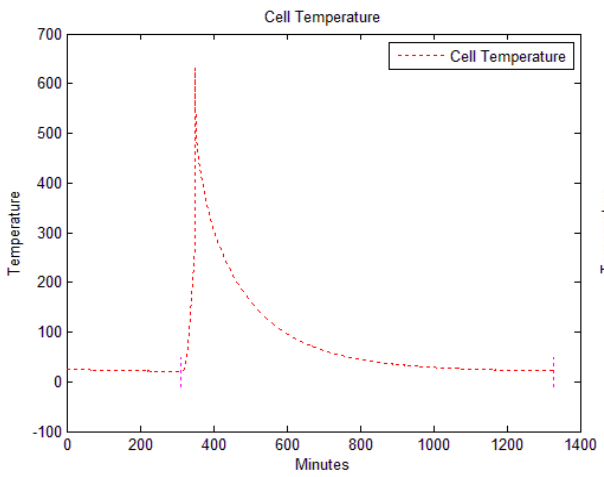

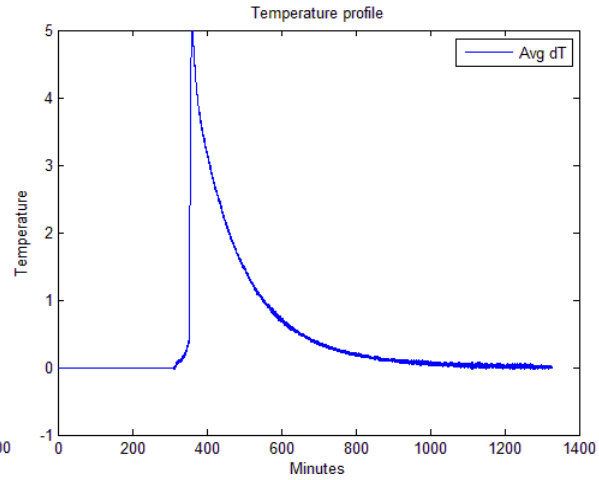

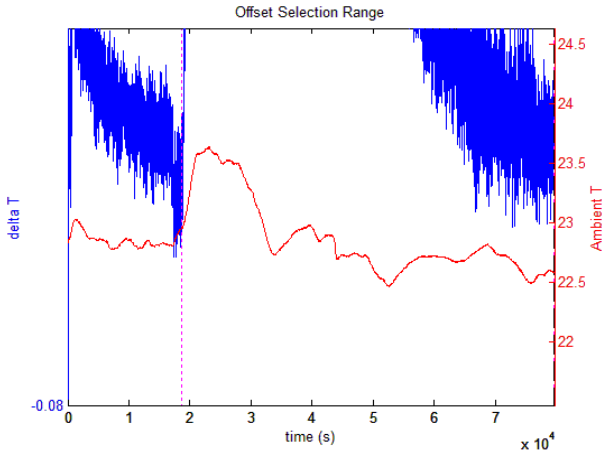

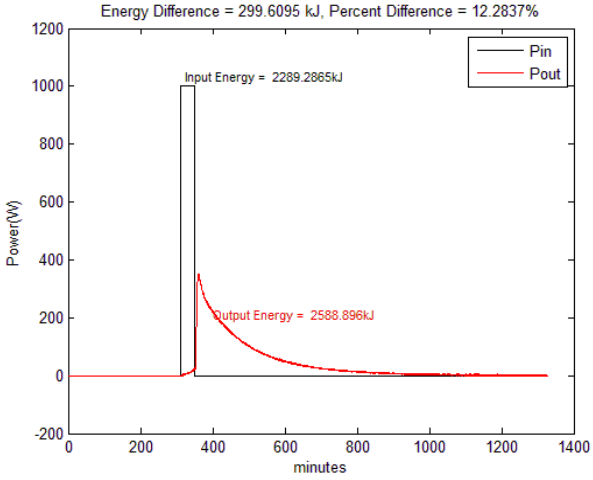

Water Flow Calorimetry, Experimental Runs and Validation Testing for BlackLight Power Inc.

Performed at Rowan University
Glassboro, New Jersey

January 2009 – May 2009

College of Engineering
Departments of Electrical, Chemical and Mechanical Engineering
Prof. Peter Mark Jansson PP PE
Ulrich K.W. Schwabe BSECE
Matthew Abdallah ChE
Nathaniel Downes ECE
Patrick Hoffman ME

May 2009

Table of Contents

Executive Summary

The company BlackLight Power (BLP) of Cranbury, NJ has been conducting experiments on the heat generation from materials which demonstrate what they believe is a proprietary process capable of relaxing the hydrogen atom below its normally considered ground state. For some time now, teams of engineering professors and their students at Rowan University have been involved in validating many of the heat experiments performed by BlackLight Power in our own campus laboratory facilities. The project described herein is the most recent continuation of previous calorimetry experiments which were completed over the last few months with the assistance of professors and students from the Chemistry and Biochemistry departments within the University. The findings which will be highlighted in this report confirm the water flow calorimeter can precisely and accurately measure heat from known chemical reactions. The specific reactions examined were the thermal decomposition of ammonium nitrate (NH_4NO_3) to form nitrogen, oxygen and water as well as the reaction of magnesium (Mg) and iron oxide (Fe_2O_3) to form magnesium oxide (MgO). By completing these well known, easily modeled reactions, it was possible to validate the calorimeter's performance when its reactants contained a known quantity of energy.

Rowan University Laboratory Setup

Materials and Equipment

The laboratory setup remained unchanged since the last report of our results, being based around a water flow calorimeter containing a simple test cell. The test cell in which chemical reactants are loaded is housed inside a vacuum chamber around which is wrapped ¼" copper tubing. A water chiller in conjunction with a pump supplies a constant flow of 20°C water to the vacuum chamber tubing. The test cell is surrounded by an electric resistive heater that is powered by a Xantrex XDC 600-10 power supply. A second precision power supply (HP) provides power and a reference voltage to the rest of the instrumentation, such as various thermistors used in the process. Once a test and any reaction inside the cell has completed, helium is introduced into the vacuum chamber to allow for a faster cool-down cycle.

All measurements are recorded with the help of a simple LabView program. Time, cell temperature, inlet and outlet water temperature, water flow rates were all recorded at 5s-10 s interval. Data are then analyzed to calculate the input energy from DC heater and the output energy from the water flow rate and change in inlet and outlet water temperature using a program written in MatLab. Profiles of the change in water temperature, cell temperature and comparing the input and output energies were plotted. This work is done mostly with the help of a simple MATLAB program, which analyzes the many data points and performs all the necessary calculations.

During the course of testing from January 2009 to May 2009, two different cell sizes were used with the 1 kW BLP reactor for chemical control heat experiments. The first was the traditional 1" diameter heavy duty cell used for small exothermic reactions, the second being a new 2" diameter heavy-duty cell used for greater exothermic reactions (Figure 1). As recommended by BLP, the 1" heavy duty cells were used for the magnesium and iron-oxide thermite reaction, while the 2" heavy-duty cells were used for decomposition ammonium nitrate experiment.

Figure 1: Showcasing the 1" (bottom) and 2" (top) heavy duty cell sizes

Calibration and Experimental Run Procedures

Before and after every test or calibration it is crucial to manually measure the water flow rate to ensure it remains relatively constant throughout each run. The heater power supply is briefly turned on with low limits to ensure proper and safe connection with the heater circuit. All valves and lines for the helium and vacuum pump are checked for leaks, and data is recorded until equilibrium of the cell temperature has been reached.

For all the chemical control heat experiments, the chemistry department procured chemicals. The graduate students of the chemistry department in the presence of project team carried out the chemical loading of the cell. In order to improve the conversion rate of the reaction, magnesium and iron oxide were thoroughly mixed during the cell loading.

For all runs, after thermal equilibrium of the cell temperature is reached, the vacuum chamber is pumped down to below 10 mTorr, ensuring that almost none of the supplied and generated heat is released to the calorimeter during the cell heating stage. Once the desired vacuum in the chamber is reached, varying methods of heating are applied

depending on the type of run to be completed. During a calibration run a predetermined amount of energy is supplied to the heater core, which will subsequently be compared to the energy (in terms of heat) measured by the calorimeter. A heat run is completed in almost the same fashion, with the exception that the input energy necessary to start the reaction is unknown. This input energy is recorded as the output voltage and current of the power supply, along with the output energy (again in terms of output heat) measured by the calorimeter. For all types of runs these input and output measurements are compared, providing the researcher with an accurate account of the accuracy of the calorimeter, and the energy produced by the reaction in the cell. The cool-down process, consisting of the infusion of helium into the vacated chamber, speeds up the process of recovering the generated heat, while also reducing observed losses.

Results and Discussion

Calibration Results

A total of 15 successful calibration runs were completed during the spring 2009 semester. Calibration runs were performed frequently between heat runs to ensure energy coupling efficiency of the calorimeter ranged in the high 98-99% . Table 1 gives the data for these calibrations, all of which having a high coupling efficiency. Figures 2, 3 and 4 below represent the energy profile, cell temperature and delta temperature respectively for a calibration run with an input energy of 120 kJ.

Table 1: Data recorded from calibration runs

Run	Date	Input	Output (kJ)	ΔkJ	% Difference	Coupling
1	1/21/2009	150.57	152.43	1.86	1.23	1.012
2	1/27/2009	120.16	119.75	-0.41	0.34	0.997
3	1/29/2009	200.72	200.30	-0.42	0.21	0.998
4	1/30/2009	150.32	148.37	-1.95	1.31	0.987
5	2/2/2009	180.22	179.06	-1.16	0.65	0.994
6	2/5/2009	200.21	199.93	-0.27	0.14	0.999
7	2/6/2009	94.03	94.72	0.70	0.74	1.007
8	2/9/2009	120.41	121.53	1.13	0.93	1.009
9	2/10/2009	149.96	152.49	2.53	1.67	1.017
10	2/13/2009	150.32	152.41	2.09	1.38	1.014
11	2/24/2009	49.67	49.99	0.33	0.52	1.007
12	2/27/2009	99.59	99.42	-0.18	0.18	0.998
13	3/23/2009	99.91	99.80	-0.11	0.11	0.999
14	4/7/2009	198.63	194.76	-3.87	1.97	0.981
15	4/16/2009	109.87	109.42	-0.46	0.42	0.996

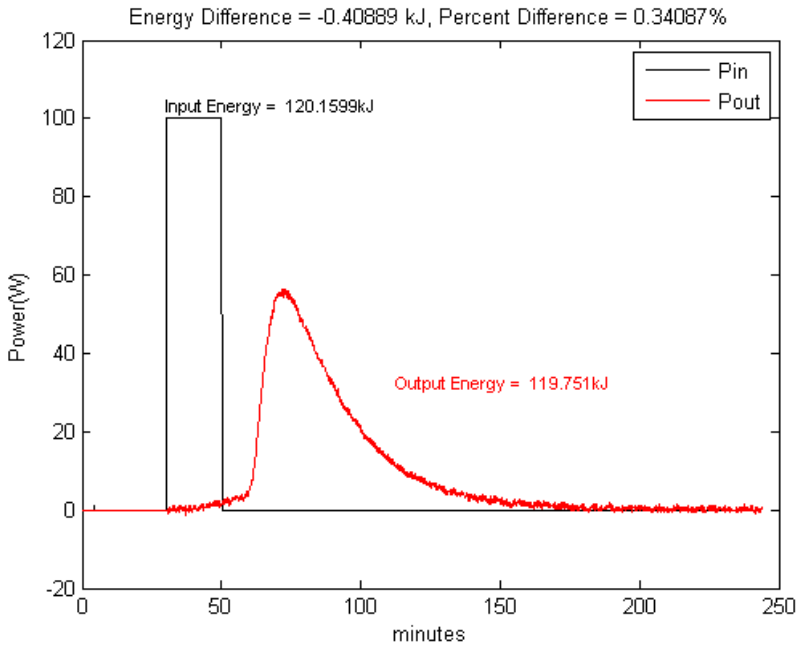

Figure 2: Input energy vs. output energy

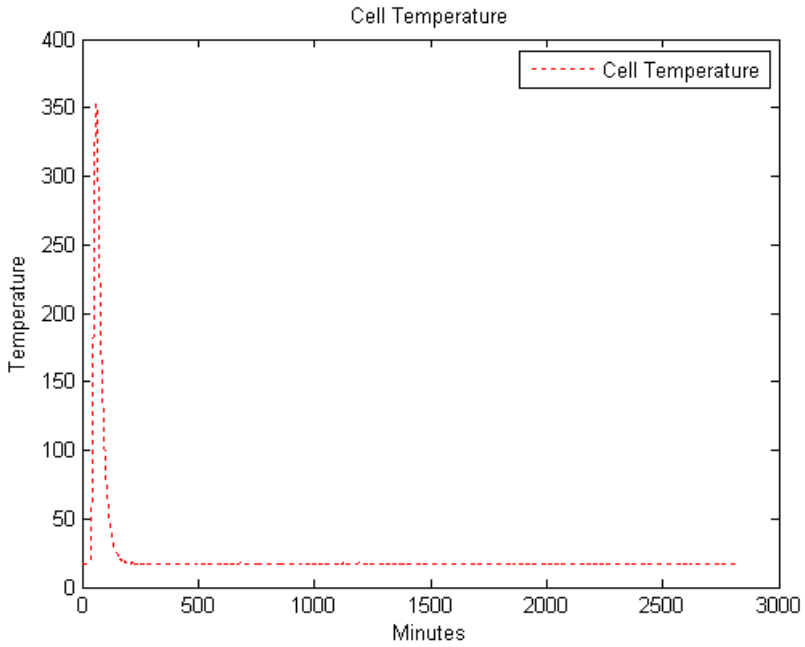

Figure 3: Cell temperature

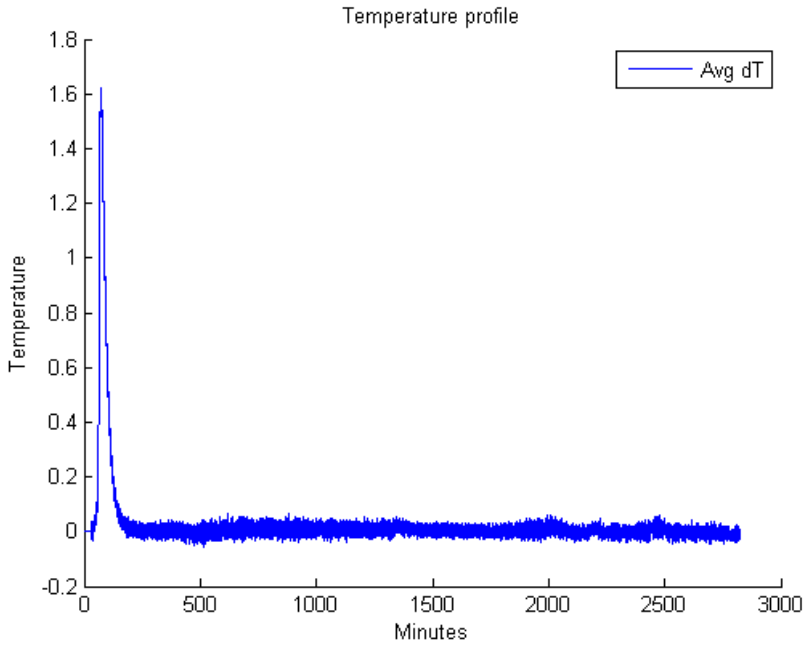

Figure 4: Change in Water Coolant Temperature

It is important to note the difference in the time-span of these figures. When calculating the output of a given run, the equipment is allowed to cool down for several hours. This is crucial in determining the offset due to thermocouple inconsistencies, later to be added or subtracted from the all data. The cool-down period is not incorporated into the final projections for output energy, as its value consists only of environmental factors such as ambient temperatures. Figure 2 represents the entire span used in the calculation of output energy, whereas Figures 3 and 4 plot the entire set of recorded data.

Experimental Results

Example results from control heat runs, three using the reactants Mg and Fe_2O_3 and one using the reactant NH_4NO_3 are listed in Table 2. Figure 5, 6 and 7 represent the energy profile, cell temperature, and change in water temperature recorded during run 3, the second control heat run with Mg and Fe_2O_3.

Table 2: Recorded Heat run data for $MgFe_2O_3$ and NH_4NO_3

Run	Date	Chemicals	Cell Size	Input (kJ)	Output (kJ)	ΔkJ	Theoretical
1	3/12/2009	NH_4NO_3	2"	443.95	481.65	**37.691**	41.2
2	4/9/2009	$MgFe_2O_3$	1"	240.62	271.83	**31.70**	32.75
3	4/12/2009	$MgFe_2O_3$	1"	227.51	256.46	**28.95**	32.75
4	4/22/2009	$MgFe_2O_3$	1"	177.83	210.21	**32.37**	32.75

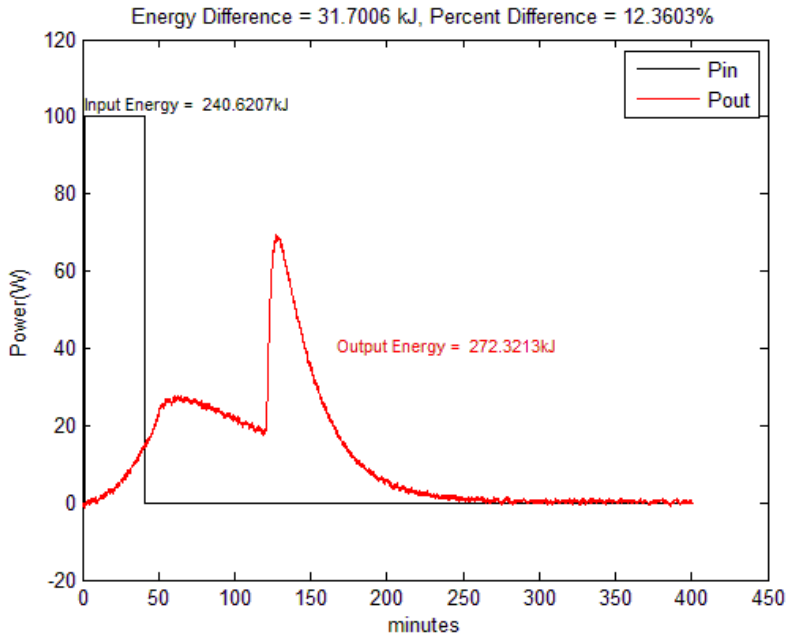

Figure 5: Heat run energy profile of Magnesium Iron Oxide on 4/9/09

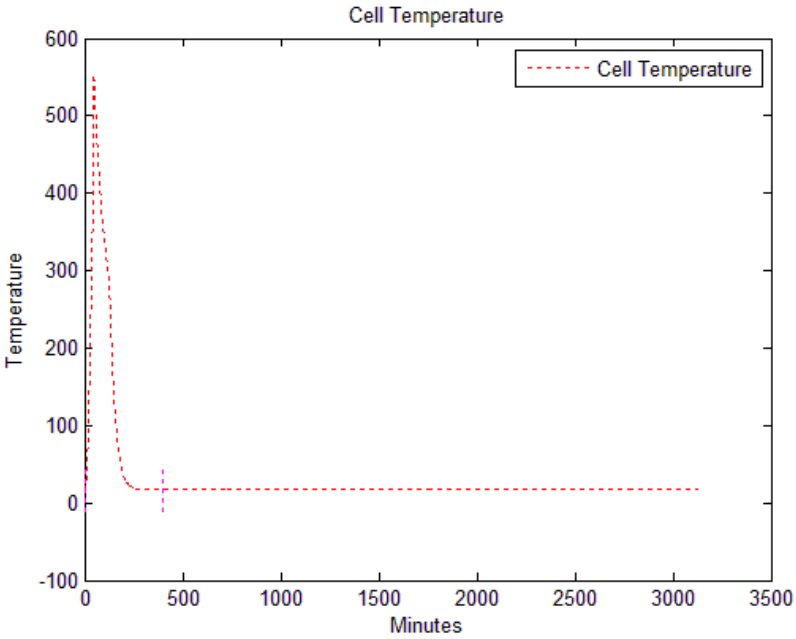

Figure 6: Cell temperature profile of heat run for $MgFe_2O_3$ on 4/9/09

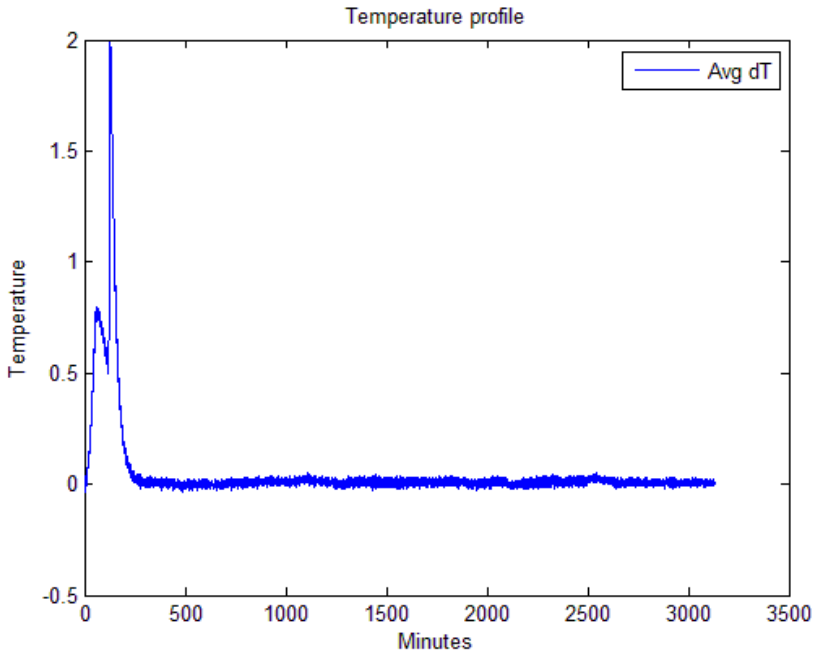

Figure 7: Change in water coolant temperature of heat run for $MgFe_2O_3$ on 4/9/09

Background calculations

Two exothermic reactions were considered for testing in the experimental calorimeter set up as chemical control heat runs. The reactions were (1) thermal decomposition of ammonium nitrate (NH_4NO_3) and (2) the reaction of iron oxide (Fe_2O_3) and magnesium (Mg). The theoretical heats of reaction provided below are under an assumption of complete conversion.

$$2NH_4NO_3 \rightarrow 2N_2 + O_2 + 4H_2O \quad (1)$$

$$Fe_2O_3 + 3Mg \rightarrow 3MgO + 2Fe \quad (2)$$

Reaction 1 is highly exothermic, ΔH_{rxn}=-412 kJ/mol, and occurs at temperatures above 300°C. However, there is a side reaction that occurs during the thermal decomposition of ammonium nitrate.

$$NH_4NO_3 \rightarrow N_2O + 2H_2O$$

The side reaction is favored at lower temperatures (200-250°C) and constitutes a net heat of reaction of -124.4kJ/mol. Therefore, this reaction is only a minor part of the overall mechanism and can be avoided by heating cell to a temperature where reaction 1 would be dominant. The second reaction used for the experimental procedure was the reduction of iron oxide by magnesium. Reaction 2 is also an exothermic reaction with a ΔH_{rxn}=-980.6 kJ/mol. No significant side reactions were found for this process.

The quantities of reactants used by the team for heat runs during the semester were identical to those used by BLP in the supplemental materials provided. Reaction 1

required 16 g of ammonium nitrate, which yielded a theoretical energy output of 41.2 kJ. The quantities of reactants used for reaction 2 were 5.34 g and 2.43 g of iron (III) oxide and magnesium respectively. The energy released by reaction 2, using reactant quantities above, was calculated to be 32.75 kJ. These calculations represent the maximum theoretical amount of energy being generated. In order to ensure the completion of the reaction, chemical cells were heated to a significantly higher temperature. Still full completion of the reaction is very difficult to achieve and this is evident from the calorimetric measurements which are off by a few kJ.

Conclusions

From the experimental results obtained, it can be concluded that the calorimeter system is both accurate and precise at measuring the heat evolved from a thermal decomposition of known reactants. The accuracy of the calorimeter was established with heater calibration runs, since DC current and voltage measurements and hence input power and energy measurement can be performed more accurately than chemical reactions. It was possible to provide a measure of the calorimeter accuracy using the energy generated by a known chemical reaction. All in all, the calibration runs proved that the calorimeter is accurate within one percent of the power input by a resistive heater, and the chemical control heat runs gave strong indication that there are no significant differences between heat loss mechanisms. The Rowan University team is confident that the calorimeter is very accurate, and will continue to complete calibration, control and heat runs to verify BlackLight Power's claims.